

STROMAL B-CATENIN IN KIDNEY DEVELOPMENT

THE FUNCTIONAL ROLE OF STROMAL B-CATENIN IN THE PATHOGENESIS
OF RENAL DYSPLASIA AND KIDNEY DEVELOPMENT

By FELIX J. BOIVIN-LAFRAMBOISE, BSc

A Thesis Submitted to the School of Graduate Studies in Partial
Fulfillment of the Requirements for the Degree of Doctor of Philosophy

McMaster University © Copyright by Felix J. Boivin-Laframboise, July 2016

Ph.D. Thesis – Felix Boivin-Laframboise

McMaster University – Medical Sciences

DOCTOR OF PHILOSOPHY (2016)

McMaster University

(Medical Sciences, Cancer and Genetics)

Hamilton, Ontario

TITLE: The Functional Role of β -catenin in the Pathogenesis of Renal Dysplasia and Kidney Development

AUTHOR: Felix J. Boivin-Laframboise, BSc (McGill University)

SUPERVISOR: Dr. Darren Bridgewater

SUPERVISORY COMMITTEE: Dr. Bradley Doble
Dr. Judith West-Mays

NUMBER OF PAGES: xviii, 211

ABSTRACT

Renal dysplasia is a disease characterized by developmental abnormalities of the kidney that affect 1 in 250 live births. Depending on the severity of the renal abnormalities, this disorder can lead to childhood kidney failure, adult onset chronic kidney disease, and hypertension. Currently, the best treatment options for patients with renal dysplasia are renal dialysis and kidney transplant. Our limited understanding of the pathogenesis of renal dysplasia has prevented the development of better treatment strategies for those patients. A hallmark of renal dysplasia is an expansion of loosely packed fibroblast cells, termed renal stroma. Markedly elevated levels of β -catenin have been reported in the expanded stromal population in patients with dysplastic kidneys. Yet, the contribution of stromal β -catenin to the pathogenesis of renal dysplasia is not known. Additionally, the role of stromal β -catenin in the developing kidney is not clear. *The overall hypothesis of this PhD thesis is that β -catenin in stromal cells controls key signalling molecules that regulate proper kidney development. Furthermore, we hypothesize that elevated levels of β -catenin contribute to the pathogenesis of renal dysplasia.* To mimic the human condition, we generated a mouse model that overexpresses β -catenin specifically in the stroma (termed β -cat^{GOF-S}). In addition, to gain a better understanding of its role in kidney development, we generated a second mouse model deficient for β -catenin exclusively in stromal cells (termed β -cat^{S^{-/-}}). The goal of this study is to utilize these models to understand the role of stromal β -catenin in kidney formation and investigate its contribution to renal dysplasia.

The first objective defines the contribution of stromal β -catenin to the genesis of renal dysplasia. We provide evidence for a mechanism whereby the overexpression of stromal β -catenin disrupts proper differentiation of stromal progenitors and leads to an expansion of stroma-like fibroblast cells and vascular morphogenesis defects. In the second objective, we establish a mechanism where stromal β -catenin modulates Wnt9b signaling in epithelial cells to control proliferation of the nephron progenitors. In the third objective, we define a role for stromal β -catenin in proper formation and survival of the medullary stroma. Finally, in a technical report, we outline a protocol to isolate stromal cells in the developing kidney and provide potential downstream applications to further our understanding of stromal β -catenin in the developing kidney.

Taken together, our findings establish a crucial role for stromal β -catenin in the genesis of renal dysplasia and demonstrate, using two mouse models, that stromal β -catenin must be tightly regulated for proper formation of the stroma lineages and development of the kidney.

“What it all boils down to is that no one’s really got it figured out just yet”

ACKNOWLEDGEMENTS

Thank you to my supervisor, Dr. Darren Bridgewater, for his constant support and guidance during my PhD. But most importantly, thank you for trusting me and allowing me to make mistakes. These mistakes have helped me grow as a scientist and as a person.

Thank you to my supervisory committee, Dr. Judith West-Mays and Dr. Bradley Doble, for their advice and support during my PhD. I am very grateful for the time and interest you have devoted to my project.

Thank you to the members of the Bridgewater lab, past and present, for your tremendous help with the β -catenin projects. You have all played a big part in the realization and completion of this thesis.

Thank you to all my friends. All of you. There's nothing like friends to help you put things into perspective.

Thank you to my family for always being so respectful and understanding. My crippling anxiety often gets the best of me, but it is always comforting to know that no matter what happens I can always count on you guys.

Thank you Jay for all your silences. You may not realize it but sometimes those silences are all I need.

PREFACE

This is a “sandwich” style thesis. Chapter 1 is a general introduction that includes parts of a review article I have published during my PhD. To provide further background information to the introduction, I have also included additional sections on renal anatomy and kidney development. Chapters 2, 3, and 4 have been published or will be submitted to peer-reviewed journals for publication. A preface of each chapter is included to highlight the significance of the studies and to describe my contribution to the publications. A technical report is included in Chapter 5 to address the limitations of the studies. Finally, the significance, contribution, and limitations of the work presented in this thesis are discussed in Chapter 6.

TABLE OF CONTENTS

ABSTRACT.....	iv
ACKNOWLEDGEMENTS.....	vii
PREFACE.....	viii
TABLE OF CONTENTS.....	ix
LIST OF FIGURES.....	xii
LIST OF SUPPLEMENTAL FIGURES.....	xiv
LIST OF ABBREVIATIONS.....	xv
CHAPTER 1 - INTRODUCTION.....	1
1.1 Chronic Kidney Disease in Children.....	2
1.2 Kidney Anatomy and Physiology.....	4
1.2.1 Gross Anatomy and Physiology of the Kidney.....	4
1.2.2 Anatomy and function of the nephron.....	6
1.3 Kidney Development.....	8
1.3.1 Branching Morphogenesis.....	8
1.3.2 Nephrogenesis.....	11
1.4 The Renal Stroma.....	14
1.4.1 The functional role of the renal stroma.....	18
1.5 β-catenin.....	21
1.5.1 Junctional and Wnt-dependent roles for β -catenin.....	21
1.5.2 Wnt-independent transcriptional roles for β -catenin.....	24
1.6 β-catenin in the Developing Kidney.....	26
1.6.1 β -catenin in the ureteric epithelium.....	26
1.6.2 β -catenin in the mesenchyme.....	28
1.6.3 β -catenin in the renal stroma.....	30
1.7 Renal Dysplasia.....	32
1.7.1 Human renal dysplasia.....	32
1.7.2 β -catenin in Renal Dysplasia.....	36
1.8 Rationale and Hypothesis.....	38
CHAPTER 2 - Stromal β-catenin Overexpression Contributes to the Pathogenesis of Renal Dysplasia.....	39
PREFACE.....	40
ABSTRACT.....	42
INTRODUCTION.....	44
METHODS.....	47
RESULTS.....	49
Stabilization of β -catenin in Stromal Cells Contributes to Renal Dysplasia.....	49
Elevated levels of Stromal β -catenin Result in a Disrupted Stromal Cell differentiation.....	55

Stromal Defects Result in Disrupted Vasculature Morphogenesis.....	59
Human dysplastic tissue exhibits similar stromal abnormalities	67
DISCUSSION	70
Stromal β -catenin overexpression leads to renal dysplasia	70
Characterization of the β -catenin overexpressing stromal-like population	73
Stromal β -catenin overexpression disrupts endothelial cell organization and vascular patterning	74
AUTHOR CONTRIBUTION	77
SUPPORTING INFORMATION – FIGURES.....	78
SUPPORTING INFORMATION - METHODS.....	85
CHAPTER 3 - Stromally Expressed β-catenin Modulates Wnt9b Signaling in the Ureteric Epithelium	89
PREFACE.....	90
ABSTRACT.....	92
INTRODUCTION	93
MATERIALS AND METHODS	97
RESULTS / DISCUSSION.....	101
β -catenin is expressed in distinctive patterns in the renal stroma.....	101
Ablation of β -catenin in stromal cells leads to multiple kidney abnormalities	107
Stromally expressed β -catenin modulates Wnt9b expression in the ureteric epithelium	117
Deletion of β -catenin in stromal cells impairs Wnt9b signaling to the nephrogenic progenitors	123
ACKNOWLEDGMENTS	129
SUPPLEMENTARY MATERIAL	130
CHAPTER 4 - Stromally expressed β-catenin controls medullary stromal development via regulation of cell survival	136
PREFACE.....	137
ABSTRACT.....	138
INTRODUCTION	139
METHODS	142
RESULTS	148
The ablation of stromal β -catenin results in reduced medullary stroma.....	148
β -catenin is not required for the development of stromal progenitors.....	153
The loss of stromal β -catenin results in increased apoptosis of stromal cells	156
Stromal β -catenin modulates the expression of anti-apoptotic genes.....	160
DISCUSSION	167
β -catenin controls medullary stroma development.....	167
β -catenin regulates cell survival in the renal stroma.....	169

CHAPTER 5 - Technical Report: Isolation of Renal Stromal Cells From <i>WT</i> AND β-<i>cat</i>^{-/-} Mouse Strains	172
PREFACE	173
ABSTRACT	174
INTRODUCTION	175
METHODS	177
RESULTS	180
Isolation of renal stromal cells from <i>WT</i> and β - <i>cat</i> ^{S-/-} mice	180
RNA extraction of FACS sorted stromal cells.....	186
Identification of FACS sorted stromal cells.....	187
CHAPTER 6 – DISCUSSION	190
The Role of Stromal β-catenin in Renal Dysplasia	191
The Functional Role of Stromal β-catenin in Kidney Development	192
Limitations and Future Directions	196
REFERENCES	198

LIST OF FIGURES**CHAPTER 1**

Figure 1.1 – Gross anatomy and basic structure of the kidney.....	5
Figure 1.2 - Basic structure of the nephron.....	7
Figure 1.3 - Branching morphogenesis and the Gdnf/Ret Signaling.....	10
Figure 1.4 - Overview of nephrogenesis in the developing kidney.....	12
Figure 1.5 - Development of the stromal populations.....	16
Figure 1.6 - Stromal cell differentiation.....	17
Figure 1.7 – Junctional and Wnt-dependent roles for β -catenin.....	23
Figure 1.8 – Wnt-independent transcriptional roles for β -catenin	25
Figure 1.9 – β -catenin in the ureteric epithelium.....	27
Figure 1.10 – β -catenin in the mesenchyme	29
Figure 1.11 - β -catenin in the renal stroma.....	31
Figure 1.12 - Human renal dysplasia	33
Figure 1.13 - Histopathological features of renal dysplasia.....	35

CHAPTER 2

Figure 2.1 - Human dysplastic kidneys exhibit increased levels of β -catenin in stromal cells	51
Figure 2.2 - Overexpression of β -catenin in the stroma during kidney development leads to renal dysplasia	53
Figure 2.3 - Disrupted and reduced stromal markers in β -cat ^{GOF-S} kidneys.....	57
Figure 2.4 - Overexpression of stromal β -catenin leads to disrupted vascular morphogenesis.....	61
Figure 2.5 - Overexpression of stromal β -catenin results in ectopic localization of Bmp4 and Wnt4.....	65
Figure 2.6 - Human dysplastic kidney display a heterogeneous stromal cell population similar to β -cat ^{GOF-S} kidneys.....	68

CHAPTER 3

Figure 3.1 – β -catenin is expressed in distinctive patterns in the renal stroma	102
Figure 3.2 - Intracellular localization of β -catenin in capsular, cortical, and medullary stroma.....	106
Figure 3.3 – β -cat ^{S-/-} mutants demonstrate multiple kidney abnormalities.....	109
Figure 3.4 – Temporal analysis of the embryonic kidney phenotype in β -cat ^{S-/-} mutant	113
Figure 3.5 – Investigation of the renal stroma in β -cat ^{S-/-} mutant kidneys	115
Figure 3.6 – The condensing mesenchyme cell population is reduced in β -cat ^{S-/-} mutant kidneys	118
Figure 3.7 – β -catenin in the renal stroma modulates Wnt9b expression in ureteric epithelial cells.....	121

Figure 3.8 - β -cat ^{S-/-} mutants demonstrate altered Wnt9b signaling to the condensing mesenchyme	125
--	-----

CHAPTER 4

Figure 4.1 - The ablation of stromal β -catenin results in reduced medullary stroma	151
Figure 4.2 - β -catenin is not essential for cortical stroma development.....	155
Figure 4.3 - β -catenin deficiency increases apoptosis in the medullary stroma.....	158
Figure 4.4 – Stromal β -catenin regulates the expression of anti-apoptotic genes...	163
Figure 4.5 – β -catenin forms a complex with Tbx5 and Yap, which binds to the promoter region of <i>Bcl2l1</i>	166

CHAPTER 5

Figure 5.1 – Lineage tracing analysis in <i>FoxD1-eGFP</i> Cre kidneys.....	182
Figure 5.2 – Isolation of stromal cells using FACS.....	185
Figure 5.3 – Identification of the stromal markers in FACS stromal cells.....	189

LIST OF SUPPLEMENTAL FIGURES**CHAPTER 2**

Supplemental Figure S2.1 – Characterization of β -catenin expression in β -cat ^{GOF-S} mutant mice.....	78
Supplemental Figure S2.2– β -cat ^{GOF-S} kidneys display disrupted branching morphogenesis and nephrogenesis.....	80
Supplemental Figure S2.3– Analysis of stromal factors in FoxD1 knockouts.....	81
Supplemental Figure S2.4– The expanded stroma-like population originates from the FoxD1 stromal progenitor population.....	82
Supplemental Figure S2.5 - β -cat ^{GOF-S} kidneys display disorganized vasculature patterning.....	83
Supplemental Figure S2.6 – Analysis of the endothelial markers in FoxD1 ^{GC/GC} mice (FoxD1 ^{-/-} knockouts).....	84

CHAPTER 3

Supplemental Figure 3.1 - The Pbx1 antibody targets the capsular, cortical, and medullary stroma.....	130
Supplemental Figure 3.2 - Generation of mutant mice with stroma specific deletion of β -catenin.....	131
Supplemental Figure 3.3 – Characterization of cyst origin in β -cat ^{S-/-}	133
Supplemental Figure 3.4 – Branching morphogenesis and Nephrogenesis are not disrupted in β -cat ^{S-/-} kidneys.....	134

LIST OF ABBREVIATIONS

A	Apoptosis
ad	Adrenal Gland
Amph	Amphiphysin
APC	Adenomatous Polyposis Coli
Aqp-3	Aquaporin 3
b	Bladder
B2M	β -2-microglobulin
Bag3	Bcl2-Associated Athanogene 3
BAT	Beta-catenin Activated Transgene
Bax	Bcl2-associated X protein
Bcl2	B-cell Lymphoma 2
Bcl2l1	Bcl2-like 1
Birc5	Baculoviral IAP Repeat Containing 5
Bmp4	Bone Morphogenic protein 4
BrdU	Bromodeoxyuridine
CD44	Cluster of Differentiation 44
cDNA	Complimentary Deoxyribonucleic Acid
ChIP	Chromatin Immunoprecipitation
Cited1	Cbp/p300-interacting transactivator 1
CKD	Chronic Kidney Disease
cm	Condensed Mesenchyme
Co-IP	Co-Immunoprecipitation
cs	Cortical Stroma
DAB	3,3'-diaminobenzidine
DAPI	4',6-diamidino-2-phenylindole
Dchs1	Dachsous Cadherin-Related 1
Dkk1	Dickkopf-related protein 1
DMEM	Dulbecco's Modified Eagle Medium
DNA	Deoxyribonucleic Acid
E	Embryonic Day
Ecm1	Extra Cellular Matrix Protein 1
Emx2	Empty Spiracles Homeobox 2
Erg	ETS-related Gene
ESR1	Estrogen Receptor 1
Eya1	Eye Absent Homolog 1
FACS	Fluorescence Activated Cell Sorting

FasI	Fas Ligand
Fat4	FAT atypical cadherin 4
FBS	Fetal Bovine Serum
Fgf8	Fibroblast Growth Factor 8
Flk1	Fetal Liver Kinase 1
FoxD1	Forkhead Box D1
g	Glomerulus
Gata3	Gata Binding Protein 3
GDNF	Glial cell line Derived Neurotrophic Factor
GFP	Green Fluorescent Protein
GFR- α 1	GDNF receptor α 1
GOF	Gain of Function
GSK3	Glycogen Synthase Kinase 3
HRP	Horseradish Peroxidase
IF	Immunofluorescence
IgG	Immunoglobulin G
IHC	Immuno Histochemistry
ISH	<i>In Situ</i> Hybridization
Jag1	Jagged1
k	Kidney
Kcni1	Kv Channel Interacting Protein 1
Lhx1	LIM Homeobox 1
LoxP	Locus of X(cross)-over in P1
LRP5/6	Lipoprotein Receptor-related Proteins 5/6
MED	Mediator
Meis1	Meis Homeobox 1
MET	Mesenchymal-to-Epithelial Transition
MM	Metanephric Mesenchyme
mRNA	Messenger Ribonucleic Acid
ms	Medullary Stroma
Msx2	Msh Homeobox 2
MULAN	Multiple Sequence Local Alignment and Visualization
Mybl2	Myb Related Protein B
NCAM	Neural Cell Adhesion Molecule
NZ	Nephrogenic Zone
p300/CBP	p300 CREB Binding Protein
Pax2	Paired Box 2
Pax8	Paired Box 8

PBS	Phosphate-Buffered Saline
Pbx1	Pre-B-Cell Leukemia Homeobox 1
PCR	Polymerase Chain Reaction
PDGFR- β	Platelet-Derived Growth Factor Receptor - β
PECAM	Platelet Endothelial Cell Adhesion Molecule
PFA	Paraformaldehyde
Pla2g7	Phospholipase A2, Group 7
Plgf1	Placenta Growth Factor 1
PN	Post Natal Day
qRT-PCR	Quantitative Real-Time Polymerase Chain Reaction
RA	Retinoic Acid
Raldh2	Retinaldehyde Dehydrogenase 2
Rar α	Retinoic Acid Receptor α
Rar β 2	Retinoic Acid Receptor β 2
rbc	Red Blood Cells
rc	Renal Capsule
Ret	Receptor Tyrosine Kinase
Rp	Renal Papilla
rv	Renal Vesicle
s	Stroma
SDS-PAGE	Sodium Dodecyl Sulfate Polyacrylamide gel electrophoresis
Sfrp1	Secreted Frizzled Related Protein 1
Six2	Six Homeobox 2
Snca	Synuclein alpha
t	Tubule
TBX5	T-Box 5
TCF/Lef	T-Cell Factor/ Lymphoid Enhancer Factor
TCF2	Transcription factor 2
TCF21	Transcription Factor 21
TENT	Tris EDTA NaCl Tween
TGF- β 1	Transforming Growth Factor β 1
TN-C	Tenascin-C
TUNEL	Terminal Deoxynucleotidyl Transferase dUTP Nick End Labelling
u	Ureter
ub	Ureteric bud
VEGF α	Vascular Endothelial Growth Factor α
VSMC	Vascular Smooth Muscle Cells
Wnt11	Wingless type 11

Wnt4	Wingless type 4
Wnt7b	Wingless type 7b
Wnt9b	Wingless type 9b
WT	Wild-Type
WT1	Wilms' Tumour 1
Xtwn	Xenopus Homeobox gene Twin
YAP	Yes-Associated Protein
α -SMA	α -Smooth Muscle Actin

CHAPTER 1 - INTRODUCTION

1.1 Chronic Kidney Disease in Children

Chronic kidney disease (CKD) is defined as a progressive decline in renal function. It affects more than 18.5-58.3 per million children worldwide (Gulati, Mittal et al. 1999) and more than 5500 children in North America (Seikaly, Ho et al. 2003). Although these numbers are considerably lower than in adult patients (>10% of the population worldwide), the prevalence of children diagnosed with CKD has steadily increased over the last two decades and is projected to triple over the next 20 years due to the growing population worldwide (Collins, Foley et al. 2012). The leading cause of CKD in neonates and children is *renal dysplasia* (Wingen, Fabian-Bach et al. 1997), which is classically defined as a congenital kidney malformation, resulting in poor renal function (Woolf, Price et al. 2004). Patients born with severe bilateral renal dysplasia develop complications early in life and require renal replacement therapy and dialysis. However, milder cases of renal dysplasia (unilateral and/or focal) are often never properly diagnosed and can lead to complications, such as cardiovascular disease and renal insufficiency, later in life or after kidney injury. Since our understanding of congenital renal malformations is very limited, we currently do not have the tools to identify patients with milder cases of renal dysplasia and at risk of developing kidney disease.

Several studies have highlighted a strong genetic association with the development of renal dysplasia (Woolf, Price et al. 2004, Jain, Suarez et al. 2007, Winyard and Chitty 2008), yet the mechanisms that promote abnormal kidney formation are not known. Thus, developing a better understanding of the underlying causes of *renal dysplasia* (i.e. genetic, environmental, epigenetic) will help identify patients at risk of

developing kidney disease, allow early treatment to prevent progression of CKD in patients at risk, and contribute foundational knowledge for the development of new treatment targets and strategies for children living with renal dysplasia.

1.2 Kidney Anatomy and Physiology

1.2.1 Gross Anatomy and Physiology of the Kidney

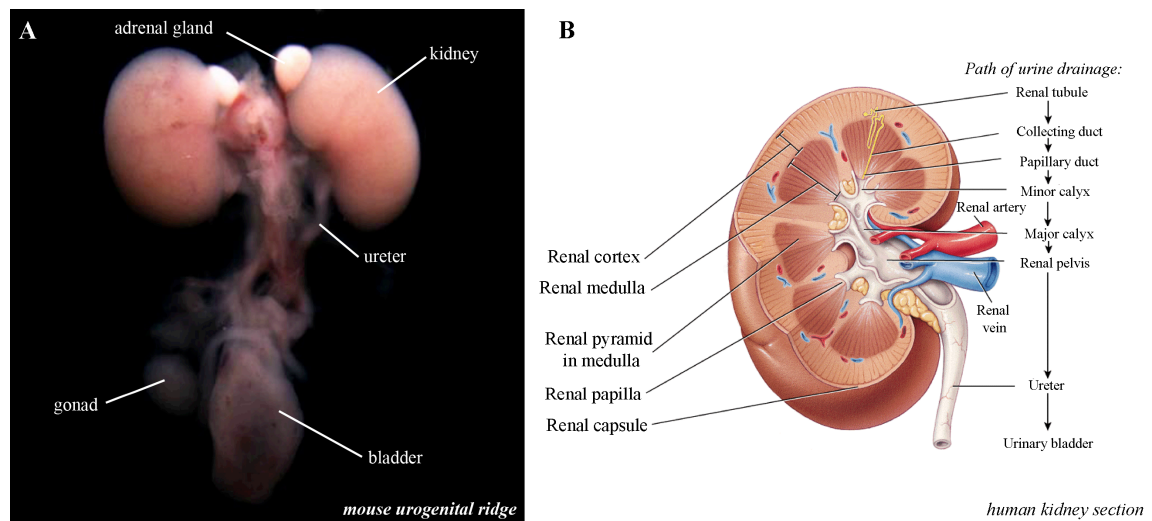
The mammalian urogenital system is comprised of the kidneys, the ureters, the bladder, and the urethra (Figure 1.1A). It is a multi-functional system involved in filtering blood by eliminating waste and balancing pH and ionic composition of body fluids. The kidneys are “bean-shaped” organs that sit on either side of the vertebral column in the posterior abdominal wall. They receive 20% of the cardiac output via the renal artery. In the kidney, blood is filtered to produce urine that is transported to the bladder via the ureter. Once filtered, blood exits the kidney via the renal vein (Figure 1.1B) (Hallgrimsson et al, 2003).

A transparent sheet of fibrous connective tissue, termed the renal capsule, surrounds the kidney to protect against trauma, help maintain the shape of the kidney, and regulate renal interstitial pressure (Slegers and Moons 1985)(Hallgrimsson et al, 2003). Within the kidney proper, three distinct regions can be observed: 1) the renal cortex, 2) the medulla, and 3) the renal pelvis. During the process of filtration, a filtrate is produced within renal cortex. This filtrate is transformed into urine in small passageways, termed renal tubules. Urine is then emptied into larger tubules, termed collecting ducts. These ducts extend within the medullary region directly below the renal cortex. The medulla is divided into inverted renal pyramids, with the base facing the cortical region and the tip facing the renal pelvis. The tips of these pyramids merge into minor calyces to form the renal papilla. Urine drains from the collecting ducts into these minor calyces and is transported into a bigger passageway called the major calyx. These major calyces merge

to form a passageway called the renal pelvis, which is connected to the ureter. Urine then exits the kidney via the ureter and is excreted into the bladder.

Developmental anomalies in the orientation of these three distinct regions (cortex, medulla, and renal pelvis) greatly affect kidney function and urinary flow, resulting in several complications, such as tubular cyst formation and hydronephrosis, defined as the swelling of the kidney due to urine build-up. In more severe cases, these complications can lead to chronic kidney disease and kidney failure while milder cases lead to cardiovascular complications, such as hypertension.

Figure 1.1 – Gross anatomy and basic structure of the kidney



Gross anatomy and basic structure of the kidney: (A) – Mouse urogenital ridge at post-natal (PN) day 0. The urogenital ridge is composed of two kidneys connected to the ureters and bladder. The adrenal glands sit atop the kidneys, and the gonads are found on either side of the bladder. (B) – Cross section of the human kidney. The kidney is divided into three distinct regions: 1) the renal cortex, 2) the renal medulla, and 3) the renal pelvis. Blood enters the kidney via the renal artery and is filtered in the renal cortex. Filtered blood exits the kidney via the renal vein. The path of urine drainage following filtration is outlined in figure 1B (adapted from Fox I.S., 2008)

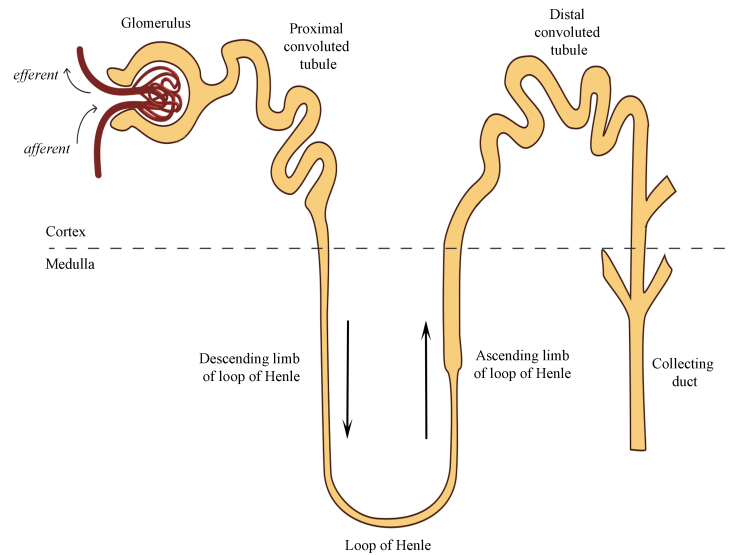
1.2.2 Anatomy and function of the nephron

The functional unit of the kidney is called the nephron. It is made up of two main parts: 1) a renal corpuscle located in the renal cortex and 2) tubules that extend within the medulla alongside the collecting ducts. The renal corpuscle consists of a glomerular tuft and fenestrated capillary network enclosed by a Bowman's capsule. Blood enters the Bowman's capsule through renal arterioles and is filtered by a filtration barrier made up of fenestrated endothelial cells, interdigitated podocytes, and a glomerular basement membrane. Ultrafiltrate is forced through the filtration barrier into the Bowman's space. The lumen of the Bowman's space is directly connected with the renal tubule. The renal tubule is divided into three sections: 1) the proximal tubule, 2) the loop of Henle, and 3) the distal tubule. The ultrafiltrate exits the Bowman's space and travels through the different sections of the renal tubule where its composition is modified into urine, by a process of water reabsorption and salt excretion. The distal tubule is connected to the collecting duct. Urine drains into the collecting ducts and travels to the medulla (Figure 1.2).

The nephron plays a crucial role in the proper functioning of the kidney. Subtle abnormalities in the development of the different sections of the nephron and collecting ducts can affect filtration and reabsorption. Similarly, nephron endowment is directly correlated with kidney function and efficacy (Hoy, Hughson et al. 2005). The human adult kidney contains approximately 800,000 to 1,200,000 nephrons. These units do not regenerate following injury, which means patients born with a lower number of nephrons are predisposed to developing chronic kidney disease following injury, and can then

develop other complications associated with kidney disease such as hypertension (Brenner, Garcia et al. 1988, Kett and Bertram 2004).

Figure 1.2 - Basic structure of the nephron



Basic structure of the nephron: Cartoon diagram outlining the regions of the mammalian nephron. Arrows indicate the direction of the filtrate as it moves through the nephron and into the collecting duct (adapted from McMaster Pathophysiology review, Sultan Chaudhry).

1.3 Kidney Development

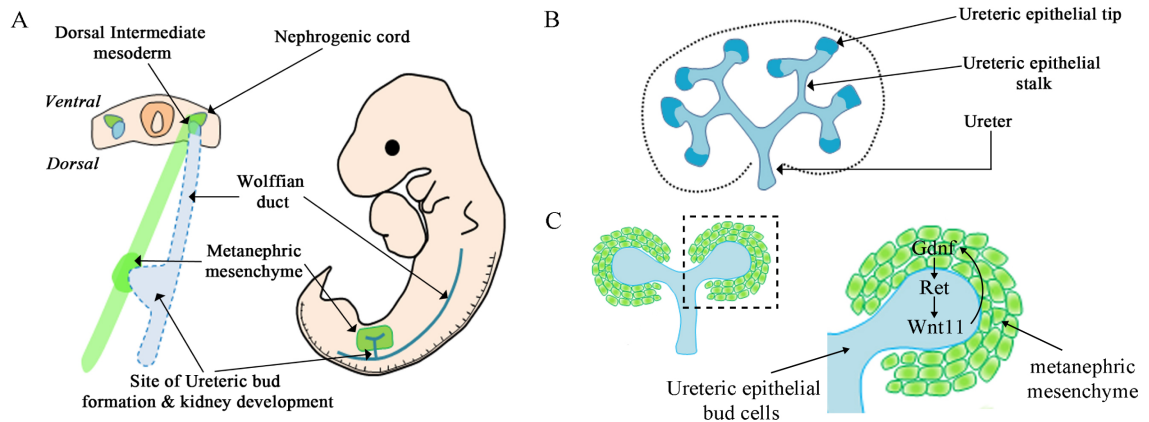
Formation of the mammalian kidney relies on two developmental processes: 1) branching morphogenesis, which gives rise to the collecting ducts and 2) nephrogenesis, which is the process of nephron formation. Proper formation of these two units relies on tightly regulated interactions between three cell populations: 1) the ureteric epithelium, the metanephric mesenchyme, and the renal stroma. Disrupted communication between these cell populations results in abnormal collecting duct and nephron formation and negatively impact nephron endowment.

1.3.1 Branching Morphogenesis

Kidney development is initiated at around embryonic day (E) 9.5 in the mouse and 4 weeks gestation in humans when a tube of epithelial cells, termed the Wolffian duct, emerges from the intermediate mesoderm and migrates caudally toward the urogenital sinus. At E10.5 in the mouse and 5 weeks gestation in humans, the caudal portion of the Wolffian duct forms an outgrowth called the ureteric bud that migrates into an adjacent pool of specified mesenchymal cells, called the metanephric mesenchyme (Figure 1.3A). Signals from the metanephric mesenchyme, such as the secreted factor GDNF, induce the ureteric bud to undergo a first branching event to form a T-shaped branch (Figure 1.3A), at around E11.5 in the mouse (Saxen and Sariola 1987). Each ureteric bud tip subsequently undergoes rounds of reiterative branching, bifurcation, elongation, and differentiation to form the collecting duct system (Figure 1.3B). Several factors are essential to ensure proper reiterative branching of the ureteric epithelium. However, for

the purpose of this study we will focus solely on GDNF, Ret, and Wnt11. Excellent reviews on signaling molecules involved in branching and elongation of the ureteric epithelium are available elsewhere (Costantini and Kopan 2010, Little and McMahon 2012).

The GDNF/Ret/Wnt11 feedback loop is central to the initial formation of the ureteric bud tip, at E10.5, and for subsequent branching events. Mesenchymal factor GDNF signals to the adjacent ureteric epithelial cells to activate co-receptors GFR- α 1 and receptor tyrosine kinase Ret and promote cell proliferation and movement (Takahashi 2001). In response to GDNF, the Ret receptor activates the expression of Wnt11, a secreted factor expressed and secreted by the ureteric bud tip cells. Wnt11 signals to the metanephric mesenchymal cells and increases the transcriptional activation of GDNF, thereby creating a positive feedback loop (Majumdar, Vainio et al. 2003). Targeted deletion of these factors in mice results in severely disrupted branching morphogenesis and renal hypoplasia (Majumdar, Vainio et al. 2003). These studies highlight the central role of the GDNF/Ret/Wnt11 feedback loop and the importance of proper epithelial-mesenchymal communication to branching morphogenesis.

Figure 1.3 - Branching morphogenesis and the Gdnf/Ret Signaling

Branching morphogenesis and the Gdnf/Ret signaling: (A) – At E10.5, a ureteric bud form off the Wolffian duct and migrates into a pool of undifferentiated metanephric mesenchyme. At E11.5, the ureteric bud undergoes a first round a branching to form a T-shaped branch. (B) – The ureteric bud tip undergoes rounds of branching, while the ureteric epithelial stalk elongates to form branches. (C) – The Gdnf/Ret/Wnt11 signaling controls the initial ureteric budding and branching morphogenesis. Gdnf is expressed and secreted by the metanephric mesenchyme and signals to the ureteric bud tip cells to activate the Ret receptor. Activation of the Ret receptor triggers the transcription of the Wnt11 ligand, which in turn signals to the metanephric mesenchyme to increase Gdnf expression, thereby creating a positive feedback loop (adapted from (Boivin, Sarin et al. 2015)).

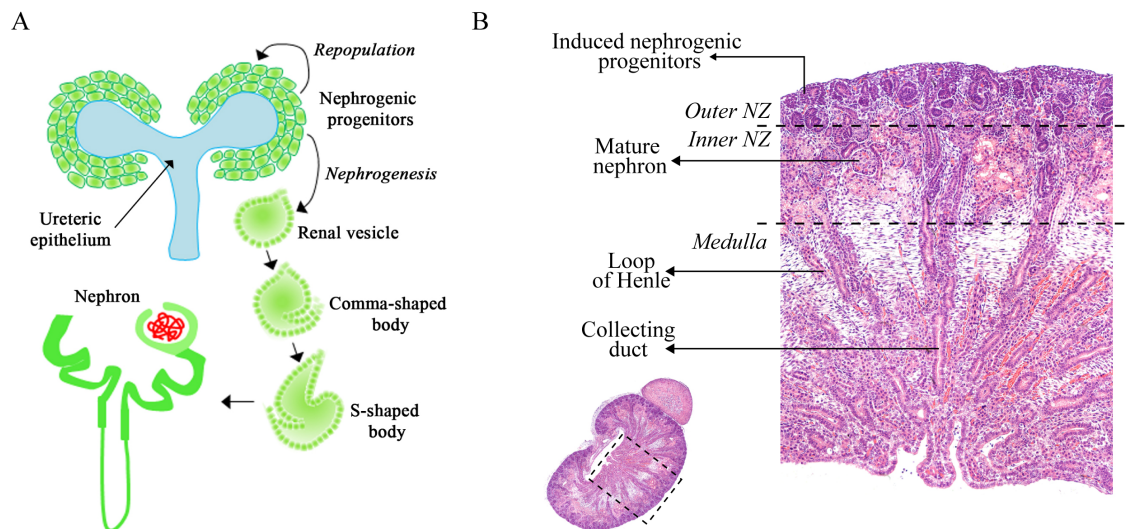
1.3.2 Nephrogenesis

Shortly after the initial formation of the ureteric outgrowth, the ureteric epithelial cells induce the metanephric mesenchyme to tightly cluster around the ureteric bud tips. These condensed mesenchymal cells are known as the nephrogenic progenitors. Signals from the ureteric bud tip cells instruct these nephrogenic progenitors to either undergo proliferation to repopulate the condensed mesenchyme population or to differentiate into epithelial cells (Karner, Das et al. 2011). Excellent reviews are available for more information on the various factors modulating the balance between proliferation and differentiation of the nephrogenic progenitors (Costantini and Kopan 2010, Little and McMahon 2012). However, for the purpose of these studies, we will focus on Wnt9b. Wnt9b is a key ureteric epithelial marker that signals to the nephrogenic progenitors to activate the Wnt/ β -catenin pathway and promote epithelial differentiation (Carroll, Park et al. 2005, Karner, Das et al. 2011). The nephrogenic progenitors undergo a series of morphological changes via mesenchymal-to-epithelial transition (i.e. renal vesicles, comma-shaped bodies, s-shaped bodies) (Figure 1.4A) to form the different structures of the mature nephron. This process gives rise to approximately 10,000 nephrons in the mouse (Cebrian, Borodo et al. 2004) and 800,000 to 1.2 million nephrons in humans (Saxen and Sariola 1987, Cebrian, Borodo et al. 2004, Cain, Di Giovanni et al. 2010). Wnt9b deficient mice exhibit severely hypoplastic kidneys and no mature nephrons, due to the absence of nephron induction (Carroll, Park et al. 2005). This demonstrates the importance of proper communication between the ureteric epithelium and the

metanephric mesenchyme. Disruptions between the epithelium and mesenchyme affect nephrogenesis and lead to a lower nephron endowment.

The process of nephron formation takes place in two distinct regions in the renal cortex: the outer nephrogenic zone where nephrogenesis is initiated and the inner nephrogenic zone where mature nephrons reside. The tubules and loops of Henle of mature nephrons extend within the inner part of the kidney to form the medulla. Glomeruli are never observed in the medullary region (Figure 1.4B).

Figure 1.4 - Overview of nephrogenesis in the developing kidney



Overview of nephrogenesis in the developing kidney: (A) – Signals from the ureteric epithelium induce the metanephric mesenchyme to condense around the ureteric bud tip. These cells are defined as nephrogenic progenitors. These progenitor cells can either repopulate the mesenchyme population or undergo nephrogenesis by mesenchymal-to-epithelial transition. Once induced, the mesenchymal cells undergo morphological changes (Renal vesicle, comma-shaped, and s-shaped body) to form the mature nephron. (B) – The process of nephrogenesis takes place in the outer nephrogenic zone (NZ) of the renal cortex, while mature nephrons lie within the inner NZ of the renal cortex. The loops of henle of the mature kidneys and collecting ducts extend within the medulla. Mature

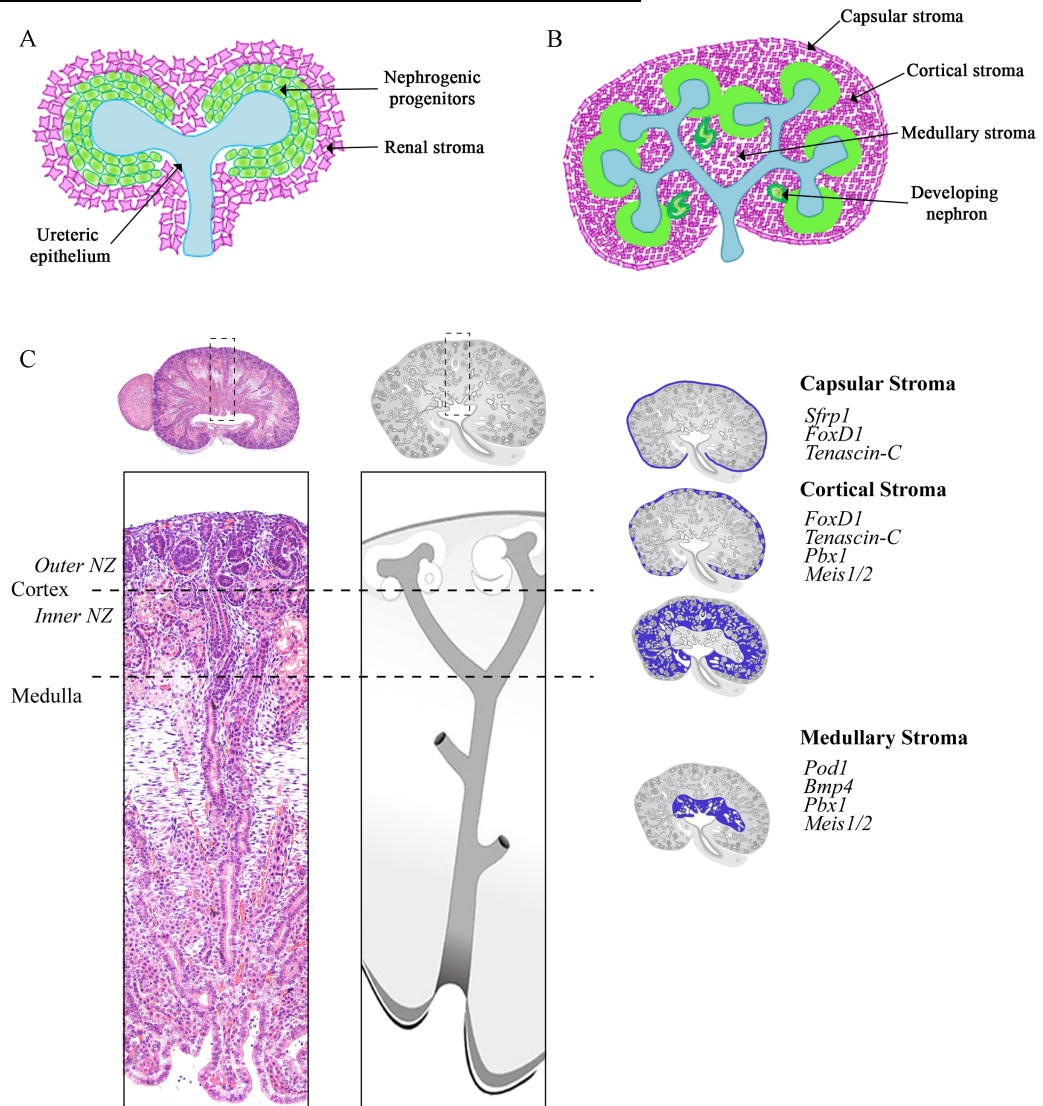
nephrons are never observed within the medulla (adapted from (Boivin, Sarin et al. 2015)).

1.4 The Renal Stroma

As the ureteric bud invades the undifferentiated pool of metanephric mesenchyme, a third cell population, termed the renal stroma, is observed surrounding the condensed mesenchyme (Figure 1.5A). The earliest marker of renal stroma is FoxD1, a member of the forkhead family of transcription factors. It marks a population of self-renewing multipotent stromal progenitors that gives rise to all stromal lineages in the kidney (Kobayashi, Mugford et al. 2014). FoxD1 is weakly expressed in the metanephric mesenchyme at E10.5 upon invasion of the ureteric bud. By E11.5, FoxD1 is strongly expressed in all stromal progenitors surrounding the condensed mesenchyme (Figure 1.5A)(Hatini, Huh et al. 1996, Kobayashi, Mugford et al. 2014). The developmental origin of stromal progenitors is not well understood. Similar to epithelial and mesenchymal progenitors in the developing kidney, stromal progenitors are thought to originate from a common pool of undifferentiated *Osr1*⁺ intermediate mesoderm (Mugford, Sipila et al. 2008). Lineage tracing studies have demonstrated that two molecularly distinct *Six2*⁺ and *FoxD1*⁺ cell populations are present within the *Osr1*⁺ cell pool prior to the onset of kidney development and ureteric bud invasion (Mugford, Sipila et al. 2008). However, the factors that instruct the *FoxD1*⁺ population are not known.

As the kidney develops, the *FoxD1*⁺ stromal progenitors integrate the nephrogenic zone surrounding the developing nephrons and collecting ducts. These stromal progenitors give rise to all stromal lineages in the mature kidney. By E14.5, three molecularly distinct stromal populations are observed: the capsular, cortical, and medullary stroma (Figure 1.5B)(Levinson, Batourina et al. 2005). The renal capsule

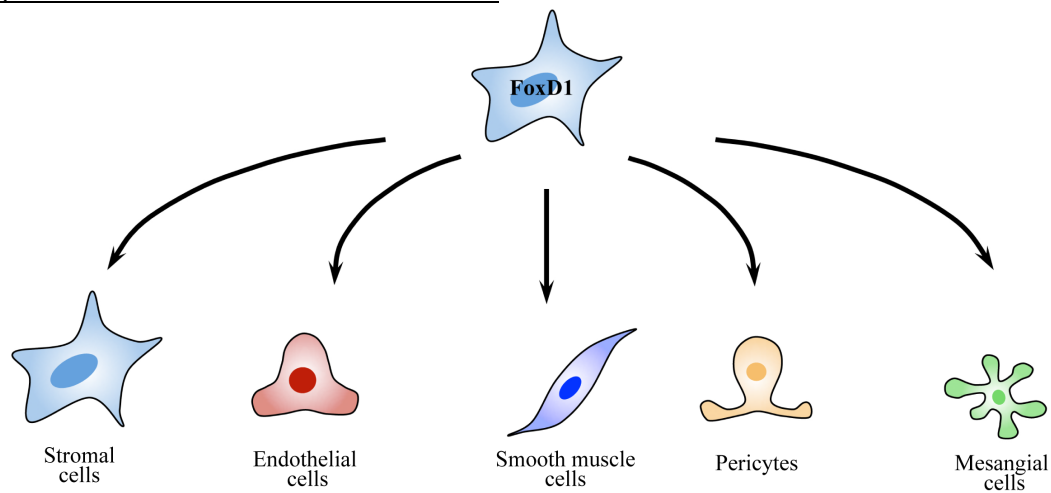
consists of a continuous layer of capsular stromal cells that strongly express the secreted frizzled-related protein Sfrp1 (Levinson, Batourina et al. 2005). Directly below the renal capsule is a population of cortical stromal cells found between the developing nephrogenic structures. Capsular and cortical stroma cells both strongly express FoxD1 and the glycoprotein Tenascin-C throughout kidney development (Figure 1.5C). Deeper into the kidney, below the nephrogenic zone, is the medullary stroma surrounding the collecting ducts, extended tubules, and loops of Henle (Figure 1.5C). These medullary stromal cells strongly express the transcription factor Pod1 (also known as TCF21) and secreted growth factor Bmp4 (Cui, Schwartz et al. 2003, Levinson, Batourina et al. 2005). Other more general factors, such as transcription factor Pbx1 and its binding partner Meis1, mark all stromal cells (capsular, cortical, and medullary) of the developing kidney (Schnabel, Godin et al. 2003, Hum, Rymer et al. 2014)(Figure 1.5C).

Figure 1.5 - Development of the stromal populations

Development of the stromal populations: (A) – Shortly after the formation of the T-shaped branch (blue), a third population of fibroblast cells is observed surrounding the nephrogenic progenitors (green). These cells are the stromal progenitors (pink). (B) – As the kidney develops, the renal stroma subdivides into three molecularly distinct populations: the capsular stroma, the cortical stroma, and the medullary stroma. (C) – Sagittal section of a mouse kidney outlining the three stromal compartments and their main stromal markers (picture adapted from the GudMap Atlas website).

Stromal progenitors also give rise to various non-epithelial cells in the kidney, such as endothelial cells, mesangial cells, smooth muscle cells, and pericytes (Figure 1.6)(Sims-Lucas, Schaefer et al. 2013, Boyle, Liu et al. 2014, Kobayashi, Mugford et al. 2014, Sequeira-Lopez, Lin et al. 2015). However, the factors that control stromal cell differentiation are not well defined.

Figure 1.6 - Stromal cell differentiation



Stromal cell differentiation: Stromal cells can differentiate into capsular, cortical, and medullary stromal cells, but they also give rise to various cell types essential for vascular morphogenesis, such as endothelial cells, smooth muscle cells, pericytes, and mesangial cells (adapted from (Li, Hartwig et al. 2014)).

1.4.1 The functional role of the renal stroma

The renal stroma is a population of matrix-producing fibroblast cells. It was traditionally thought to act purely as a supportive cell population for the developing nephrogenic structures of the kidney. However, gene ablation studies have demonstrated important roles for stromal cells in the control of stromal differentiation, nephrogenesis, and branching morphogenesis.

Cortical stromal cells in the nephrogenic zone play an important role in nephron differentiation. The process of nephrogenesis relies on a tightly regulated balance between proliferation and differentiation of the nephron progenitors, which is primarily regulated by the ureteric epithelial factor Wnt9b. Interestingly, the ablation of all stromal progenitors results in stalled nephrogenesis and increased proliferation of the nephron progenitors (Das, Tanigawa et al. 2013, Hum, Rymer et al. 2014), suggesting stromal cells modulate communication between the epithelium and mesenchyme. Several cortical stromal factors have recently been shown to regulate the nephron progenitors. Fat4, an atypical cadherin expressed in cortical stromal cells, forms direct cell-cell interactions with the adjacent nephron progenitors to regulate proliferation via the hippo signaling effectors (Das, Tanigawa et al. 2013, Bagherie-Lachidan, Reginensi et al. 2015). Similarly, Decorin, a proteoglycan protein expressed in the cortical stroma signals to the nephron progenitors to repress Bmp-Smad signaling and prevent nephron differentiation (Fetting, Guay et al. 2014). The deletion of FoxD1 results in a similar expansion of the nephron progenitors, suggesting FoxD1 controls the expression of several stromal factors

important for nephron differentiation. However, the transcriptional activity of FoxD1 in stromal cells has not been investigated.

Stromal cells also play a critical role in the formation and regulation of the collecting duct system. Retinoic acid (RA) controls *Ret* expression in epithelial cells and is essential for proper branching morphogenesis. The cortical stroma strongly expresses *Raldh2*, the enzyme responsible for RA synthesis (Rosselot, Spraggon et al. 2010). Additionally, several RA receptors (*Rarβ2* and *Rarα*) are expressed in stromal cells (Mendelsohn, Batourina et al. 1999, Batourina, Gim et al. 2001) and ureteric bud cells (Schmidt-Ott, Chen et al. 2006). The deletion of these factors results in reduced *Ret* expression and impaired branching morphogenesis, demonstrating critical communication between stromal and ureteric epithelial cells for branching morphogenesis. Medullary stromal markers are also thought to be essential for branching morphogenesis. The ablation of *Pod1* results in the mis-expression of the *Ret* receptor and reduced branching morphogenesis, leading to medullary hypoplasia (lack of medulla) (Quaggin, Schwartz et al. 1999, Cui, Schwartz et al. 2003). Similarly, deletion of *Pbx1* results in severe branching defects and renal dysplasia (Schnabel, Godin et al. 2003). Combined these studies demonstrate that stromal cells do not simply act as a supportive framework for the developing units of the kidney, but can communicate with the metanephric mesenchyme and the ureteric epithelium to modulate nephrogenesis and branching morphogenesis.

Stromal cells also play a critical role in vascular development. Fate tracing studies have demonstrated that stromal progenitors give rise to various supportive cells essential for vascular development, such as vascular smooth muscle cells, mesangial cells, and

pericytes (Figure 1.6)(Humphreys, Lin et al. 2010, Kobayashi, Mugford et al. 2014).

Furthermore, a subset of stromal cells can differentiate into endothelial cells to contribute to peritubular capillary formation (Sims-Lucas, Schaefer et al. 2013). Ablation of stromal

progenitors leads to severe vascular morphogenesis defects (Hum et al. 2014) and

abnormal development of vascular smooth muscle cells (Sequeira-Lopez, Lin et al. 2015).

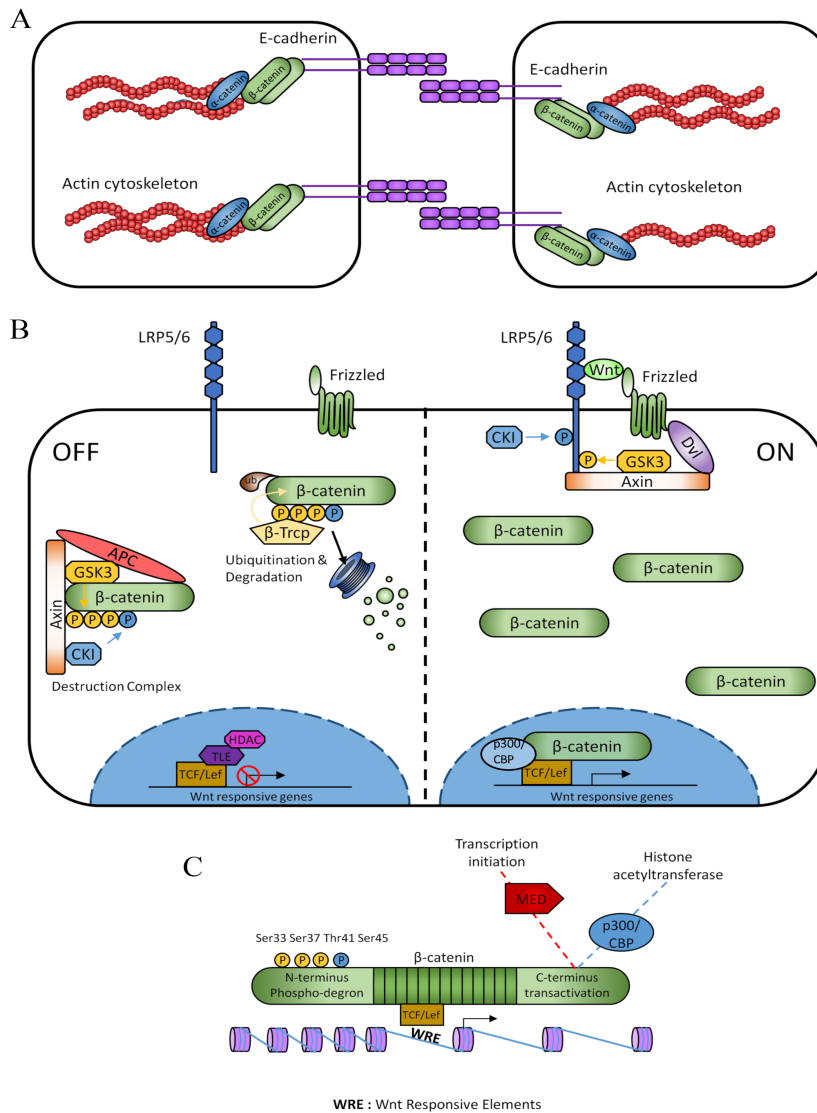
However, the factors that promote stromal cell differentiation are not well characterized.

1.5 β -catenin

1.5.1 Junctional and Wnt-dependent roles for β -catenin

β -catenin is an evolutionarily conserved multifunctional protein with various intra-cellular functions (Heuberger and Birchmeier 2010). At the cell membrane, β -catenin binds to the intracellular domain of E-cadherin to form adherens junctions. It forms a complex with α -catenin to link the cytoskeleton with E-cadherin. This complex is essential for cell movements during morphogenesis (Figure 1.7A)(Gumbiner 2000, Gumbiner 2005). Traditionally, β -catenin has been characterized as the central effector of the Wnt/ β -catenin signaling pathway (Clevers and Nusse 2012). In the absence of a Wnt ligand, β -catenin is targeted for degradation by a destruction complex that consists of axin, adenomatosis polyposis coli (Apc), glycogen synthase kinase 3 (Gsk3), and Casein Kinase 1 (CK1). This destruction complex binds to β -catenin and phosphorylates serine/threonine residues within the N-terminal domain (GSK3 phosphorylates Serine33, Serine37, and Threonine41, whereas CK1 phosphorylates Serine45) leading to its ubiquitination and proteosomal destruction (Figure 1.7B & C). In this inactive state, Wnt downstream target genes are repressed by the transcriptional co-repressor transducin-like enhancer (TLE) protein. The TLE protein binds TCF/Lef DNA-bound transcription factors and recruits histone deacetylases (HDAC). This leads to deacetylation of H3 and H4 histone tails, resulting in a silenced chromatin structure and gene silencing. Upon binding of a Wnt ligand to a Frizzled (Fz) receptor and LRP5/6 co-receptor, the intracellular domain of the Fz receptor recruits a protein called Disheveled (Dsh) to the cell membrane. The mechanism of action of Dsh is not clear, however it sequesters the

destruction complex to the cell membrane by interacting with Axin via shared DIX domains. This results in a disassembly of the destruction complex, thereby preventing phosphorylation of β -catenin and leading to its stabilization in the cytoplasm (Figure 1.7B). The accumulation of β -catenin in the cytoplasm allows it to translocate to the nucleus where it interacts with TCF/Lef transcription factors, inducing the dissociation of co-repressors and promoting the recruitment of co-activators (Zeng, Huang et al. 2008, MacDonald, Tamai et al. 2009)(Figure 1.7B). The C-terminus domain of β -catenin serves as a platform to recruit transcriptional co-activators involved in chromatin remodeling, such as the histone acetyltransferase p300/CBP, and transcription initiation such as the Mediator (MED) protein (Figure 1.7C)(MacDonald, Tamai et al, 2009). Once recruited to the TCF/ β -catenin complex, MED promotes the recruitment of the RNA polymerase II complex to the transcription initiation site. This transcription complex then regulates the expression of genes involved in cell proliferation, cell fate determination, and differentiation (MacDonald , Tamai et al, 2009, Logan and Nusse 2004).

Figure 1.7 – Junctional and Wnt-dependent roles for β -catenin

Junctional and Wnt-dependent roles for β -catenin – (A) Junctional role for β -catenin. β -catenin localizes to the cell membrane by interacting with the intracellular domain of E-cadherin and the actin cytoskeleton. (B) – Wnt-dependent role for β -catenin. In the absence of a Wnt ligand (left) β -catenin is targeted for degradation by a destruction complex (Apc, Axin, Gsk-3). In the presence of a Wnt ligand (right), the destruction complex is sequestered to the cell membrane. This prevents degradation of β -catenin and results in its cytoplasmic stabilization. β -catenin can then freely translocate to the nucleus, where it interacts with transcription factors (Tcf/Lef) to regulate gene expression. (C) Linear depiction of β -catenin. The β -catenin protein is comprised of an N-terminal phospho-degron, a central armadillo repeat domain that binds TCF/Lef and E-cadherin, and a C-terminal transactivation domain involved in the recruitment of co-activators, such as MED and p300/CBP.

1.5.2 Wnt-independent transcriptional roles for β -catenin

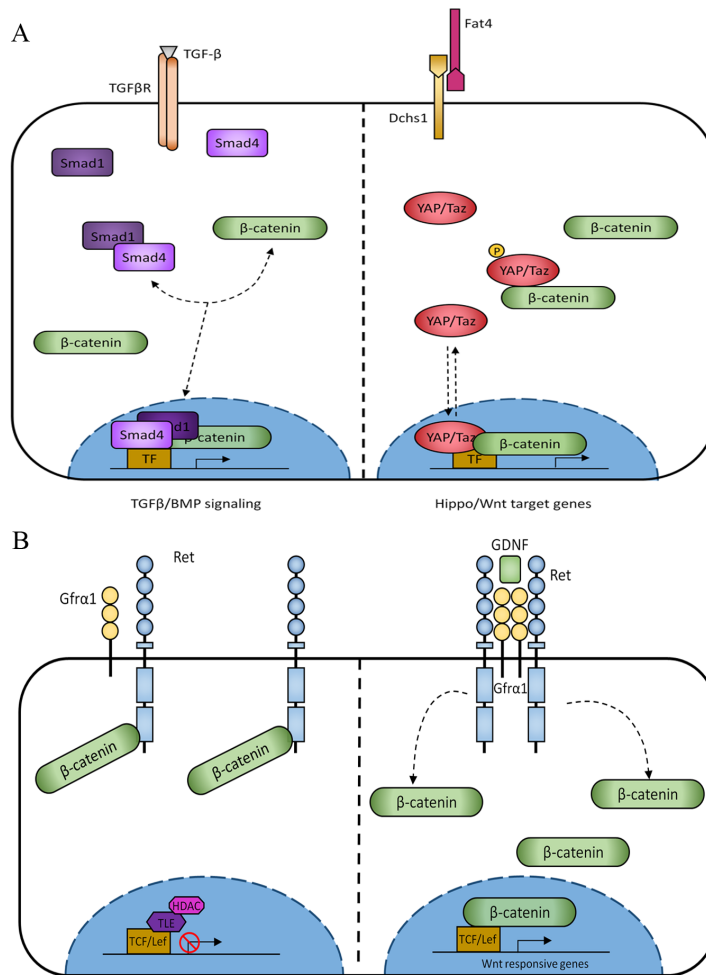
While traditionally involved in the Wnt/ β -catenin signaling pathway, β -catenin has been shown to interact with other signaling pathways. In the context of kidney development, β -catenin interacts with Smad1 and Smad4 to form a transcription complex (Figure 1.8A)(Hu, Piscione et al. 2003) that regulates the expression of genes important for cell proliferation and differentiation, such as c-myc (Hu and Rosenblum 2005). Similarly, β -catenin also interacts with Smad proteins in other developing organs to control the expression of *Xtwn* and *Msx2* and control cell fate determination (Labbe, Letamendia et al. 2000, Hussein, Duff et al. 2003).

Recent studies have demonstrated an interaction between β -catenin and the hippo signaling effector Yap in the developing heart. β -catenin forms a transcriptional complex with Yap to control cardiomyocyte proliferation (Heallen, Zhang et al. 2011). Other studies have demonstrated that β -catenin forms a transcription complex with YAP, Yes, and TBX5 in several human cancer cell lines to promote proliferation (Rosenbluh, Nijhawan et al. 2012). While there is no evidence for this interaction in the developing kidney, deletion of YAP specifically in the condensed mesenchyme results in a down-regulation of β -catenin target genes such as *Amph*, *Tafa5*, *Cited1*, and *Pla2g7*, leading to reduced proliferation (Reginensi, Scott et al. 2013). This suggests β -catenin and the Hippo signaling effectors interact to promote proliferation of the condensed mesenchyme.

β -catenin also binds to the intracellular domain of the Ret receptor in the ureteric epithelium. Upon activation of the Ret receptor by Gdnf, β -catenin is released from the Ret receptor and translocates to the nucleus to regulate the expression of genes important

for kidney development (Figure 1.8B) (Sarin, Boivin et al. 2014). This interaction is also observed in models of thyroid carcinomas (Gujral, van Veelen et al. 2008). Together, these studies demonstrate that β -catenin is a promiscuous protein that interacts with several transcription factors and effectors to regulate cell proliferation and differentiation.

Figure 1.8 – Wnt-independent transcriptional roles for β -catenin



Wnt-independent transcriptional roles for β -catenin - (A) β -catenin interacts with members of the TGF- β /Bmp signaling (Smad1/4) and hippo signaling (β -catenin/YAP). (B) β -catenin acts downstream of the Ret receptor in response to the Gdnf ligand in ureteric epithelial cells.

1.6 β -catenin in the Developing Kidney

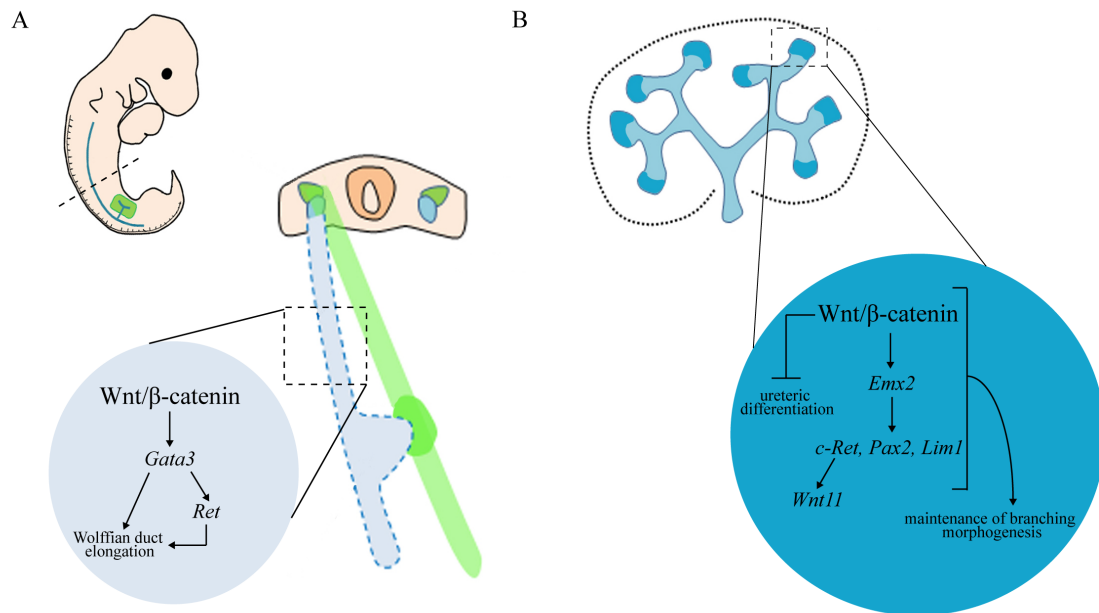
During mouse and human kidney development, β -catenin demonstrates a distinct spatial and temporal expression pattern in epithelial, mesenchymal, and stromal cells (Bridgewater, Cox et al. 2008, Sarin, Boivin et al. 2014). Analysis of transgenic Tcf/Lef reporter mice suggests β -catenin is transcriptionally active in the Wolffian duct, ureteric epithelium, condensed mesenchyme, and renal stroma (Iglesias, Hueber et al. 2007, Bridgewater, Cox et al. 2008, Yu, Carroll et al. 2009).

1.6.1 β -catenin in the ureteric epithelium

Important roles for β -catenin have been established in the Wolffian duct and the ureteric epithelium. Prior to metanephric development, β -catenin controls proliferation and extension of the Wolffian duct by maintaining the expression of transcription factor *Gata3* (Figure 1.9A). The deletion of β -catenin from the Wolffian duct results in a loss of *Gata3* expression and failure to initiate normal ureteric budding, which ultimately leads to renal agenesis (Grote, Boualia et al. 2008). Once metanephric development is initiated, β -catenin plays a critical role in regulating and maintaining the ureteric bud cell tip identity. During branching morphogenesis, the ureteric epithelium is divided into molecularly distinct ureteric bud tip and stalk cell populations (Bridgewater and Rosenblum 2009). The deletion of β -catenin specifically in epithelial cells results in a loss of ureteric bud tip associated genes (Bridgewater, Cox et al. 2008) and an activation of genes associated with fully differentiated epithelial stalk cells (Marose, Merkel et al. 2008). Furthermore, a loss of β -catenin in the ureteric epithelium results in reduced expression of *Emx2*, a transcription factor important for the maintenance of ureteric bud

tip cells (Bridgewater, Cox et al. 2008). The loss of *Emx2* in those cells results in reduced expression of branching factors *Ret* and *Wnt11*, which leads to branching morphogenesis defects and severe renal hypoplasia (Bridgewater, Cox et al. 2008, Marose, Merkel et al. 2008)(Figure 1.9B). Together, these studies demonstrate β -catenin in the ureteric epithelium controls branching morphogenesis by controlling a hierarchy of key branching genes and maintaining ureteric bud tip identity.

Figure 1.9 – β -catenin in the ureteric epithelium



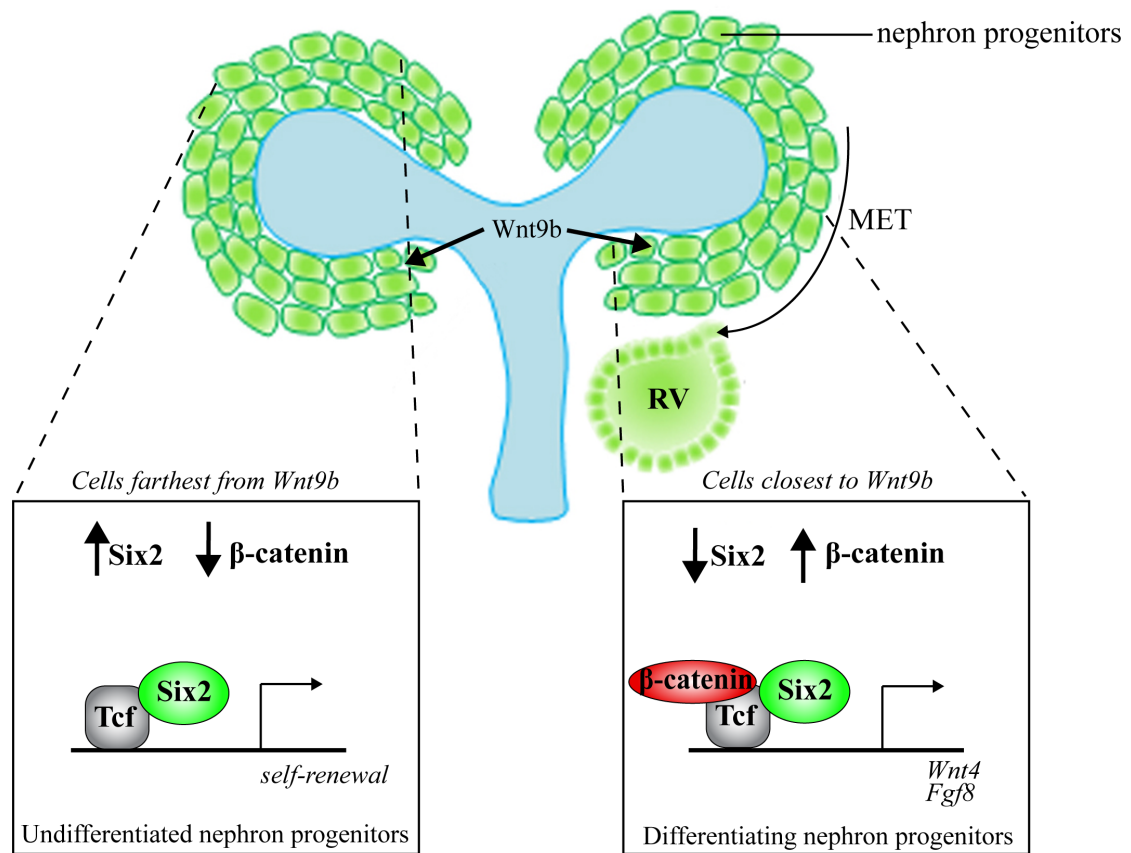
β -catenin in the ureteric epithelium: (A) – The Wnt/ β -catenin pathway is essential for Wolffian duct elongation by regulating *Gata3* expression. (B) In ureteric bud tip cells, β -catenin maintains branching morphogenesis via regulation of *Emx2*, which in turn regulated the expression of *c-Ret*, *Pax2*, and *Lim1*. β -catenin also inhibits ureteric differentiation.

1.6.2 β -catenin in the mesenchyme

β -catenin also plays a central role in the induction of the condensed mesenchyme. Shortly after the formation of the ureteric bud, the metanephric mesenchyme is induced to condense around the ureteric bud tip. This process is initiated by the Wnt9b ligand, which is secreted by the ureteric bud cells. It signals to the adjacent mesenchyme population to activate the Wnt/ β -catenin signaling pathway (Carroll, Park et al. 2005, Park, Valerius et al. 2007). This inductive β -catenin-mediated signal then up-regulates Wnt4 expression, which in turn activates the expression of key mesenchymal-to-epithelial transition (MET) factors, such as Pax8, Lhx1, and Fgf8, in a β -catenin dependent manner (Figure 1.10)(Stark, Vainio et al. 1994, Kispert, Vainio et al. 1998, Park, Valerius et al. 2007, Schmidt-Ott, Masckauchan et al. 2007). The deletion of β -catenin in the condensed mesenchyme results in reduced expression of these key MET markers and a depletion of the nephrogenic progenitors. More recently, studies have highlighted the importance of β -catenin in the maintenance of the nephrogenic progenitors of the condensed mesenchyme. In these cells, β -catenin forms a complex with Six2, a transcription factor essential for self-renewal of the nephrogenic progenitors, and regulates the expression of key nephrogenic progenitor genes, such as *Cited1*, *Pla2g7*, *Tafa5*, and *Gdnf* (Karner, Das et al. 2011, Sarin, Boivin et al. 2014). Interestingly, Six2 and the Wnt9b/ β -catenin signaling form opposing gradients within the condensed mesenchyme to maintain the balance between proliferation and induction of the nephrogenic progenitors. The condensed mesenchymal cells farthest from the ureteric bud tip receive a low β -catenin inductive signal, which allows Six2 to promote self-renewal of the nephrogenic progenitors.

Conversely, the cells closest to the ureteric bud tip receive a high β -catenin inductive signal, which allows the up-regulation of Wnt4 and MET markers (Figure 1.10) (Park, Ma et al. 2012). Taken together, these studies demonstrate the central role of β -catenin in balancing self-renewal of nephrogenic progenitors and the induction of nephrogenesis.

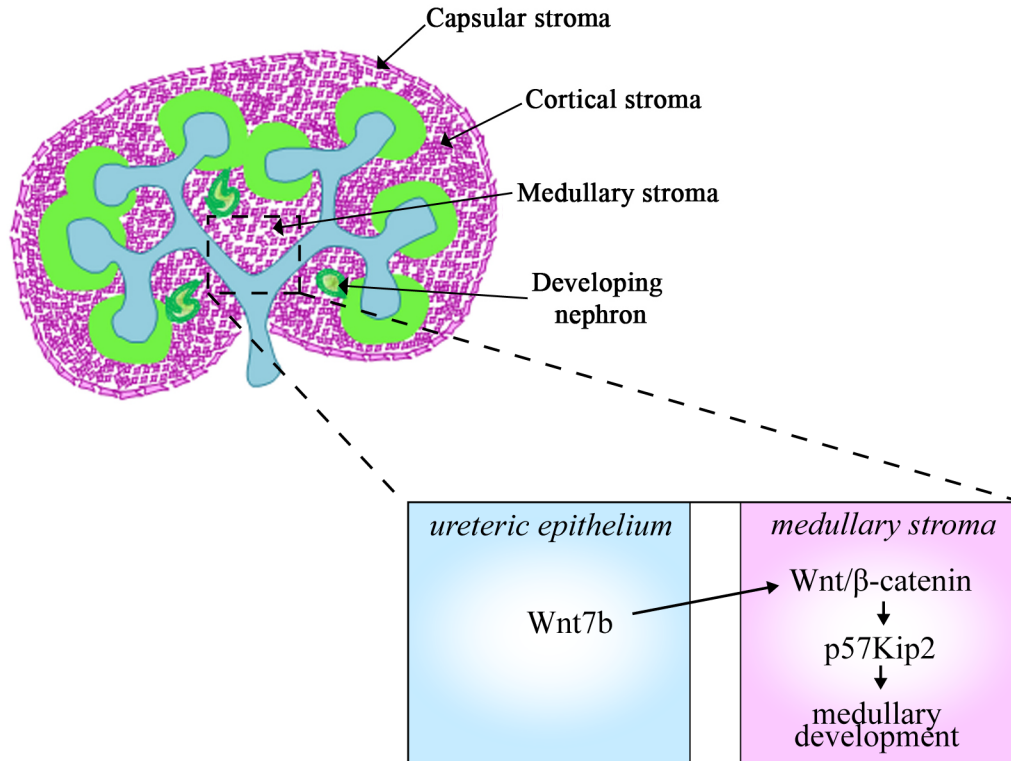
Figure 1.10 – β -catenin in the mesenchyme



β -catenin in the mesenchyme: β -catenin and Six2 create opposing gradients in the mesenchymal nephron progenitors. The cells closest to the ureteric bud tip receive (right) high levels of Wnt9b signal, which stabilizes the levels of β -catenin and increases the expression of MET genes such as Wnt4 and Fgf8. The cells farthest from the ureteric bud tip (left) receive low levels of Wnt9b signaling, which results in low levels of β -catenin and allows Six2 to promote self-renewal of nephron progenitors (adapted from (Park, Ma et al. 2012)).

1.6.3 β -catenin in the renal stroma

Although strong nuclear localization of β -catenin is observed in stromal cells of human fetal kidneys (Eberhart and Argani 2001), the functional contributions of stromal β -catenin to kidney development and the renal stroma are not well defined. A possible role for stromal β -catenin was shown in the development of the medulla. Studies have demonstrated Wnt7b, which is secreted from the ureteric epithelium, signals to neighbouring stromal cells to activate the Wnt/ β -catenin signaling pathway and regulate proper cortico-medullary patterning and epithelial tubule elongation. The inactivation of β -catenin specifically in stromal cells results in cortico-medullary axis defects and impaired medullary development (Yu, Carroll et al. 2009). The specific role of β -catenin in those medullary stromal cells is not clear, however, the cyclin-dependent kinase inhibitor p57Kip2 is markedly reduced in both Wnt7b and β -catenin stromal cell mutants (Yu, Carroll et al. 2009), suggesting β -catenin regulates a genetic program that controls medullary stromal maintenance and development (Figure 1.11). While this study explores the functional role of β -catenin in medullary stroma, it is not known whether β -catenin plays a role in the other stromal populations during kidney development. Further studies are required to determine whether β -catenin is also required in the capsular and cortical stromal populations.

Figure 1.11 - β -catenin in the renal stroma

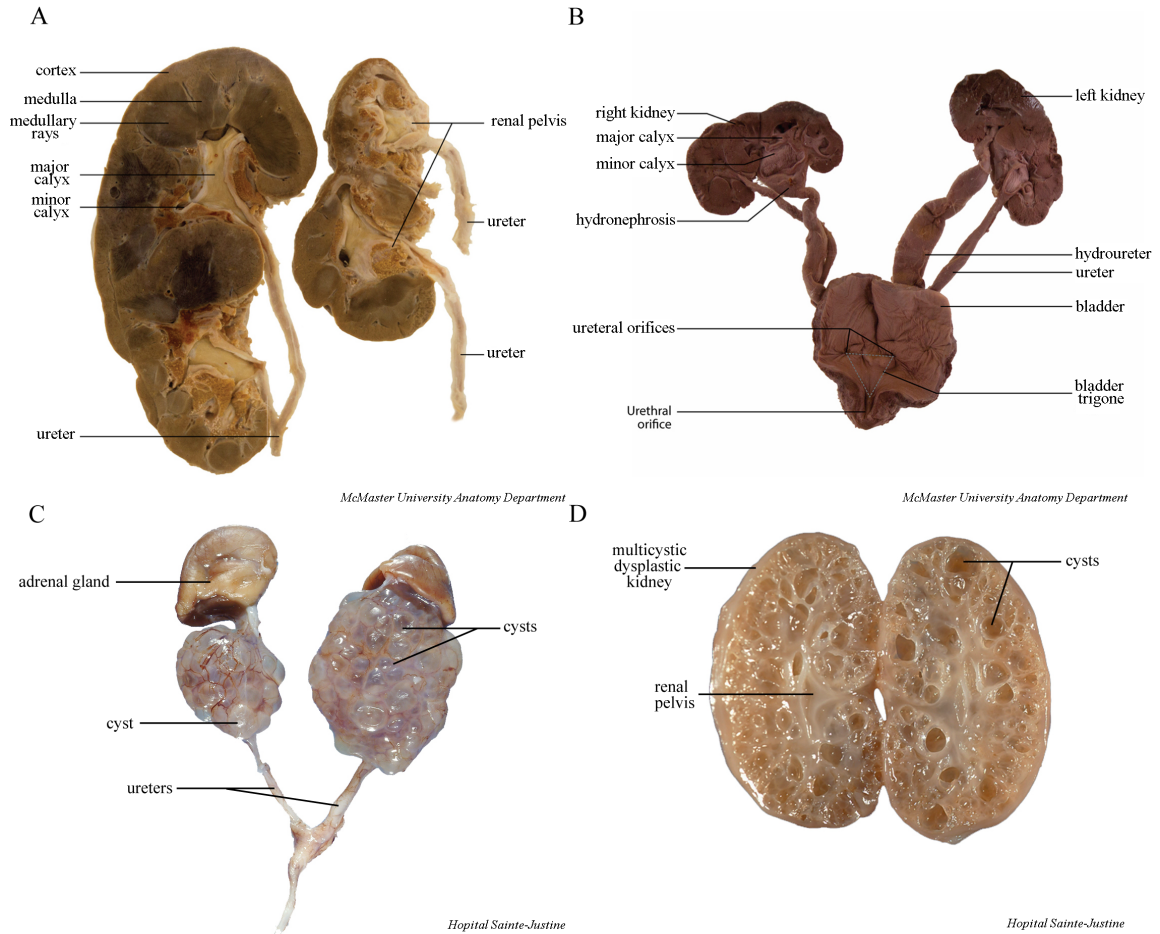
β -catenin in the renal stroma: Wnt7b, which is expressed in ureteric epithelial stalk cells, signals to the adjacent medullary stromal cells to activate the Wnt/ β -catenin pathway. β -catenin then regulates the expression of p57Kip2, which is thought to be essential for medullary development.

1.7 Renal Dysplasia

1.7.1 Human renal dysplasia

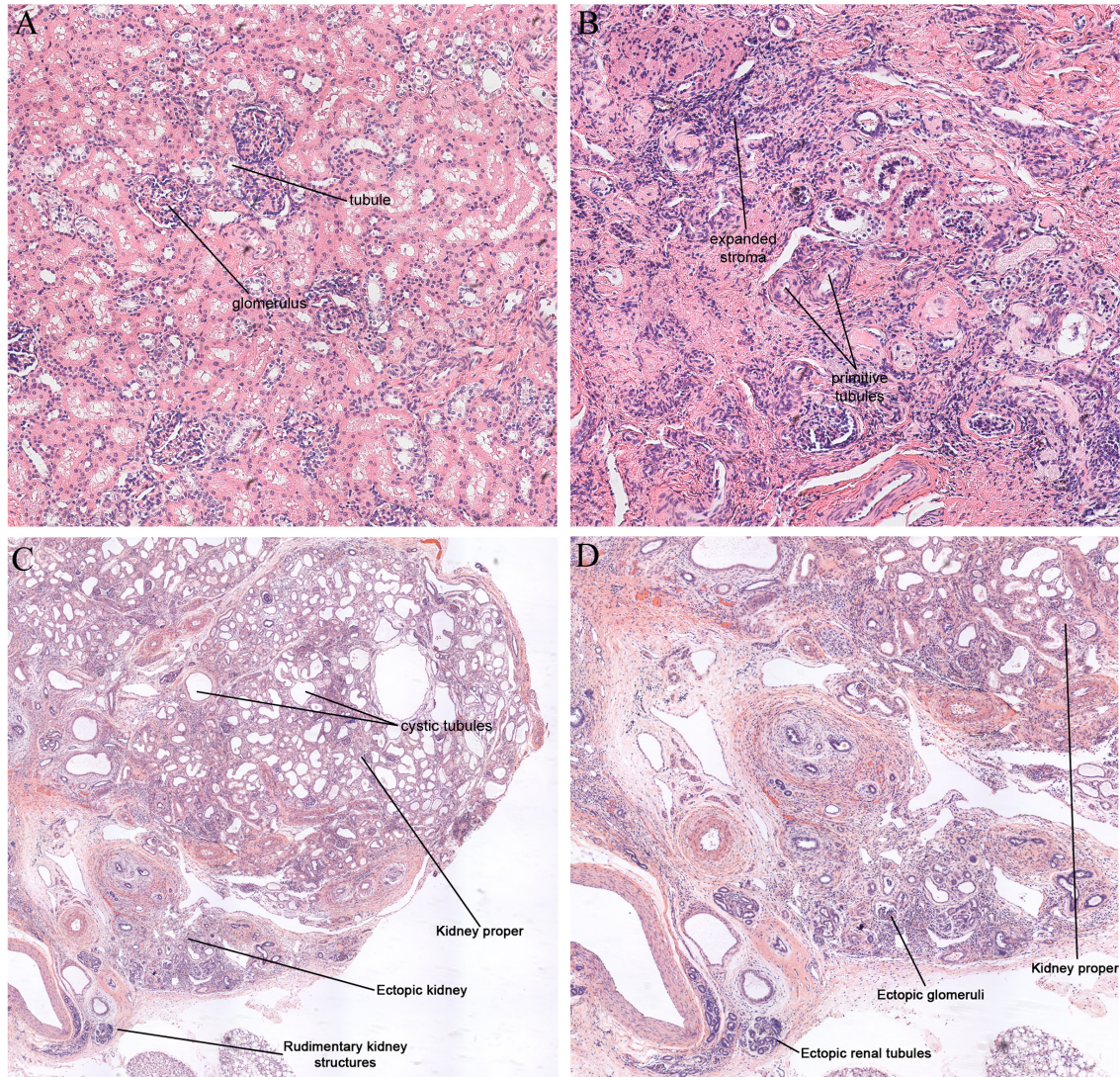
Human renal dysplasia is a congenital kidney malformation that affects 1 in 1000 live births and has an even higher incidence of 4% in fetuses and infants at autopsy (Chen and Chang 2015), thereby making it one of the leading causes of childhood end-stage renal disease (Neu, Ho et al. 2002). The label dysplasia is given to kidneys with structural abnormalities not seen in normal kidneys. At the gross level, these structural abnormalities include renal agenesis, hypoplasia, hypodysplasia, multiplex kidneys with duplicate kidneys (Figure 1.12A,B), and multicystic dysplastic kidneys (Figure 1.12C,D)(Woolf, Price et al. 2004, Winyard and Chitty 2008, Goodyer 2009). Renal dysplasia arises from disruptions between the various cell populations in the kidney (epithelial, mesenchymal, and stromal). These disruptions lead to defects in branching morphogenesis and nephrogenesis. The underlying mechanisms that contribute to the development of renal dysplasia are not well understood and are most likely due to a combination of disruptions in genetic, environmental, and epigenetic cues (El-Dahr, Harrison-Bernard et al. 2000, Jain, Suarez et al. 2007, Thomas, Sanna-Cherchi et al. 2011, Nicolaou, Renkema et al. 2015).

Figure 1.12 - Human renal dysplasia



Human renal dysplasia – (A) Post-natal multiplex dysplastic kidneys with multiple ureters. (B) Embryonic multiplex dysplastic kidneys with bilateral bifid ureters. (C) Embryonic (15 weeks) multicystic dysplastic kidneys. (D) Sagittal section of an embryonic multicystic dysplastic kidney. (A&B – adapted from (Boivin, Sarin et al. 2015), C&D – retrieved from <http://www.humpath.com/spip.php?article4882>).

At the histopathological level, dysplastic kidneys display a wide range of developmental abnormalities in the cortical and medullary regions that result from disrupted branching morphogenesis and nephrogenesis (Piscione and Rosenblum 1999). These abnormalities can be diffuse (involving the whole kidney), focal (involving abnormal regions intermingled with normal regions), or segmental (involving segments of the kidney). Dysplastic kidneys exhibit a disorganized collecting duct system and primitive nephrogenic structures (Figure 1.13A-B)(Woolf, Price et al. 2004), dilated/cystic tubules and epithelial structures (Figure 1.13C)(Hu, Piscione et al. 2003, Katabathina, Kota et al. 2010), undifferentiated mesenchyme, (Winyard and Chitty 2008), and cystic glomeruli (Figure 1.13B)(Sanna-Cherchi, Caridi et al. 2007). Notably, dysplastic kidneys also exhibit a marked expansion of loosely arranged stromal cells surrounding the primitive tubules and collecting ducts (Figure 1.13B)(Winyard and Chitty 2008), suggesting disruptions in the stromal population.

Figure 1.13 - Histopathological features of renal dysplasia

Histopathological features of renal dysplasia: (A) – Histological analysis of embryonic human kidney displaying glomeruli surrounded by their associated tubules. (B) – Embryonic human dysplastic kidney exhibiting primitive tubules surrounded by an expanded stroma population. (C) – Post-natal human multiplex dysplastic kidneys displaying cystic tubules and ectopic rudimentary kidney structure. (D) – Post-natal multiplex dysplastic kidneys displaying ectopic glomeruli and renal tubules. (adapted from (Boivin, Sarin et al. 2015)).

1.7.2 β -catenin in Renal Dysplasia

The exact cause of renal dysplasia in humans is not known but is likely due to a combination of environmental and genetic alterations (Nicolaou, Renkema et al. 2015). While most cases of renal dysplasia are sporadic, many cases have been linked to genetic syndromes and hereditary factors (McPherson, Carey et al. 1987, Squiers, Morden et al. 1987, Murugasu, Cole et al. 1991, Moerman, Fryns et al. 1994). Several genomic mutations in key developmental genes such as *TCF2*, *PAX2*, *RET*, *GDNF*, and *GATA3* (Weber, Moriniere et al. 2006) have been linked to the pathogenesis of renal dysplasia. Additionally, increased levels of β -catenin are observed in the primitive epithelial structures and expanded stromal cell population in many patients with renal dysplasia (Hu, Piscione et al. 2003, Sarin, Boivin et al. 2014). Furthermore, several misregulated markers observed in renal dysplasia, such as Gata3 and GDNF, are known to be regulated by β -catenin (Grote, Boualia et al. 2008, Sarin, Boivin et al. 2014), suggesting the misregulation of β -catenin is a major contributor to the pathogenesis of renal dysplasia. Conditional mouse models where the levels of β -catenin are overexpressed specifically in the ureteric epithelium or metanephric mesenchyme were generated to understand the contribution of β -catenin to the development of renal dysplasia. The overexpression of β -catenin specifically in the ureteric epithelium results in severe renal hypodysplasia, caused by defects in branching morphogenesis and nephrogenesis (Bridgewater, Di Giovanni et al. 2011). In these mice, the increased levels of β -catenin in the ureteric epithelium lead to an upregulation of secreted factors Tgf β 2 and Dkk1, resulting in reduced branching morphogenesis and increased apoptosis in the metanephric

mesenchyme (Bridgewater, Di Giovanni et al. 2011). Similarly, the overexpression of β -catenin specifically in the nephrogenic progenitors (Six2+ population) results in severe hypodysplasia and in some cases renal agenesis at birth (Park, Valerius et al. 2007). Increased levels of β -catenin prevent nephrogenic progenitors to form the renal vesicle and undergo nephrogenesis, resulting in severely hypodysplastic kidneys. Conversely, the overexpression of β -catenin in the metanephric mesenchyme, which encompasses both the nephrogenic and stromal progenitors, results in large and misshapen lobular kidneys at birth and are consistent with the histopathological features of human renal dysplasia (Maezawa, Binnie et al. 2012, Sarin, Boivin et al. 2014). The discrepancy between these two models suggests an important contribution from the stromal population to the dysplastic phenotype. While increased nuclear β -catenin is observed in the expanded stromal population (Sarin, Boivin et al. 2014), its contribution to the pathogenesis of renal dysplasia has not been characterized.

1.8 Rationale and Hypothesis

Elevated levels of β -catenin have been reported in epithelial, mesenchymal, and stromal cells in patients with dysplastic kidneys. Roles for β -catenin have been demonstrated in the metanephric mesenchyme and ureteric epithelium in the pathogenesis of renal dysplasia. However, the role of β -catenin in stromal cells remains poorly understood and it is not known whether a dysregulation of stromal β -catenin contributes to the pathogenesis of renal dysplasia. A role for stromal β -catenin has been suggested in the context of cortico-medullary axis formation, however the mechanisms by which stromal β -catenin regulates kidney development are not known. *My hypothesis is that β -catenin is essential for kidney development and that a dysregulation of β -catenin contributes to the pathogenesis of renal dysplasia.*

To test this hypothesis, I developed three separate research projects, which resulted in two publications and a manuscript in preparation.

1. Determine the contribution of an overexpression of β -catenin in stromal cells to renal dysplasia.
2. Explore the mechanism by which β -catenin in stromal cells controls proliferation of the nephrogenic progenitors.
3. Investigate the contribution of β -catenin to the development of the medullary stroma compartment via the regulation of cell survival.

CHAPTER 2

Stromal β -catenin Overexpression Contributes to the Pathogenesis of Renal Dysplasia

Authors: Felix J Boivin, Sanjay Sarin, Pari Dabas, Michele Karolak, Leif Oxburgh, Darren Bridgewater

Corresponding Author: Darren Bridgewater, Pathology and Molecular Medicine, McMaster University Medical Centre, 1200 Main St. West, Hamilton, Ontario, Canada L8N 3Z5. Phone (905) 525-9140 ext. 20754, Fax (905)-546-1129, Email: Bridgew@mcmaster.ca

Citation: Boivin FJ, Sarin S, Dabas P, Karolak M, Oxburgh L, Bridgewater D. Stromal β -catenin Overexpression Contributes to the Pathogenesis of Renal Dysplasia, J Pathol. 2016 Mar, doi: 10.1002.

PREFACE

Significance to thesis

Renal dysplasia is characterized by disrupted branching of the collecting duct system, primitive nephrogenic tubules, and an expansion of the renal stroma. The use of transgenic mouse models has demonstrated important contributions from the epithelial and mesenchymal cell populations to the genesis of renal dysplasia. However, the contribution of the expanded stromal population to renal dysplasia is not known. We, and others, have shown elevated levels of β -catenin in epithelial, mesenchymal, and stromal cells in dysplastic kidneys. In mice, the conditional overexpression of β -catenin in the metanephric mesenchyme or ureteric epithelium promotes histopathological features consistent with renal dysplasia. However, it is not known whether elevated levels of β -catenin in stromal cells contribute to the abnormalities observed in renal dysplasia. The primary goal of this chapter is to understand the contribution of increased β -catenin to the stromal population and to the genesis of renal dysplasia. To do so, we generated a mouse model where the levels of β -catenin are specifically stabilized in stromal cells from the onset of stromal development. Additionally, we compared our findings with human renal dysplastic tissue to determine whether our mouse model is representative of the human renal disease.

Authors' Contribution

Felix J. Boivin designed the study, performed and supervised all experiments, performed and supervised all data analysis, wrote the original draft of the manuscript, and edited and revised the manuscript based on the reviewers' comments.

Ph.D. Thesis – Felix Boivin-Laframboise McMaster University – Medical Sciences

Sanjay Sarin contributed to the design of the study, assisted in the interpretation of the data, and assisted in drafting the manuscript and addressing the reviewers' comments.

Pari Dabas assisted in experiments and data analysis.

Michelle Karolak assisted in experiments.

Leif Oxburgh assisted in the revisions of the manuscript.

Darren Bridgewater contributed to the design of the study, assisted in the interpretation of the data, contributed to refining the original draft of the manuscript, and assisted in editing and revising the manuscript.

ABSTRACT

Renal dysplasia, the leading cause of renal failure in children, is characterized by disrupted branching of the collecting ducts, primitive tubules, and an expansion of the stroma. Yet a role for the renal stroma in the genesis of renal dysplasia is not known. Here, we demonstrate that β -catenin, a key transcriptional co-activator in renal development, is markedly increased in the expanded stroma in human dysplastic tissue. To understand its contribution to the genesis of renal dysplasia, we generated a mouse model that overexpresses β -catenin specifically in stromal progenitors, termed β -cat^{GOF-S}. Histopathological analysis of β -cat^{GOF-S} mice revealed a marked expansion of fibroblast cells surrounding primitive ducts and tubules, similar to defects observed in human dysplastic kidneys. Characterization of the renal stroma in β -cat^{GOF-S} mice revealed altered stromal cell differentiation in the expanded renal stroma demonstrating this is not renal stroma, and instead a population of stroma-like cells. These cells overexpress ectopic Wnt4 and Bmp4, factors necessary for endothelial cell migration and blood vessel formation. The characterization of the renal vasculature demonstrated disrupted endothelial cell migration, organization, and vascular morphogenesis in β -cat^{GOF-S} mice. Analysis of human dysplastic tissue demonstrated a remarkably similar phenotype as observed in our mouse model including altered stromal cell differentiation, ectopic Wnt4 expression in the stroma-like cells, and disrupted endothelial cell migration and vessel formation. Our findings demonstrate that the overexpression of β -catenin in stromal cells is sufficient to cause renal dysplasia. Further the pathogenesis of renal dysplasia is one of disrupted stromal differentiation and vascular morphogenesis. Combined, this study

demonstrates for the first time the contribution of stromal β -catenin overexpression to the genesis of renal dysplasia.

Key words: Renal Dysplasia, Stroma, B-catenin, Vascular Morphogenesis

INTRODUCTION

Renal dysplasia affects up to 1 in 1000 of the general population (Winyard and Chitty 2008). It is one of the leading causes of childhood end-stage kidney disease, and no treatments are currently available (Neu, Ho et al. 2002). Human renal dysplasia is characterized at the gross level as complete absence of the kidneys, small kidneys with normal renal architecture, or massive multicystic kidneys (Sanna-Cherchi, Caridi et al. 2007). Histologically, dysplastic kidneys are characterized by abnormal cortical and medullary patterning (Piscione and Rosenblum 1999), disorganization of the collecting system and nephrons (Winyard and Chitty 2008, Rosenblum 2012), dilated/cystic epithelial tubules and collecting ducts (Hu, Piscione et al. 2003, Katabathina, Kota et al. 2010, Trnka, Hiatt et al. 2010), undifferentiated tubules and mesenchyme (Winyard and Chitty 2008), cystic glomeruli (Sanna-Cherchi, Caridi et al. 2007), metaplastic cartilage transformation (Woolf, Price et al. 2004), and an expanded population of loosely arranged stroma (Woolf, Price et al. 2004, Winyard and Chitty 2008). Renal dysplasia arises from the improper formation of kidney tissue elements. Normally the kidney develops from two main cell populations: 1) the ureteric epithelium and 2) the metanephric mesenchyme. Metanephric kidney development is initiated at embryonic day (E) 10.5 in the mouse, or 6-8 weeks in the human, with the formation of a ureteric bud from a tube of ureteric epithelial cells, termed Wolffian duct (Saxen and Sariola 1987). In response to signals emanating from the adjacent metanephric mesenchyme (MM), the ureteric bud migrates into the MM population and undergoes branching morphogenesis to form the collecting duct system of the kidney. Simultaneously, signals from the ureteric epithelium

induce the MM to form a population of condensed mesenchyme. These condensed MM cells undergo mesenchymal-to-epithelial transformation and progress through morphological stages to form the kidney nephrons (Saxen and Sariola 1987, Cebrian, Borodo et al. 2004, Little and McMahon 2012). Shortly after the invasion of the ureteric bud, at around E11.5, the renal stroma arises and surrounds the MM (Hatini, Huh et al. 1996, Kobayashi, Mugford et al. 2014).

The renal stroma is a population of fibroblast cells originating from the MM pool (Mugford, Sipila et al. 2008). The initial formation of the renal stromal cells is dependent on Foxd1 (Hatini, Huh et al. 1996, Levinson, Batourina et al. 2005, Fetting, Guay et al. 2014). The FoxD1 stromal cells form a population of multipotent progenitors maintained via self-renewal around the MM and newly forming nephrons (Kobayashi, Mugford et al. 2014). As kidney development progresses, the FoxD1 progenitors can differentiate into pericytes, mesangial, smooth muscle, interstitial, and endothelial cells (Sims-Lucas, Schaefer et al. 2013, Kobayashi, Mugford et al. 2014, Sequeira-Lopez, Lin et al. 2015). Studies have recently shown the stromal cells play important roles in kidney development (Li, Hartwig et al. 2014) and may also modulate the pathogenesis of renal dysplasia.

β -catenin is a multi-functional protein involved in adherens junctions (Gumbiner 2000) and cell signaling by acting as a transcriptional co-activator (Logan and Nusse 2004). The misregulation of β -catenin in epithelial and mesenchymal populations of the kidney contributes to the genesis of renal dysplasia (Bridgewater, Di Giovanni et al. 2011, Sarin, Boivin et al. 2014). Previous studies have demonstrated increased levels of β -catenin in the stromal compartment in human dysplastic kidneys (Sarin, Boivin et al.

2014). However, it is not known whether the misregulation of β -catenin in stromal cells contributes to the pathogenesis of renal dysplasia.

In this study, we investigated the contribution of stromally expressed β -catenin to the development of renal dysplasia. We show that β -catenin overexpression in stromal cells results in severe renal dysplasia characterized by an expansion of abnormally differentiated stromal cells. The stromal cells overexpress Bmp4 and Wnt4, growth factors involved in vascular morphogenesis and blood vessel formation (Itaranta, Chi et al. 2006, Wiley and Jin 2011). We demonstrate the renal endothelial cells are sporadically distributed throughout the dysplastic tissue and do not form proper blood vessels. Interestingly, we observe identical findings in human dysplastic kidney tissue. Combined these studies demonstrate the overexpression of β -catenin in the stroma contributes to renal dysplasia by altering the stromal cell fate and disrupting endothelial cell organization.

METHODS

Mouse strains: β -catenin stabilized mice, termed β -cat^{GOF-S}, were generated by crossing *Foxd1eGFPCre* mice (described in (Humphreys, Lin et al. 2010) and (Kobayashi, Mugford et al. 2014)) with mice containing LoxP sites flanking exon 3 of the β -catenin allele (β -cat^{A3/A3})(described in (Brault, Moore et al. 2001)). Both mouse lines were maintained on a CD1 genetic background. Mice that did not express the eGFPCre allele were used as *WT* littermate controls. FoxD1 knockin mice, termed *FoxDI*^{GC/GC}, were generated by crossing FoxD1^{GC/+} heterozygous mice, as described in (Humphreys, Lin et al. 2010). (See Online Supplemental Information for details).

Human Kidney Tissue: Human renal tissues were obtained from the McMaster University pathology department in accordance with research ethics (Research Ethics Board approval 13-160-T) (See Online Supplemental Information for details).

Histology and Immunofluorescence: Tissue slides were generated and subsequent staining was performed with hematoxylin and eosin. For immunofluorescence and immunohistochemistry, the following primary antibodies were used on *WT*, β -cat^{GOF-S}, *FoxDI*^{GC/GC} sections: β -catenin, Pbx1, Pax2, Six2, Foxd1, Meis1/2, Erg, PECAM, α -SMA, PDGFR- β , GFP. (See Online Supplemental Information for details).

Whole-Mount Immunofluorescence: *WT* and β -cat^{GOF-S} kidneys were flattened, blocked in serum, and incubated with primary antibodies to Cytokeratin or PECAM. Kidneys were subsequently incubated with secondary antibodies (See Online Supplemental Information for details).

In Situ Hybridization: *In Situ* Hybridization for *BMP4*, *Wnt4*, *SMA- α* , and *Pod1* was performed on mouse and human renal tissues using the *Affymetrix QuantiGene ViewRNA* assay (Please see online supplement for details).

Real-time reverse transcriptase-PCR: Real-time PCR was performed using the SYBR green PCR Master Mix and run on the Applied Biosystems 7900HT fast RT-PCR system. Relative levels of mRNA expression were determined using the $2^{(-\Delta\Delta C_t)}$ method (Livak and Schmittgen 2001). (Please see online supplement for details).

Statistical Analysis: The qRT-PCR and endothelial cell count were analyzed using a two-tailed Student's t-test using GraphPad Prism software, version 5.0c. $P < 0.05$ indicates statistical significance.

Ethics Statement: All studies were performed in accordance with animal care and guidelines put forth by the Canadian Council for Animal Care and McMaster's Animal Research Ethics Board (AREB) (Animal Utilization Protocol #100855) and approved the project described in this study.

RESULTS

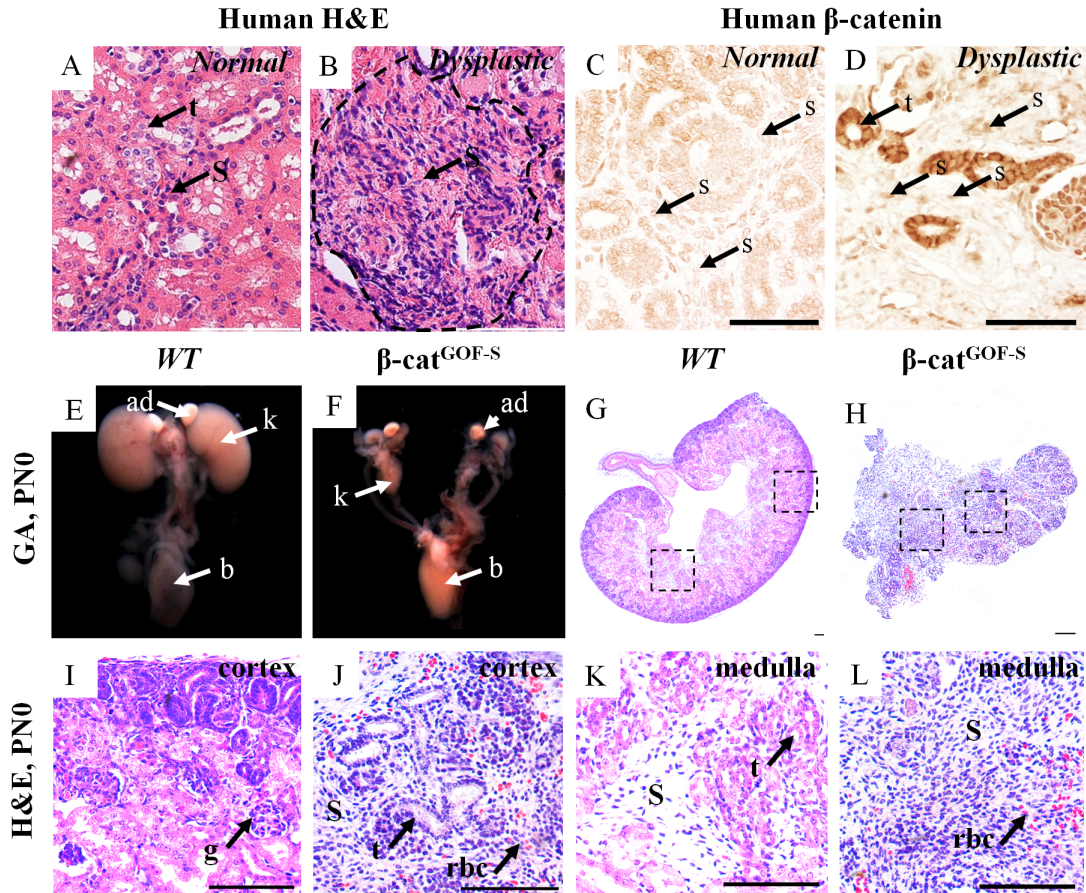
Stabilization of β -catenin in Stromal Cells Contributes to Renal Dysplasia

One of the histopathological hallmarks of human renal dysplasia is the focal expansion of stromal cells (Figure 2.1A, B). We analyzed 3 different human renal dysplastic tissues and observed increased nuclear β -catenin within the expanded stromal cells (Figure 2.1C, D), which is also observed in our previous reports (Sarin, Boivin et al. 2014). Next, we sought to determine the functional significance of β -catenin overexpression in the renal stroma. Using the Cre-LoxP system, we crossed *FoxD1eGFPCre* (Humphreys, Lin et al. 2010, Kobayashi, Mugford et al. 2014) mice with *β -cat^{A3/A3}* mice (Harada, Tamai et al. 1999), which stabilizes β -catenin leading to its overexpression in the cytoplasm and nucleus of the renal stroma (termed *β -cat^{GOF-S}*). The analysis of β -catenin by IF at E11.5, E12.5, and E14.5 confirmed β -catenin overexpression in *β -cat^{GOF-S}* mice exclusively in the expanded kidney stromal cell population (Supplemental Figure 2.1).

β -cat^{GOF-S} mutants died shortly after birth and renal tissue was isolated for gross and histological analysis. In contrast to *WT* littermates, the majority of *β -cat^{GOF-S}* kidneys (n=5/6) demonstrated severe bilateral renal dysplasia and one mutant demonstrated unilateral aplasia at PN0 (n=1/6) (Figure 2.1E, F). Further analysis of *β -cat^{GOF-S}* at PN0 confirmed numerous histological characteristics of renal dysplasia in *β -cat^{GOF-S}* kidneys (Figure 2.1G, H) including disorganized kidney tissue patterning, poorly differentiated tubules, and a lack of glomeruli (Figure 2.1I, J). Of note, similar to human renal dysplasia, we observed a marked expansion of stromal cells between primitive tubules

(Figure 2.1H, L). The cells within the expanded cell population appeared more rounded and lacked the distinctive stellate-like morphology observed in *WT* kidney stroma (Figure 2.1K, L). Moreover, we observed several red blood cells within the expanded stroma population surrounding the tubules (Figure 2.1J-L).

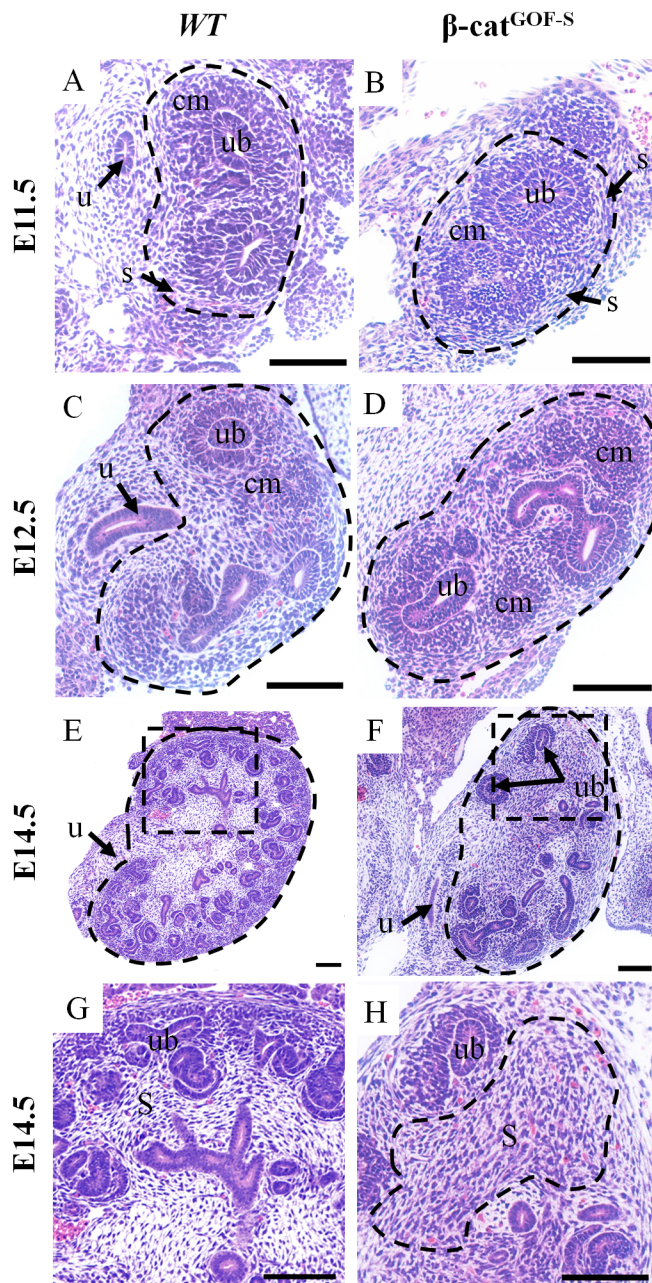
Due to the severe malformation of kidneys at PN0 we analyzed kidney tissue for abnormalities during kidney development. At E11.5 and E12.5 no overt changes were observed in kidney morphology or in the stromal cell population in $\beta\text{-cat}^{GOF-S}$ mutants (Figure 2.2A-D and Supplemental Figure 2.2). However, at E12.5 $\beta\text{-cat}^{GOF-S}$ kidneys did display increased condensed mesenchyme surrounding the ureteric epithelium (Figure 2.2C,D and Supplemental Figure 2.2G,H). By E14.5 $\beta\text{-cat}^{GOF-S}$ kidneys demonstrated abnormal kidney morphology characterized by a marked reduction in nephrogenesis and ureteric branching (Figure 2.2E,F and Supplemental Figure 2.2I-L). Notably, at E14.5 the stromal population in $\beta\text{-cat}^{GOF-S}$ kidneys was forming clusters that occupied the majority of the renal interstitium (Figure 2.2G,H). Taken together, the overexpression of β -catenin in the renal stroma is sufficient to cause renal dysplasia. Moreover, the overexpression of β -catenin in the renal stroma leads to an expansion and clustering of stromal cells, a key feature of renal dysplasia.

Figure 2.1 - Human dysplastic kidneys exhibit increased levels of β -catenin in stromal cells

Human dysplastic kidneys exhibit increased levels of β -catenin in stromal cells: (A) Normal human kidneys showing stromal cells (s) between tubules (t) (B) Dysplastic human kidneys displaying a focal zone of expanded stromal cell population (s). (C-D) Protein expression of the active form of β -catenin in postnatal normal (C) and dysplastic (D) human kidneys. β -catenin expression is markedly increased in stromal cells (s) and tubules (t) in dysplastic kidneys compared to normal kidneys. (E) Gross anatomy of *wild-type* (*WT*) kidneys at PN0. (F) Gross anatomy of β -cat^{GOF-S} kidneys at PN0 showing severe gross abnormalities (G-H) Hematoxylin and Eosin stains of *WT* (G) and β -cat^{GOF-S} (H) kidneys at PN0. (I-L) Higher magnifications of the cortical and medullary regions in *WT* and β -cat^{GOF-S} kidneys. (I) Several glomeruli (g) are observed in the cortex in *WT* kidneys. (J) β -cat^{GOF-S} kidneys are devoid of mature nephrons and exhibit focal zones of expanded renal stroma (s) between poorly developed tubules (t). (K) Medullary stromal cells (s) are observed between the tubules (t) in *WT* kidneys. (L) The stromal population (s) is increased in β -cat^{GOF-S} kidneys and many red blood cells (rbc) are observed in the expanded stroma population. No tubules are observed in the medulla in β -cat^{GOF-S}

kidneys. ad = adrenal gland, b = bladder, k = kidney, rbc = red blood cells, s = stroma, t = tubule. Scale bars = 100 μm .

Figure 2.2 - Overexpression of β -catenin in the stroma during kidney development leads to renal dysplasia



Overexpression of β -catenin in the stroma during kidney development leads to renal dysplasia: (A-B) H&E stain of WT (A) and β -cat^{GOF-S} (B) kidneys at E11.5. No noticeable differences are observed. (C-D) H&E stain of WT (C) and β -cat^{GOF-S} (D) kidneys at E12.5. The condensed mesenchyme (cm) is increased in β -cat^{GOF-S} but no

stromal alterations are observed. (E-F) H&E stains of *WT* (E) and β -*cat*^{GOF-S} (F) kidneys at E14.5. β -*cat*^{GOF-S} kidneys display fewer ureteric bud tips with increased condensed mesenchyme around the ub tips. An increased population of loosely packed fibroblast cells is also observed. (G-H) Higher magnification of *WT* (G) and β -*cat*^{GOF-S} (H) kidneys at E14.5. An expanded population of stromal cells is observed in β -*cat*^{GOF-S} kidneys between collecting ducts and condensed mesenchyme. cm =condensed mesenchyme, s = stroma, ub = ureteric bud, u = ureter. Scale = 100 μ m.

Elevated levels of Stromal β -catenin Result in a Disrupted Stromal Cell differentiation

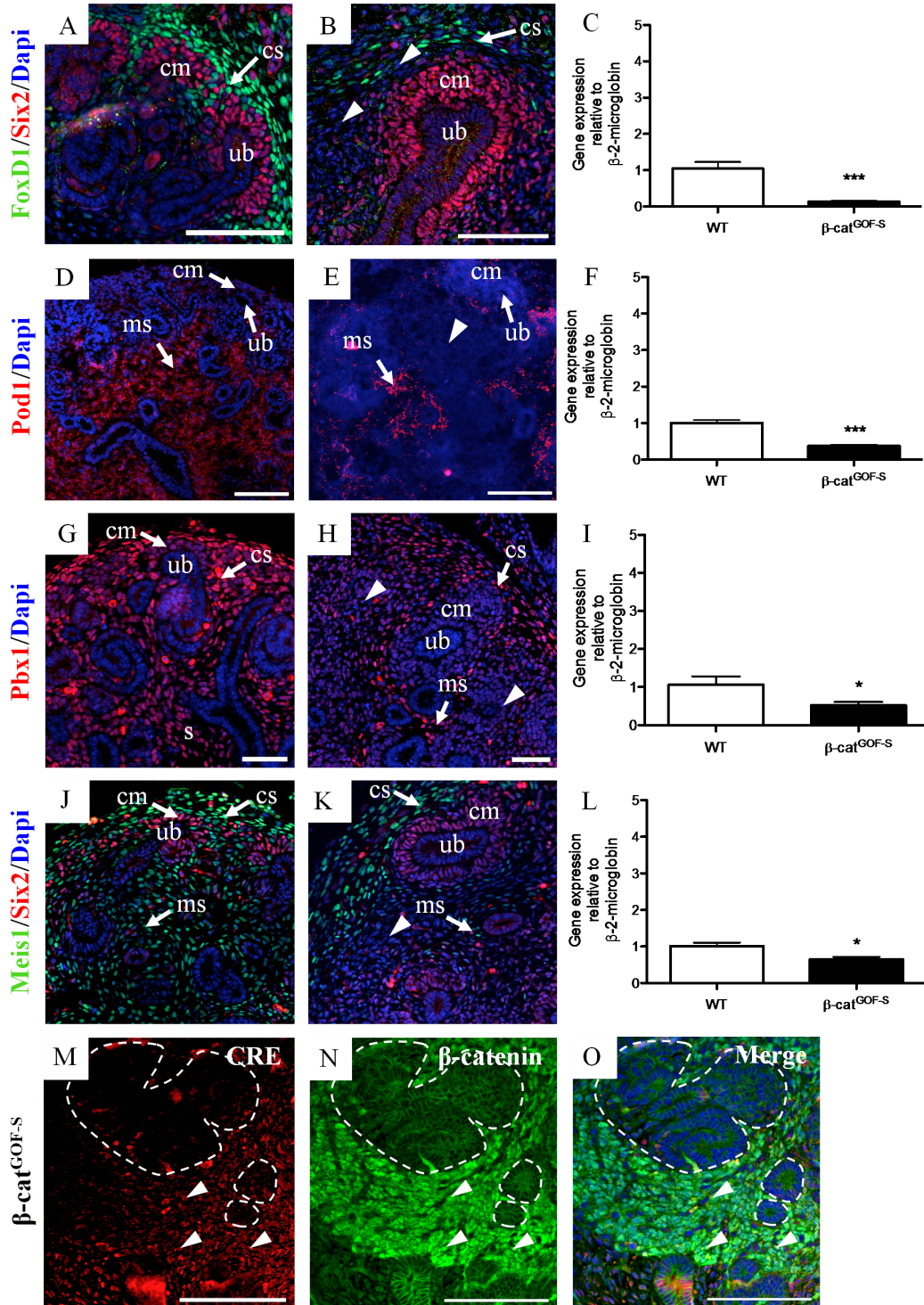
We next characterized the renal stroma in β -cat^{GOF-S} kidneys to gain further insight into the stromal population. We first analyzed FoxD1, as this is the earliest known marker expressed in stromal progenitors (Kobayashi, Mugford et al. 2014). In *WT*, abundant capsular and cortical FoxD1 positive stromal cells were adjacent to the Six2 positive condensed mesenchyme (Figure 2.3A). In contrast, β -cat^{GOF-S} kidneys revealed a marked reduction in the number of FoxD1 positive cells in both the capsular and cortical compartments (Figure 2.3B). We confirmed a 91% reduction in FoxD1 expression by RT-PCR (Figure 2.3C) in β -cat^{GOF-S} kidneys (n=5) when compared to *WT* (n=4) at E14.5 (*WT*-1.049 versus 0.1392, p=0.0006). Interestingly, we noted that in the region where the cortical stroma normally resides, β -cat^{GOF-S} kidneys displayed multiple cell clusters adjacent to the Six2 positive condensed mesenchyme that were not FoxD1 or Six2 positive (white arrowheads, Figure 2.3B).

β -catenin is involved in medullary stromal cell differentiation or maintenance (Yu, Carroll et al. 2009, Boivin, Sarin et al. 2015). Therefore we suspected that β -catenin overexpression might alter the differentiation of the stromal progenitors. We utilized the medullary stromal marker Pod1 to determine if, by overexpressing β -catenin, we have prematurely differentiated the stromal cells into medullary stroma. Surprisingly β -cat^{GOF-S} kidneys exhibited a virtual absence of Pod1 expression throughout the kidney including in the expanded stromal cell clusters (white arrowhead)(Figure 2.3D-E). We confirmed a 63% reduction of Pod1 expression in β -cat^{GOF-S} mutants at E14.5 by RT-PCR (1.00 vs 0.37, p<0.0001)(Figure 2.3F). Furthermore using Pbx1 and Meis1/2, markers of all renal

stromal cells (Hum, Rymer et al. 2014, Boivin, Sarin et al. 2015), the majority of the expanded population of stromal cells in β -cat^{GOF-S} kidneys did not express Pbx1 (Figure 2.3G-H) or Meis1/2 (Figure 2.3J-K). These results were confirmed by RT-PCR, which showed a 54% reduction in Pbx1 (WT 1.1 vs. β -cat^{GOF-S} 0.52, p=0.044) (Figure 2.3I) and a 36% reduction in Meis1/2 (WT 1.01 vs β -cat^{GOF-S} 0.654, p=0.02) at E14.5 (Figure 2.3L). These results demonstrate the cells occupying the stromal compartment do not express classic markers of the renal stroma. We next analyzed FoxD1 mutant mice (termed *FoxD1*^{GC/GC}) since the marked reduction in FoxD1 in β -cat^{GOF-S} mice may account for the disruptions in stromal differentiation. While the histological phenotype was similar to β -cat^{GOF-S} (Hatini, Huh et al. 1996, Kobayashi, Mugford et al. 2014), we did not observe any disruptions in stromal cell differentiation as analyzed by IF and ISH for FoxD1, Pod1, and Pbx1 (Supplemental Figure 2.3). This demonstrates the reduction in stromal markers in β -cat^{GOF-S} is not caused by the reduction in FoxD1 expression.

Despite the marked reductions in stromal markers, the β -cat^{GOF-S} kidneys exhibit an expanded population of cells in the compartment normally occupied by the stroma. Herein we will refer to these cells as “stroma-like” cells. We next performed a lineage tracing analysis by IF for Cre, β -catenin, and GFP to confirm these cells originate from the Foxd1 progenitors. This analysis confirmed that the stroma-like cells express GFP, Cre recombinase, and overexpress β -catenin (Figure 2.3M-O and Supplemental Figure 2.4). Combined these results demonstrate that the expanded stroma-like cells arise from the Foxd1 progenitor cell population that overexpresses β -catenin and do not express classic kidney stromal markers.

Figure 2.3 - Disrupted and reduced stromal markers in β -cat^{GOF-S} kidneys

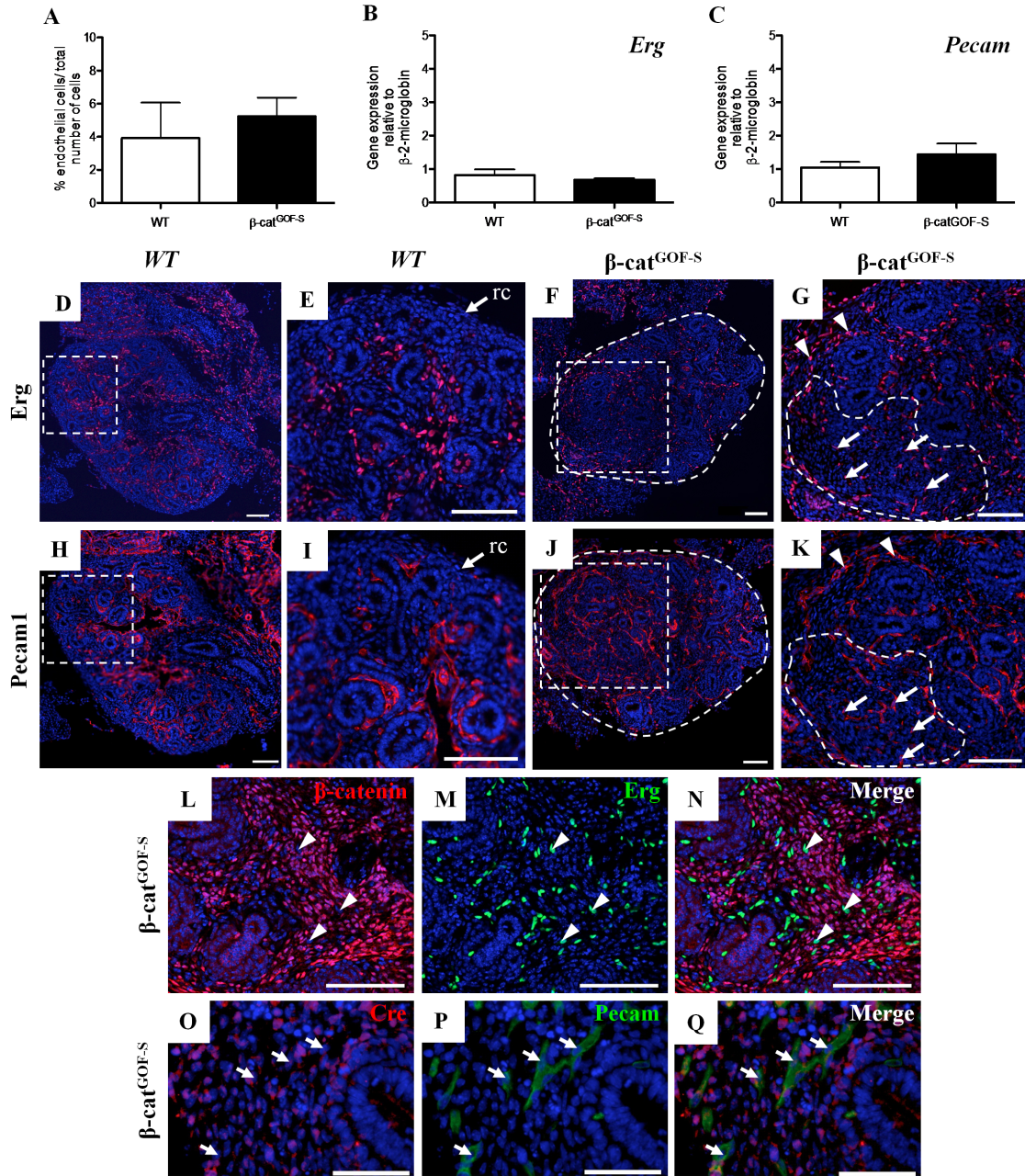


Disrupted and reduced stromal markers in β -cat^{GOF-S} kidneys: (A-B) Immunofluorescence for cortical marker FoxD1 (green) in *WT* and β -cat^{GOF-S} kidneys. The number of FoxD1 positive cells is reduced in β -cat^{GOF-S} (B) compared to *WT* (A) kidneys at E14.5. Several cells do not express FoxD1 (green) or Six2 (red), (white arrowhead). (C) FoxD1 expression is significantly reduced at E14.5 in β -cat^{GOF-S}. (D-E) In situ hybridization for medullary stromal marker Pod1 in *WT* and β -cat^{GOF-S} at E14.5. Compared to *WT* (D), the number of Pod1 expressing cells is significantly reduced in β -cat^{GOF-S} kidneys (E) and clusters of Pod1 negative cells are observed between ureteric bud tips (white arrowhead) (F) qPCR analysis demonstrating the reduced levels of Pod1 in β -cat^{GOF-S} compared to *WT*. Analysis of general stromal markers Pbx1 (G-I) and Meis1 (J-L) in *WT* and β -cat^{GOF-S}. Several cells in the regions where the renal stroma should be do not express Pbx1 (white arrowhead) between the ureteric bud tips in β -cat^{GOF-S} (H) compared to *WT* (G). The levels of Pbx1 mRNA are significantly reduced in β -cat^{GOF-S} (I). Similarly, many cells in β -cat^{GOF-S} (K) do not express Meis1 and Six2 (white arrowhead), compared to *WT* (J). The levels of Meis1 are significantly reduced in β -cat^{GOF-S} kidneys (L). (M-O) The expanded stroma-like population expresses Cre recombinase (M) and overexpresses β -catenin (N) (arrowheads). cm = condensed mesenchyme, cs = cortical stroma, ms = medullary stroma, s = stroma, ub = ureteric bud. Scale bar = 100 μ m.

Stromal Defects Result in Disrupted Vasculature Morphogenesis

Recent studies suggest that stromal cells can differentiate into endothelial cells (Sims-Lucas, Schaefer et al. 2013). Since β -catenin mediated signaling is involved in endothelial cell differentiation and angiogenesis (Cattelino, Liebner et al. 2003, Masckauchan, Shawber et al. 2005), we suspected that β -catenin overexpression might pre-maturely differentiate stromal cells into an endothelial fate. Therefore, we analyzed the stroma-like population for endothelial cell markers Erg and Pecam. We quantified the percentage of endothelial cells (Figure 2.4A) and the expression levels of Erg and Pecam (Figure 2.4B-C). While both *WT* and β -cat^{GOF-S} kidneys demonstrate a similar number of endothelial cells and equivalent expression of endothelial markers, we noted that β -cat^{GOF-S} kidneys lacked the distinct endothelial cell patterning that is observed in *WT*. In *WT*, Pecam and Erg positive endothelial cells lined the developing nephrons and collecting duct system in an organized pattern consistent with forming a blood vessel tree as previously reported (Robert, St John et al. 1998) (Figure 2.4 D-E, 2.4H-I). Conversely, β -cat^{GOF-S} kidneys exhibited disorganized, sporadic, and ectopic endothelial cell localization within the kidney and around the kidney capsule (Figure 2.4F-G, 2.4J-K, Supplemental Figure S2.5). Unlike *WT*, these endothelial cells were primarily single unconnected cells that were sporadically placed throughout the dysplastic tissue (arrows, Figure 2.4K) (arrowheads, Supplemental Figure S2.5). Notably, numerous endothelial cells localized within the expanded stromal-like cells (dashed line, Figure 2.4K). To confirm that these disruptions were not caused by marked reductions in FoxD1 expression, we performed an analysis of Erg and Pecam in *FoxD1*^{GC/GC} kidneys. No overt

changes in endothelial cell organization were observed within *FoxD1^{GC/GC}* kidneys (Supplemental Figure S2.6). We next analyzed the expression of Cre and β -catenin in the endothelial cells in *β -cat^{GOF-S}* kidneys to determine whether these cells originated from stromal progenitors. None of the endothelial cells in *β -cat^{GOF-S}* kidneys overexpressed β -catenin (Figure 2.4L-N) or expressed the Cre protein (Figure 2.4O-Q) demonstrating that overexpression of β -catenin does not result in endothelial cell differentiation, rather results in endothelial cell disorganization.

Figure 2.4 - Overexpression of stromal β -catenin leads to disrupted vascular morphogenesis

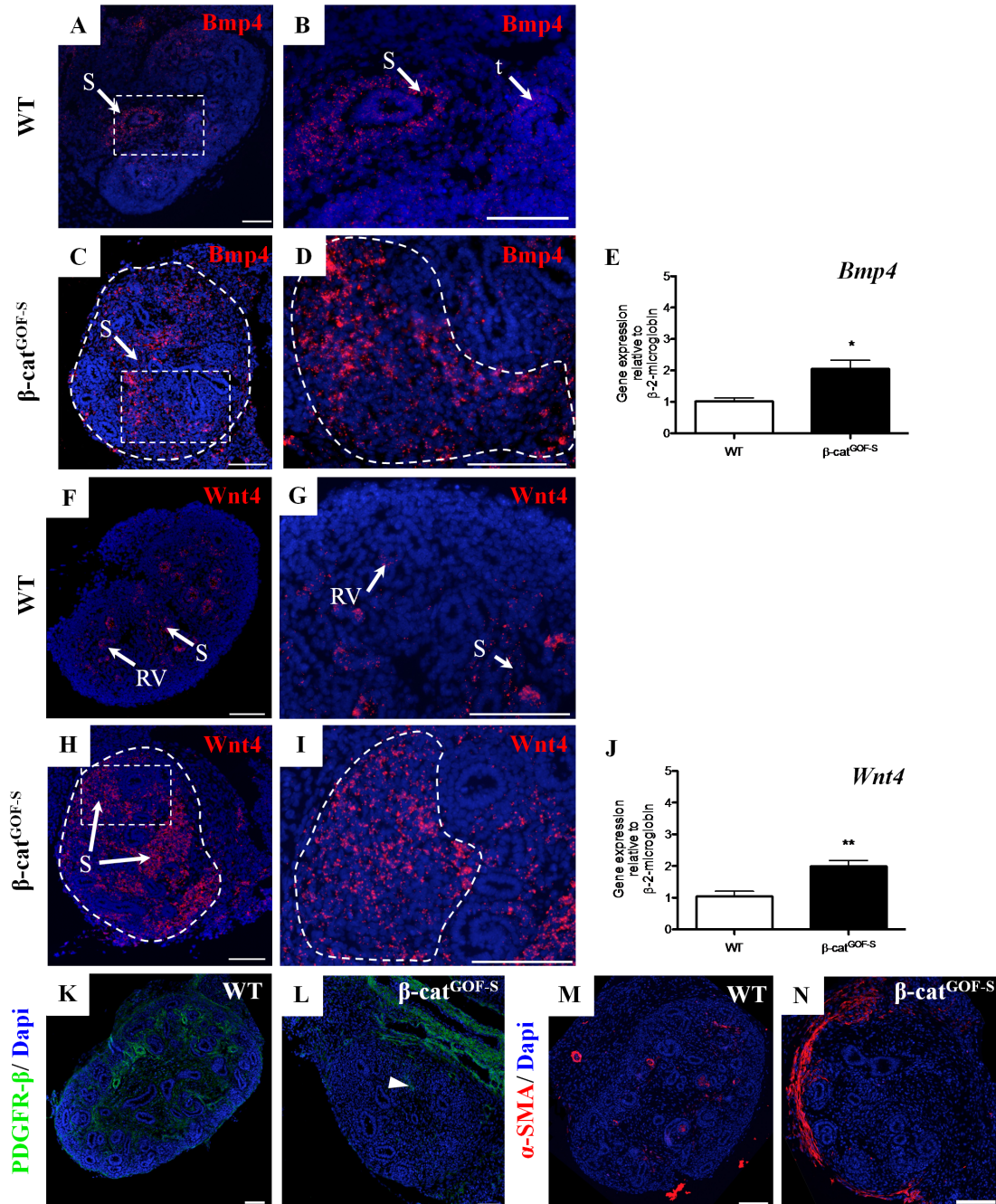
Overexpression of stromal β -catenin leads to disrupted vascular morphogenesis: (A) No significant differences are observed in the percentage of endothelial cells in *WT* and β -cat^{GOF-S} kidneys. (B-C) qPCR analysis of endothelial markers Erg (B) and PECAM (C) in *WT* and β -cat^{GOF-S}. No significant changes are observed. (D-G) IF analysis for Erg in *WT* (D-E) and β -cat^{GOF-S} kidneys (F-G). Unlike *WT* littermates, β -cat^{GOF-S} kidneys exhibit

many endothelial cells below the renal capsule (white arrowheads) and several endothelial cells in the expanded stroma-like population (arrows) (H-K) IF analysis for PECAM in *WT* (H-I) and β -*cat*^{GOF-S} kidneys (J-K). Endothelial cells are observed directly below the renal capsule (white arrowhead). Several endothelial cells in β -*cat*^{GOF-S} kidneys do not form vessels (arrows) in the expanded stroma-like population (arrow). (L-N) The endothelial cells (M) in the expanded stroma-like population do not overexpress β -catenin (L and N). (O-Q) The endothelial cells in the expanded stroma-like population do not arise from the stromal progenitors. These endothelial cells (P) do not express the Cre protein (O). rc = renal capsule, scale bar = 100 μ m.

The origin of endothelial cells in the developing kidney is not entirely understood, but studies have demonstrated endothelial cells can differentiate from stromal progenitors (Sims-Lucas, Schaefer et al. 2013) and can also migrate into the kidney from unknown sources (Robert, St John et al. 1998, Sequeira-Lopez, Lin et al. 2015). Previous studies have demonstrated that a misexpression of BMP4, a known regulator of endothelial cell migration (Wiley and Jin 2011), results in the mislocalization of PECAM+/Flk1+ endothelial cells in the kidney (Valdimarsdottir, Goumans et al. 2002, Levinson, Batourina et al. 2005). Since β -cat^{GOF-S} mutant kidneys exhibited ectopic and mislocalized endothelial cells we analyzed BMP4 mRNA expression. Similar to previous studies (Dudley and Robertson 1997), *Bmp4* was primarily expressed in the stromal cells surrounding the ureter and in the proximal tubules in *WT* kidneys (Figure 2.5A, B). Conversely, β -cat^{GOF-S} mutant kidneys displayed a marked increase in the number of cells expressing *Bmp4* (Figure 2.5C,D). Furthermore, the ectopic *Bmp4* expressing cells were mostly located in the expanded stroma-like cell population (dashed line, Figure 2.5D). We confirmed a 201% increase in *Bmp4* expression by RT-PCR (Figure 2.5E) in β -cat^{GOF-S} kidneys (n=5) when compared to *WT* (n=4) at E14.5 (*WT*-1.02 versus 2.05, p=0.01). The increase in ectopic *Bmp4* expression prompted us to investigate *Wnt4* expression since studies have shown it controls *Bmp4* expression and also promotes endothelial cell sprouting (Itaranta, Chi et al. 2006). In contrast to *WT* (Figure 2.5F,G), we observed the majority of *Wnt4* positive cells in β -cat^{GOF-S} were found in the expanded stroma-like population much like the *Bmp4* expression (Figure 2.5H,I). We confirmed a 190% increase in *Wnt4* expression by RT-PCR (Figure 2.5J) in β -cat^{GOF-S} kidneys at

E14.5 (WT-1.042 versus 1.9884, $p=0.0079$). Together our analysis reveals that overexpression of β -catenin results in ectopic expression of *Wnt4* and *Bmp4* in the expanded stroma-like population.

Studies have demonstrated the *Wnt4/Bmp4* signaling axis promotes the differentiation of stromal into smooth muscle cell types such as pericytes and mesangial cells (Itaranta, Chi et al. 2006), possibly mediated by β -catenin (DiRocco, Kobayashi et al. 2013). Therefore, we hypothesized that overexpression of β -catenin promotes differentiation of stromal cells toward a smooth muscle cell fate. We analyzed the PDGFR- β expression, which is predominantly expressed in mesangial, pericytes, and stromal cells surrounding developing vessels (Seifert, Alpers et al. 1998, Kobayashi, Mugford et al. 2014). Compared to *WT* (Figure 2.5K), PDGFR- β expression was markedly reduced in *β -cat^{GOF-S}* kidneys (Figure 2.5L). Some expression was observed adjacent to the condensed mesenchyme population and surrounding the cortical region, but the majority of the expanded stroma-like population did not express PDGFR- β (arrowhead, Figure 2.5L). Similarly, analysis of α -SMA revealed the presence of smooth muscle cells surrounding the developing vessels and in the vascular cleft in *WT* (Figure 2.5M). While strong α -SMA expression was observed surrounding the *β -cat^{GOF-S}* mutant kidneys, we did not observe the presence of α -SMA expressing cells in the expanded stroma-like population in *β -cat^{GOF-S}* kidneys (Figure 2.5N). Taken together, these results demonstrate that ectopic expression of *Wnt4* and *Bmp4* in the stroma-like population does not promote differentiation of smooth muscle cell types.

Figure 2.5 - Overexpression of stromal β -catenin results in ectopic localization of *Bmp4* and *Wnt4*

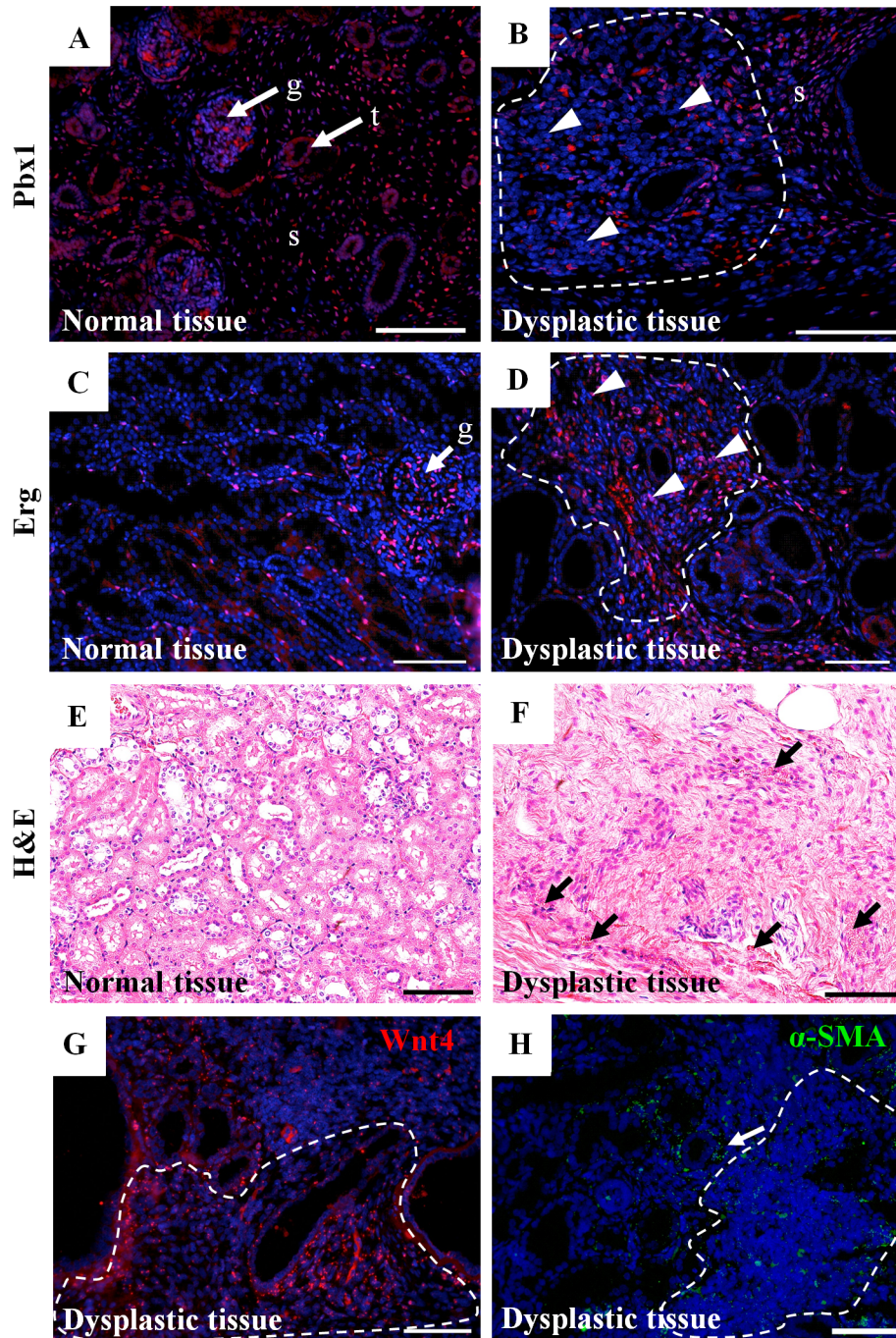
Overexpression of stromal β -catenin results in ectopic localization of *Bmp4* and *Wnt4*: (A-B) In *WT* kidneys, *Bmp4* is expressed in stromal cells (s) surrounding the ureter and in tubules (t) at E14.5. (C-D) *Bmp4* is ectopically expressed in most of the

stroma-like cell population in β -cat^{GOF-S} (white arrowheads). (E) The mRNA levels of *Bmp4* are significantly increased in β -cat^{GOF-S} kidneys. (F-G) In *WT* littermates, *Wnt4* is expressed in renal vesicles and medullary stromal cells at E14.5. (H-I) In β -cat^{GOF-S} kidneys, *Wnt4* is ectopically expressed in most of the stroma-like population. (J) *Wnt4* expression is significantly increased in β -cat^{GOF-S} kidneys. (K-L) PDGFR- β expression in *WT* (K) and β -cat^{GOF-S} kidneys at E14.5. PDGFR- β expression is reduced in β -cat^{GOF-S} kidneys. (M-N) α -SMA expression in *WT* and β -cat^{GOF-S} kidneys at E14.5. α -SMA is not expressed in the expanded stroma-like population, but is ectopically localized around the β -cat^{GOF-S} kidneys (N). RV = renal vesicle, S = stroma, t = tubule. Scale bar = 100 μ m.

Human dysplastic tissue exhibits similar stromal abnormalities

The analysis of $\beta\text{-cat}^{GOF-S}$ kidneys demonstrates an increase in stroma-like cells. To assess whether the increased levels of β -catenin in dysplastic human kidneys lead to a similar stromal phenotype as that observed in $\beta\text{-cat}^{GOF-S}$ kidneys, we analyzed the differentiation state of the renal stroma cell population in human renal dysplasia. In normal tissue all stroma cells expressed Pbx1 (Figure 2.6A). In dysplastic human renal tissue numerous cell within the expanded stromal cell compartment were not positive for the stromal marker Pbx1; a pattern identical to the $\beta\text{-cat}^{GOF-S}$ mouse model (Figure 2.6A-B). Remarkably, within the expanded stromal compartment, a vast majority of cells expressed the endothelial marker Erg (Figure 2.6C-D). Notably, the Erg⁺ cells were ectopic and sporadically placed within the human dysplastic tissue suggesting they were not organized in a manner consistent with proper blood vessel formation. Also, identical to the $\beta\text{-cat}^{GOF-S}$ mouse model we noted a significant infiltration of blood cells within the human dysplastic tissue (Figure 2.6F). These alterations were never observed in the human control tissue (Figure 2.6E). Interestingly, Wnt4 expression was also increased in the expanded stromal population (Figure 2.6G), while α -SMA expression was only observed in smooth muscle cells surrounding the dysplastic collecting ducts (Figure 2.6H). Taken together these results support our mouse model findings and demonstrate that an increase in stromal β -catenin in dysplastic renal tissue disrupts proper stromal cell differentiation and endothelial cell organization.

Figure 2.6 - Human dysplastic kidney display a heterogeneous stromal cell population similar to β -cat^{GOF-S} kidneys



Human dysplastic kidney display a heterogeneous stromal cell population similar to β -cat^{GOF-S} kidneys: (A-B) Analysis of Pbx1 in normal (A) and dysplastic (B) human kidneys. While all stromal cells stain positive for PBX1 in normal human kidneys, several

negative PBX1 cells in the stromal compartment are observed in dysplastic tissue (arrowhead, dotted line). (C-D) Analysis of Erg in normal (C) and dysplastic (D) human kidneys. Several ectopic endothelial cells are observed sporadically within the stromal population (white arrowheads, dotted line). (E-F) H&E staining of normal (E) and dysplastic (F) human kidneys. Numerous red blood cells are observed in the expanded stromal compartment identical to that observed in the $\beta\text{-cat}^{GOF-S}$ kidneys (arrows). (G) Wnt4 expression in dysplastic kidneys. Wnt4 expression is observed in the expanded stroma population (dotted line). (H) α -SMA expression in dysplastic kidneys. α -SMA is expressed around the dysplastic tubules but is not observed in the expanded stroma population (dotted line) g= glomeruli, t= tubule, s=stroma. scale bar = 100 μm .

DISCUSSION

Renal dysplasia is defined as an abnormal development of renal tissue elements yet the contribution of the renal stroma is not well understood. Here, we demonstrate the levels of β -catenin are increased in the expanded stromal population in human dysplastic renal tissue. In our mutant mouse model the increased β -catenin in stromal cells was sufficient to cause severe renal dysplasia. The β -cat^{GOF-S} mutant kidneys were characterized by an expanded stromal-like cell population that overexpressed Wnt4 and Bmp4, two known growth factors necessary for endothelial cell migration and angiogenesis in the kidney (Itaranta, Chi et al. 2006, Wiley and Jin 2011). Consequently, β -cat^{GOF-S} mutant kidneys exhibited disorganized endothelial cells and abnormal blood vessel formation. Human dysplastic kidneys also exhibit a maldifferentiated stromal cell population that also expresses ectopic Wnt4 and exhibits disorganized endothelial cells not organized into blood vessels. Combined, our data demonstrate that β -catenin overexpression in the renal stroma is sufficient to cause renal dysplasia by altering stromal cell differentiation resulting in disorganization of components of the renal vasculature in both mouse and human.

Stromal β -catenin overexpression leads to renal dysplasia

To date, the renal stroma in dysplastic tissue has been defined as an expanded population of stromal cells between the primitive collecting ducts and tubules (Winyard and Chitty 2008). However, our findings demonstrate that this expanded population, in fact, does not express classic markers of renal stroma and instead is a heterogeneous

population of stroma and stroma-like cells. Additionally, we demonstrate this disruption in stromal cells identity is a direct consequence of the β -catenin overexpression, as demonstrated by our stromal analysis of *FoxD1^{GC/GC}* kidneys where stromal cell differentiation is not disrupted. In embryonic kidney development and kidney disease models, β -catenin is a known regulator of cell differentiation (Logan and Nusse 2004). Studies have shown that the overexpression of β -catenin in mesenchymal progenitors (Kuure, Popsueva et al. 2007, Park, Valerius et al. 2007) and ureteric epithelium (Bridgewater, Di Giovanni et al. 2011) affects proper differentiation of cells in the nephrons and collecting duct system. In other model systems, for example, in the adrenal gland, overexpression of β -catenin in steroidogenic cells leads to adrenal dysplasia and promotes ectopic differentiation of the zona glomerulosa (Berthon, Sahut-Barnola et al. 2010). In the lung, β -catenin overexpression promotes stromal cell differentiation into a myofibroblast fate, leading to bronchopulmonary dysplasia (Popova, Bentley et al. 2012). Our analysis is consistent with the overexpression of stromal β -catenin playing a role in aberrant stromal cell differentiation in the kidney.

The consequences of the altered stromal cell differentiation are a disruption in the ability for the renal stroma to communicate with the neighboring ureteric epithelium and MM. To support this, we have previously demonstrated that stromal β -catenin modulates Wnt9b gene expression in the neighboring ureteric epithelium (Boivin, Sarin et al. 2015). Overexpression of β -catenin results in defects in mesenchymal proliferation which result from disruptions in Wnt9b expression and its downstream signaling to the MM (Boivin, Sarin et al. 2015). We believe that Wnt9b in the ureteric epithelium is modulated by β -

catenin controlling factors in the renal stroma that signal to the neighboring ureteric and mesenchymal cells. This mechanism has been shown in previous studies to control MM differentiation. The stromal factors Decorin and Fat4 directly interact with the MM to modify proliferation and differentiation of mesenchyme progenitors and control nephron formation (Das, Tanigawa et al. 2013, Fetting, Guay et al. 2014). Therefore, we believe the alterations in stromal cell differentiation lead to altered expression of stromal factors leading to reduced and disorganized branching morphogenesis and an absence of nephron formation and we are currently working on further identifying these factors (Hatini, Huh et al. 1996, Levinson, Batourina et al. 2005, Das, Tanigawa et al. 2013, Fetting, Guay et al. 2014, Hum, Rymer et al. 2014). A study by Brusnkill et al (Brunskill, Park et al. 2014) demonstrated by single cell RNA-seq analysis an overlap of FoxD1 and Six2/Cited1 expression in a small subset of cells in E11.5 mouse kidneys. Therefore, it is possible that some of the phenotypes seen in $\beta\text{-cat}^{GOF-S}$ are in fact nephron lineage phenotypes. While we cannot rule out this possibility, our analysis of β -catenin overexpression at E11.5, E12.5 and E14.5 did not identify β -catenin overexpressing cells within the condensed MM at any time point. While they might be present, these cells likely represent an extremely small contribution of the overall nephron progenitor population. Thus, a subset of Six2/Cited1 cells overexpressing β -catenin is unlikely to have any significant contribution to the overall phenotype. Taken together, β -catenin overexpression in the renal stroma disrupts stromal cell differentiation, which in turn disrupts the key kidney developmental processes thus contributing to renal dysplasia.

Characterization of the β -catenin overexpressing stromal-like population

Our data demonstrate the stromal cell population in renal dysplastic tissue does not express markers of the renal stroma. The stromal progenitors can differentiate into vascular smooth muscle cells (VSMC), pericytes, mesangial cells, endothelial cells, and capsular, cortical, and medullary interstitial fibroblasts (Humphreys, Lin et al. 2010, Sims-Lucas, Schaefer et al. 2013, Kobayashi, Mugford et al. 2014, Sequeira-Lopez, Lin et al. 2015). Considering the role of β -catenin in cell differentiation, we suspected β -catenin overexpression promoted differentiation of the renal stroma into its derivatives. However, we did not observe any evidence to suggest that stromal progenitors were differentiating into endothelial, pericyte, mesangial or smooth muscle cells. There also existed the possibility that β -catenin was promoting myofibroblast differentiation as reported by DiRocco and colleagues. They demonstrated β -catenin stabilization drives myofibroblast differentiation in kidney medullary fibroblasts (DiRocco, Kobayashi et al. 2013). Surprisingly, we found no evidence to suggest that stromal β -catenin overexpression resulted in myofibroblast differentiation in our mouse model as shown by an absence of smooth muscle actin expression in the stroma-like cell population. The time period at which β -catenin was overexpressed likely accounts for the differences between these two experimental models. In the DiRocco study β -catenin was overexpressed in mature fully differentiated medullary stromal cells (DiRocco, Kobayashi et al. 2013), whereas in our study β -catenin was overexpressed in the embryonic period where stromal cell differentiation was altered. This suggests medullary fibroblasts must be fully differentiated for β -catenin overexpression to promote myofibroblast differentiation. Our

data support that β -catenin does not promote differentiation of stromal progenitors into its derivatives, and thus future studies will be required to identify the fate of the stroma-like cells.

Stromal β -catenin overexpression disrupts endothelial cell organization and vascular patterning

Stromal cells are critical for proper formation and migration of renal vasculature (Hum, Rymer et al. 2014, Sequeira-Lopez, Lin et al. 2015). The deletion of FoxD1 from the kidney stromal progenitors results in the presence of ectopic sub-capsular arteries (Hum, Rymer et al. 2014, Sequeira-Lopez, Lin et al. 2015). Interestingly, our mutant model also exhibited abnormal vascular development. We observed the presence of endothelial cells in the stroma-like population in β -cat^{GOF-S} kidneys that were ectopically and sporadically distributed and not connected to other endothelial cells to form vessels. Moreover, the analysis of the vascular patterning was disorganized in our β -cat^{GOF-S} mutants. This prompted us to investigate WNT4 and BMP4 since they play critical roles in endothelial cell migration and vessel formation in the kidney and in other organ systems (Valdimarsdottir, Goumans et al. 2002, Itoh, Itoh et al. 2004, Itaranta, Chi et al. 2006, Suzuki, Montagne et al. 2008). In our mutant mouse model both *Bmp4* and *Wnt4* were ectopically overexpressed in the stroma-like cell population. Both factors are sufficient to cause migration and sprouting of endothelial cells in vitro (Itaranta, Chi et al. 2006, Suzuki, Montagne et al. 2008). Considering the high number of recruited endothelial cells not derived from the renal stroma to the stroma-like population, our data suggest that the overexpression of BMP4 and WNT4 may be factors required for

endothelial cell recruitment and organization. This role for BMP4 and WNT4 is supported by their specific spatial and temporal expression during normal kidney development. For instance, *Wnt4* expression is observed in the pre-tubular aggregates (Stark, Vainio et al. 1994) and *Bmp4* is expressed in specific segments of the developing nephrons (Miyazaki, Oshima et al. 2003), which are both regions where proper endothelial cell recruitment and formation of the vascular network are essential. Furthermore, the *Bmp* pathway is activated in developing vascular cells and in endothelial cells of the maturing glomerular tuft, which also suggests *Bmp* signaling is essential for vascular development (Blank, Seto et al. 2008). Thus, it is likely that the overexpression of *Bmp4* and *Wnt4* caused disruptions in the endothelial cell recruitment and organization leading to the disrupted vasculature patterning in the dysplastic tissue. Further investigation is required to determine whether β -catenin directly modulates *Bmp4* and *Wnt4* expression and to determine what their roles are in endothelial migration and vascular formation in the developing kidney.

The hypothesis whereby disruptions in a specific cell population affects the behavior of the other cell populations in the kidney to contribute to or worsen the dysplastic phenotype has been postulated in the pathogenesis of renal dysplasia (Hu, Piscione et al. 2003, Sarin, Boivin et al. 2014). Our data support this model. The overexpression of β -catenin in stromal progenitors is sufficient to cause renal dysplasia by first disrupting stromal cell differentiation. This results in alterations in the expression of stromal factors essential for nephrogenesis and branching morphogenesis. Secondly, the overexpression of β -catenin in the heterogeneous stroma-like population results in

increased levels of Wnt4 and Bmp4, and promotes disruptions in vascular morphogenesis.

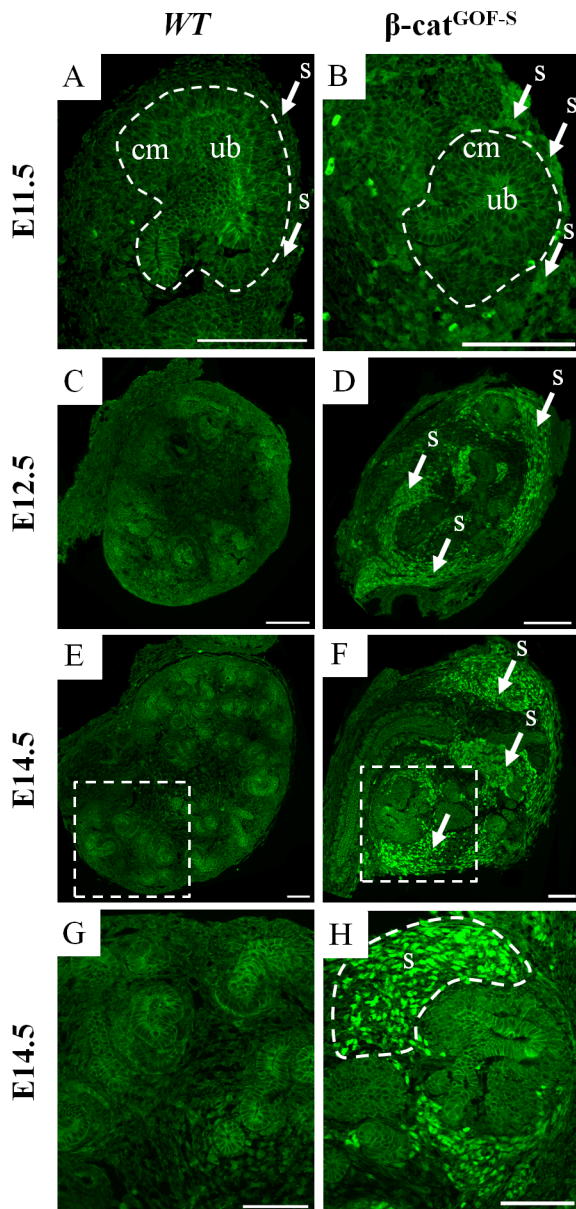
Of particular interest the characteristics and mechanisms observed in $\beta\text{-cat}^{GOF-S}$ mutant kidneys were remarkably similar in the human dysplastic kidneys we analyzed, supporting a translatable mechanism in human renal dysplasia.

AUTHOR CONTRIBUTION

Conception and design: FJB, SS, DB; Performed experiments: FJB, PD, MK; Analysis and interpretations: FJB, SS, PD, DB; Drafting the manuscript: FJB, SS, DB; Edited and revised manuscript: FJB, SS, LO, DB.

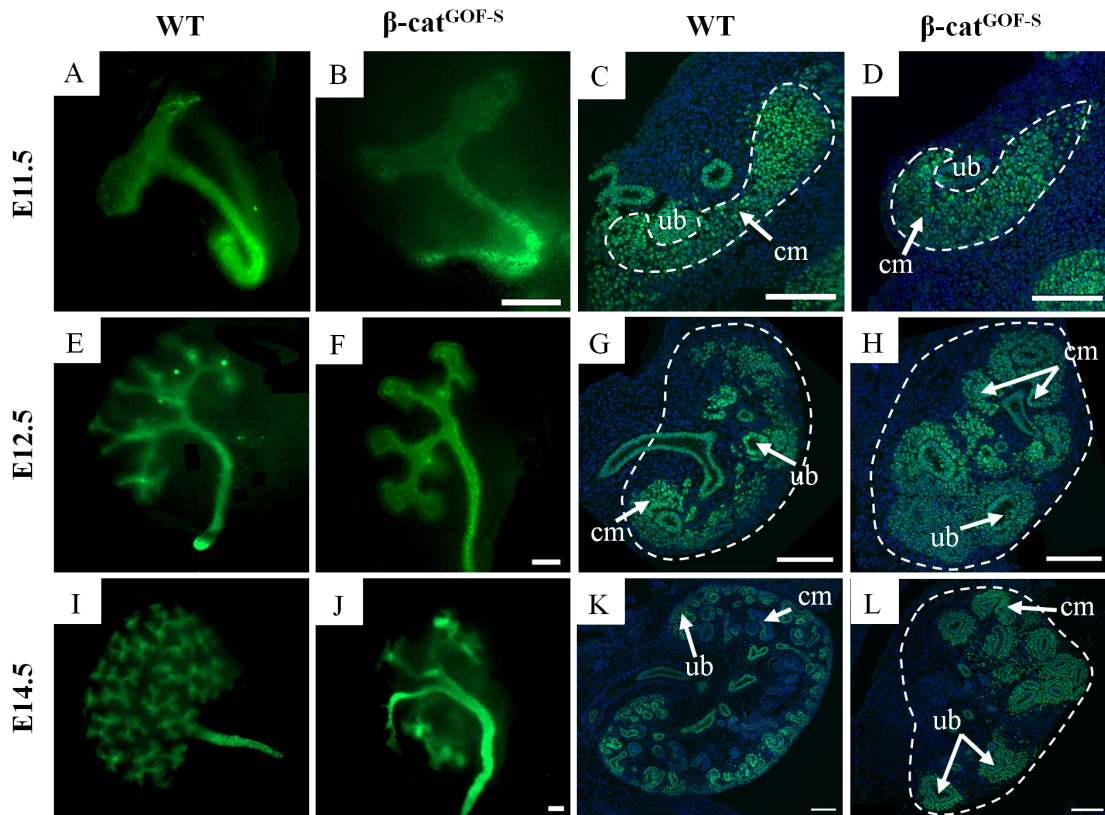
SUPPORTING INFORMATION – FIGURES

Supplemental Figure S2.1 – Characterization of β -catenin expression in β -cat^{GOF-S} mutant mice

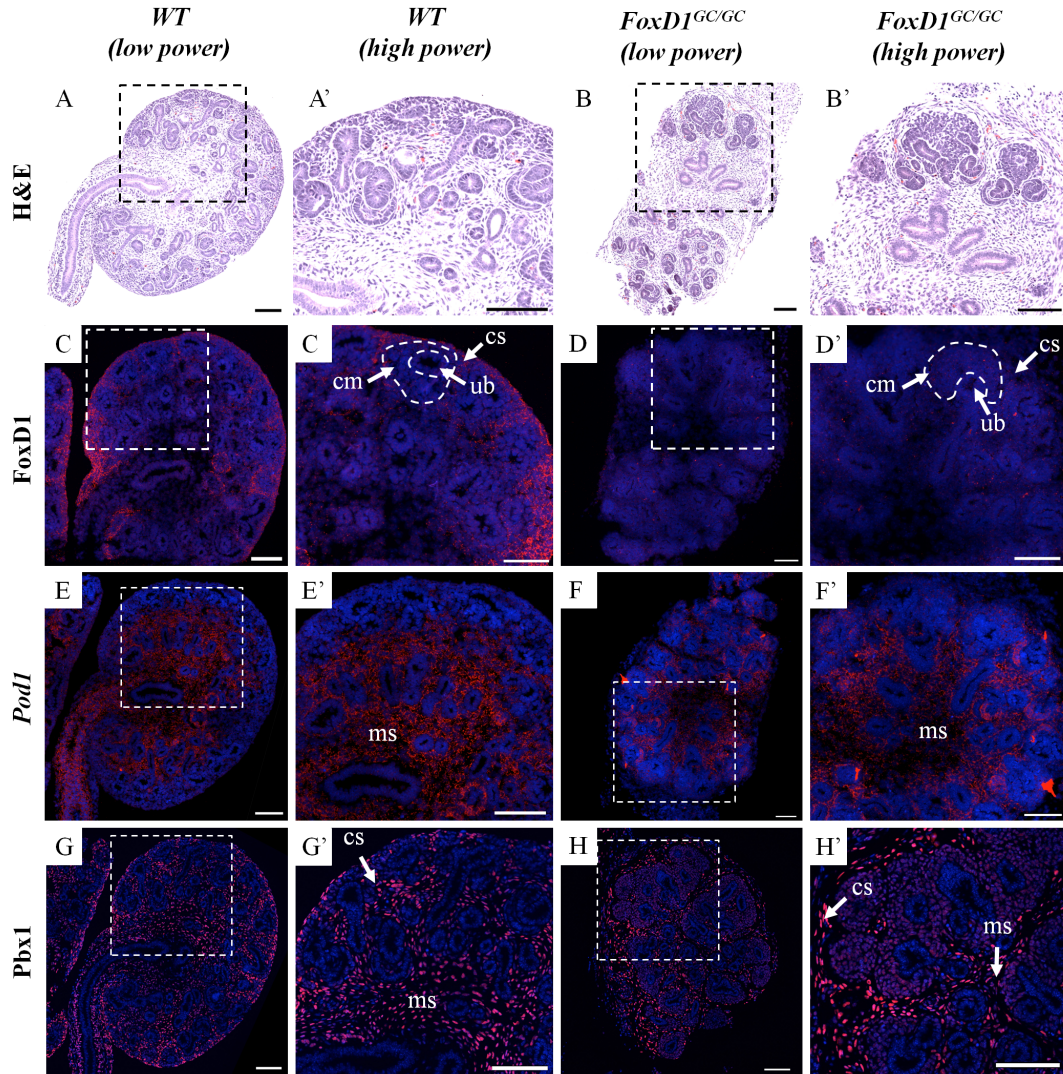


Characterization of β -catenin expression in β -cat^{GOF-S} mutant mice : (A-H) β -catenin immunofluorescence demonstrating β -catenin overexpression at E11.5, E12.5, and E14.5. β -catenin is overexpressed in the stromal cells surrounding the condensed mesenchyme and ureteric bud in β -cat^{GOF-S} kidneys (arrows). The levels of β -catenin are unchanged in ureteric bud cells and the condensed mesenchyme in β -cat^{GOF-S} kidneys. Cm=condensed mesenchyme, s= stroma, ub= ureteric bud. Scale bars = 100 μ m.

Supplemental Figure S2.2– β -cat^{GOF-S} kidneys display disrupted branching morphogenesis and nephrogenesis

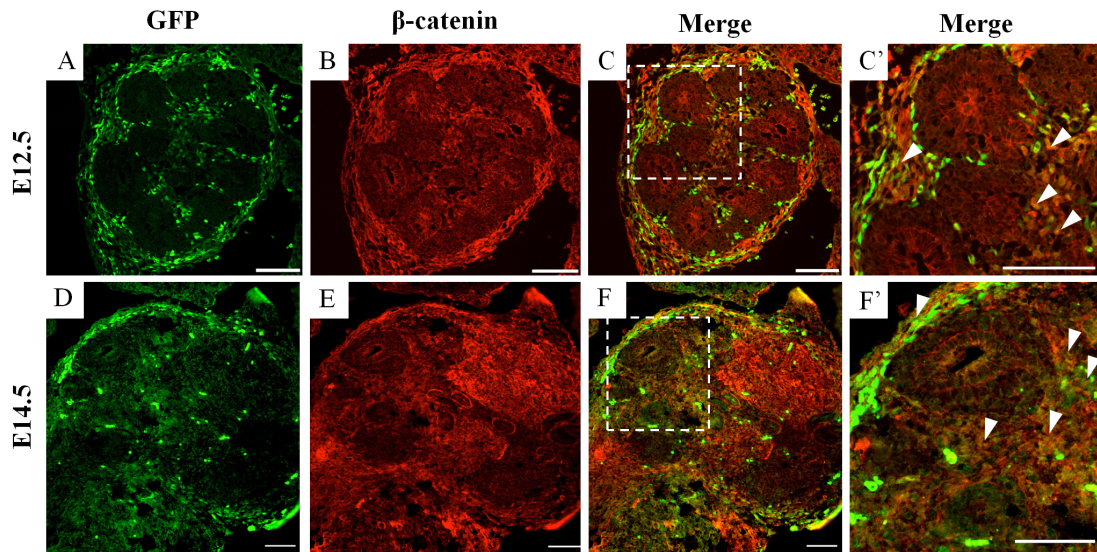


β -cat^{GOF-S} kidneys display disrupted branching morphogenesis and nephrogenesis: Analysis of branching morphogenesis analyzed by whole mount cytokeratin at E11.5 (A-B), E12.5 (E-F), and E14.5 (I-J). Analysis of nephrogenesis using Pax2, a marker of the mesenchyme and epithelium, at E11.5 (C-D), at E12.5 (G-H), and E14.5 (K-L). β -cat^{GOF-S} kidneys display disrupted branching morphogenesis and fewer ureteric bud tips as early as E12.5. Pax2 revealed increased condensed mesenchyme around the ureteric epithelium as early as E12.5 (H), and persists at E14.5 (L). cm = condensed mesenchyme, ub = ureteric bud. scale bar = 100 μ m.

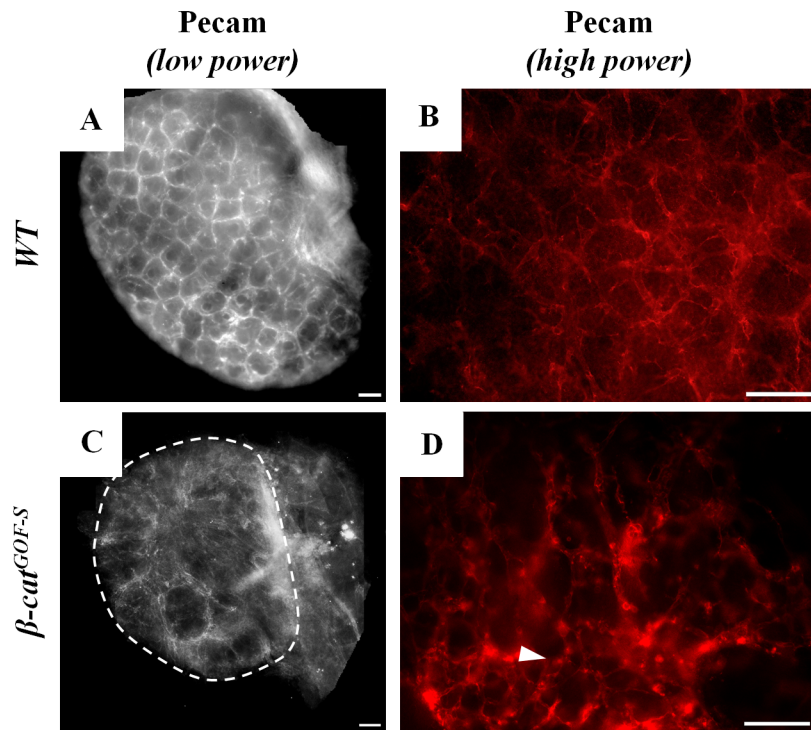
Supplemental Figure S2.3– Analysis of stromal factors in FoxD1 knockouts

Analysis of stromal factors in FoxD1 knockouts: (A-B) H&E staining of *WT* and *FoxD1^{GC/GC}* kidneys at E14.5. (C-D) *FoxD1* *in situ* hybridization in *WT* and *FoxD1^{GC/GC}* kidneys. As expected, *FoxD1* is completely absent in *FoxD1^{GC/GC}* kidneys. (E-F) *Pod1* *in situ* hybridization in *WT* and *FoxD1^{GC/GC}*. Similar to *WT*, *Pod1* is expressed in the medullary stroma in *WT* and *FoxD1^{GC/GC}*. (G-H) *Pbx1* expression is in the cortical and medullary stroma in *WT* (G') and *FoxD1^{GC/GC}*. cm= condensed mesenchyme, cs=cortical stroma, ms=medullary stroma, ub= ureteric bud. Scale bars = 100 μ m.

Supplemental Figure S2.4– The expanded stroma-like population originates from the FoxD1 stromal progenitor population

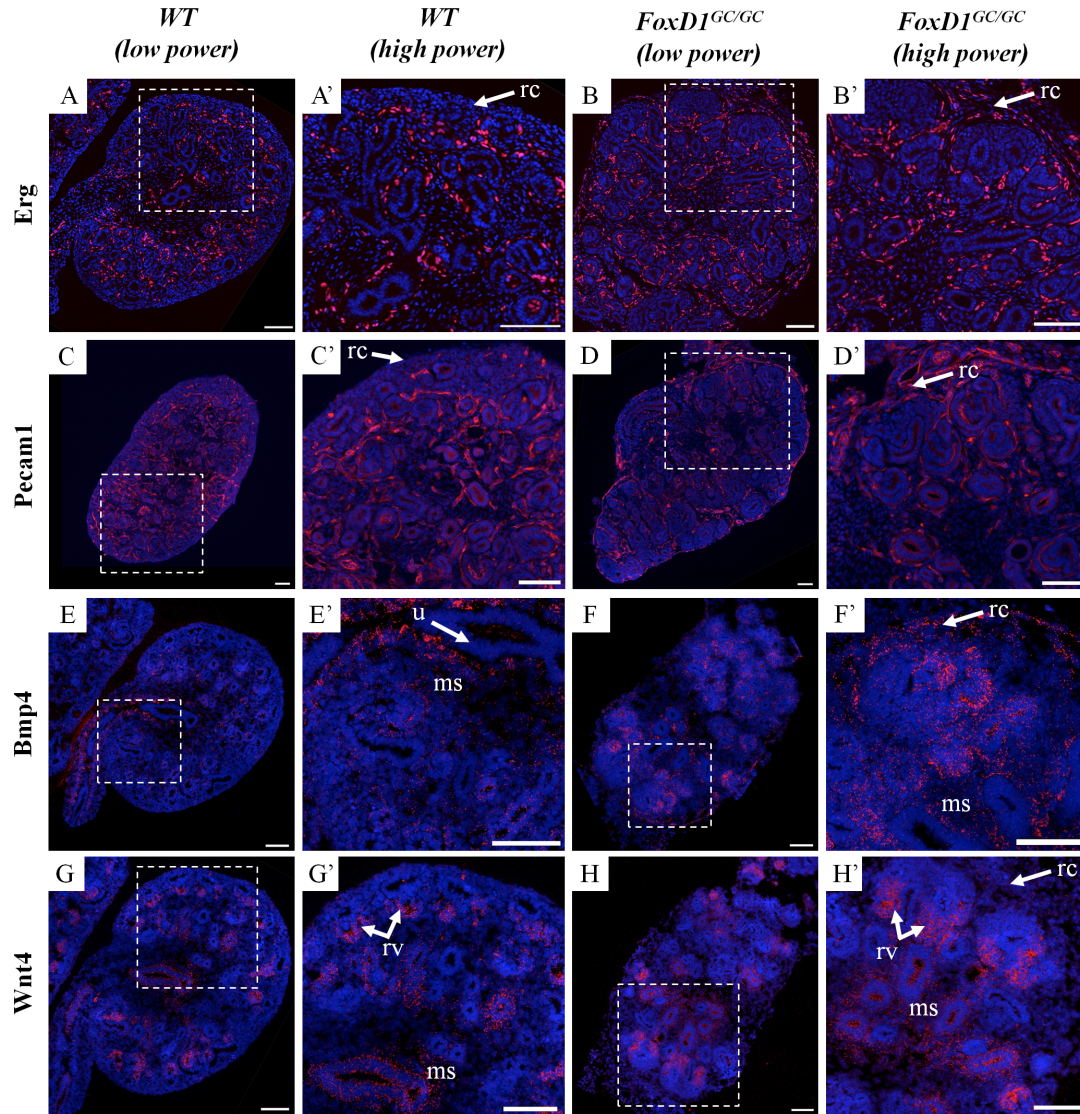


The expanded stroma-like population originates from the FoxD1 stromal progenitor population: (A-F) GFP expression co-localizes with β -catenin over-expression in β -*cat*^{GOF-S} kidneys at E12.5 (A-C) and E14.5 (D-F)(arrowheads). Scale bars = 100 μ m.

Supplemental Figure S2.5 - β -cat^{GOF-S} kidneys display disorganized vasculature patterning

β -cat^{GOF-S} kidneys display disorganized vasculature patterning: (A-D) Whole-mount IF analysis showing renal vasculature morphogenesis using a PECAM antibody. Compared to *WT* kidneys, the overall arterial tree morphogenesis is disorganized in β -cat^{GOF-S} kidneys. (B-D) The close examination revealed the presence of several single unconnected endothelial cells in β -cat^{GOF-S} kidneys (arrowhead) that were not observed in *WT*. scale bar = 100 μ m.

Supplemental Figure S2.6 – Analysis of the endothelial markers in $FoxD1^{GC/GC}$ mice ($FoxD1^{-/-}$ knockouts)



Analysis of the endothelial markers in $FoxD1^{GC/GC}$ mice ($FoxD1^{-/-}$ knockouts): (A-D) Erg and Pecam expression in WT and $FoxD1^{GC/GC}$ kidneys at E14.5. Endothelial cells demonstrate a similar organization in $FoxD1^{GC/GC}$ and WT kidneys. In $FoxD1^{GC/GC}$ kidneys endothelial cells localize to the renal capsule but are not observed in WT . (E-H) $Bmp4$ and $Wnt4$ expression in WT and $FoxD1^{GC/GC}$ kidneys. In $FoxD1^{GC/GC}$ kidneys, $Bmp4$ is observed in the medullary stroma and in the renal capsule. $Wnt4$ is predominantly observed in the renal vesicles (rv) and medullary stroma (ms) in WT (G') and $FoxD1^{GC/GC}$ (H') kidneys. (rc). ms=medullary stroma, rc=renal capsule, rv=renal vesicle, u=ureter. Scale bars = 100µm.

SUPPORTING INFORMATION - METHODS

Mouse strains and genotyping: Mice with a stabilized β -catenin allele resulting in β -catenin overexpression (termed β -cat^{GOF-S}) were generated by crossing *Foxd1eGFPCre* mice (described in [14] and [27]) with mice containing LoxP sites flanking exon 3 of the β -catenin allele (β -cat^{A3/A3})(described in [28]). Both mouse lines were maintained on a CD1 genetic background. Mice were genotyped using the following primers specific to the *FoxD1eGFPCre* allele: Forward 5'-GCGGCATGGTGCAAGTTGAAT-3' and Reverse 5'-CGTTCACCGGCATCAACGTTT-3'. Mice that did not express the eGFPCre allele were used as *WT* littermate controls. *FoxD1* knock-in mice, termed *FoxD1*^{GCE/GCE}, were generated by crossing *FoxD1*^{GCE/+} heterozygous mice, as described in [14]. All animal studies were performed in accordance with animal care and guidelines put forth by the Canadian Council for Animal Care and McMaster's Animal Research Ethics Board (AREB) (Animal Utilization Protocol #100855) and approved the project described in this manuscript.

Human Dysplastic Kidney Tissue: Dysplastic human renal tissues were obtained from the McMaster University (Hamilton, ON, Canada) pathology department in accordance with research ethics (Research Ethics Board approval 13-160-T). Whole kidney tissue was fixed in 4% paraformaldehyde for at least 24 hours at 4°C. Kidneys were paraffin embedded, cut into sections (4 μ m thick), mounted onto SuperfrostTM Plus slides (Thermo Fisher Scientific, Waltham, MA), and incubated overnight at 37°C. Sections were

deparaffinized using xylene washes and rehydrated using graded ethanol washes (100%, 95%, 75%, 50%, H₂O) and stained with H&E (Sigma, St. Louis, MO).

Histology and Immunofluorescence: Whole kidney tissue was fixed in 4% paraformaldehyde for 24 hours at 4 °C. Kidneys were paraffin-embedded, sectioned to 5µm, and mounted on Superfrost™ Plus slides (Thermo Fisher Scientific, Waltham, MA) and incubated overnight at 37°C. Sections were deparaffinized using xylene washes and rehydrated using graded ethanol washes (100%, 95%, 75%, 50%, H₂O) and stained with hematoxylin and eosin (Sigma, St. Louis, MO). For immunofluorescence, tissue was prepared as described above and antigen retrieval was performed for 5 minutes in 10mM sodium citrate solution pH 6.0 in a pressure cooker, followed by blocking with serum-free protein block (Dako Corporation, Carpinteria, CA). Sections were incubated with primary antibodies to β-catenin (cat# 610153, BDTransduction, Lexington, KY; 1:200), Pbx1 (cat# 4342S, Cell Signaling, Beverly, MA; 1:250 dilution), Pax2 (cat# PRB-276P, Covance, Montreal, QC; 1:200 dilution), Six2 (cat# 11562-1-AP, Proteintech Group, Chicago, IL; 1:250), Foxd1 (cat# SC-47585, Santa Cruz, 1:200), Meis1/2 (cat# SC-10599, Santa Cruz, 1:200), Erg (cat# 133264, AbCam, Cambridge, MA, 1:200), Pecam (cat# 553370, BD Transduction, Lexington, KY; 1:200), Flk-1 (cat# 550549, BD Transduction, Lexington, KY; 1:200), α-Sma (cat# A2547, Sigma, St. Louis, MO, 1:200), Pdgfr-β (cat# 05-1135, Millipore, Billerica, MA; 1:200), GFP (cat# ab6673, AbCam, Cambridge, MA, 1:250) overnight at 4°C. Tissue sections were washed in PBS pH 7.4, incubated with secondary antibodies AlexaFluor 488 or 568 (Invitrogen, Carlsbad, CA; 1:1000 dilution) for 1 hour at room temperature, counterstained with DAPI (Sigma, St. Louis, MO; 1:1000 dilution)

for 5 minutes and cover-slipped using Fluoromount (Sigma, St. Louis, MO) and photographed on a Nikon 90i-eclipse upright microscope. Immunohistochemistry (IHC) was performed using the Vectastain elite avidin-biotin complex kit (Vector Labs, Burlingame, CA). After antigen retrieval, endogenous peroxidase activity was blocked using 3% H₂O₂ for 10 minutes, followed by blocking endogenous biotin-binding activity using a biotin/avidin blocking kit (Vector Labs), as per the manufacturer's protocol. Incubation with β -catenin antibody (Millipore, Billerica, MA; 1:100 dilution) was performed overnight at 4°C.

Whole-Mount Immunofluorescence: Kidneys were flattened on 0.4-mm transwell filters (BD, Franklin Lakes, NJ) for 4 hours at 37°C in wells containing Dulbecco's minimal essential medium (DMEM) and stored in 100% methanol at -20°C. Kidneys were washed 3 times with PBS and blocked in 10% normal goat serum, followed by incubation with primary antibodies to cytokeratin (Sigma; 1:200 dilution) or PECAM (BD Transduction, Lexington, KY; 1:200) at 37°C for 1.5 hours. Kidneys were washed in PBS (pH 7.4), incubated with secondary antibodies Alexa Fluor 488 or 568 (Invitrogen; 1:200 dilution) for 1.5 hours at 37°C, and imaged on a Nikon 90i-eclipse inverted microscope.

In Situ Hybridization: *In situ* hybridization using mouse probes for *Wnt4*, *Bmp4*, *Pod1* was performed using the Affymetrix QuantiGene ViewRNA assay. Separate human probes for *WNT4*, *BMP4*, and α -SMA were used on human samples. Briefly, paraffin-embedded *WT* and β -cat^{GOF-S} kidneys and normal and dysplastic human renal tissue were sectioned at a thickness of 5 μ m, deparaffinized, boiled in pre-treatment solution (Affymetrix, Santa Clara, CA) and digested with proteinase K. Sections were incubated

with a custom designed QuantiGene ViewRNA *Wnt4* probe for 2 hrs at 40°C. Signal was amplified with Pre-Amp and Amp solutions and then developed Fast-Red substrate. Slides were counter-stained with DAPI, mounted with Fluoromount (Sigma, St. Louis, MO) and photographed on a Nikon 90i-eclipse upright microscope.

Reverse transcription-PCR: Complementary DNA was generated from total RNA using first strand cDNA synthesis (Invitrogen Carlsbad, CA). QPCR was performed using the Applied Biosystems 7900HT fast RT-PCR system (Applied Biosystems, Burlington, ON) Real-time PCR reaction mix contained 12.5ng/ul of each cDNA sample, SYBR green PCR Master Mix (Applied Biosystems, Burlington, ON) and 300nM of each primer to a total volume of 25 µl. Primers for *Foxd1*, *Pbx1*, *Meis1/2*, *Pod-1*, *Erg*, *Pecam*, *Wnt4*, and *Bmp4* were designed using the Primer 3 software (<http://bioinfo.ut.ee/primer3-0.4.0/>) and verified using the UCSC genome bioinformatics website (genome.ucsc.edu). Relative levels of mRNA expression were determined using the $2^{(-\Delta\Delta Ct)}$ method. Individual expression values were normalized by comparison to β -2-microglobin.

Statistical Analysis: The qRT-PCR and endothelial cell count were analyzed using a two-tailed Student's t-test using GraphPad Prism software, version 5.0c. $P < 0.05$ indicates statistical significance.

Ethics Statement: All studies were performed in accordance with animal care and guidelines put forth by the Canadian Council for Animal Care and McMaster's Animal Research Ethics Board (AREB) (Animal Utilization Protocol #100855) and approved the project described in this study.

CHAPTER 3

Stromally Expressed β -catenin Modulates Wnt9b Signaling in the Ureteric Epithelium

Authors: Felix J Boivin, Sanjay Sarin, Janice Lim, Ashkan Javidan, Bruno Svajger, Hadiseh Khalili. Darren Bridgewater

Corresponding Author: Darren Bridgewater, Pathology and Molecular Medicine, McMaster University Medical Centre, 1200 Main St. West, Hamilton, Ontario, Canada L8N 3Z5. Phone (905) 525-9140 ext. 20754, Fax (905)-546-1129, Email: Bridgew@mcmaster.ca

Citation: Boivin FJ, Sarin S, Lim J, Javidan A, Svajger B, Bridgewater D. Stromally Expressed β -catenin Modulates Wnt9b Signaling in the Ureteric Epithelium, PLoS One. 2015 Mar 24;10(3).

PREFACE***Significance to thesis:***

The primary goal of this chapter is to investigate the role of stromal β -catenin in kidney development. In Chapter 2 we investigated the contribution of an overexpression of stromal β -catenin to the genesis of renal dysplasia. This approach provides insights into the mechanisms that contribute to renal dysplasia by mimicking the human disease. However, to gain a better understanding of the role of stromal β -catenin in the context of proper kidney development, we generated a model deficient for β -catenin specifically in stromal cells. In this chapter we demonstrate the role of stromal β -catenin in regulating proliferation of the nephrogenic progenitors. In addition, we utilize the gain of function model established in Chapter 2 to demonstrate the direct contribution of β -catenin to this mechanism.

Authors' Contribution

Felix J. Boivin conceived and designed the study, performed and supervised all experiments, performed and supervised all data analysis, wrote the original draft of the manuscript, and edited and revised the manuscript based on the reviewers' comments.

Sanjay Sarin contributed to the design of the study, assisted in the interpretation and analysis of the data, assisted in drafting the manuscript, and helped in addressing the reviewers' comments.

Janice Lim contributed to experiments and data analysis.

Ashkan Javidan contributed to experiments and data analysis.

Hadiseh Khalili assisted in data analysis.

Bruno Svajger assisted in data analysis.

Darren Bridgewater contributed to the design of the study, assisted in the interpretation and analysis of the data, contributed to refining the original draft of the manuscript, and assisted in editing and revising the manuscript.

ABSTRACT

The mammalian kidney undergoes cell interactions between the epithelium and mesenchyme to form the essential filtration unit of the kidney, termed the nephron. A third cell type, the kidney stroma, is a population of fibroblasts located in the kidney capsule, cortex and medulla and is ideally located to affect kidney formation. We found β -catenin, a transcriptional co-activator, is strongly expressed in distinctive intracellular patterns in the capsular, cortical, and medullary renal stroma. We investigated β -catenin function in the renal stroma using a conditional knockout strategy that genetically deleted β -catenin specifically in the renal stroma cell lineage (β -cat^{s/-}). β -cat^{s/-} mutant mice demonstrate marked kidney abnormalities, and surprisingly we show β -catenin in the renal stroma is essential for regulating the condensing mesenchyme cell population. We show that the population of induced mesenchyme cells is significantly reduced in β -cat^{s/-} mutants and exhibited decreased cell proliferation and a specific loss of Cited 1, while maintaining the expression of other essential nephron progenitor proteins. *Wnt9b*, the key signal for the induction of nephron progenitors, was markedly reduced in adjacent ureteric epithelial cells in β -cat^{s/-}. Analysis of *Wnt9b*-dependent genes in the neighboring nephron progenitors was significantly reduced while *Wnt9b*-independent genes remained unchanged. In contrast mice overexpressing β -catenin exclusively in the renal stroma demonstrated massive increases in the condensing mesenchyme population and *Wnt9b* was markedly elevated. We propose that β -catenin in the renal stroma modulates a genetic program in ureteric epithelium that is required for the induction of nephron progenitors.

INTRODUCTION

Development of the mammalian kidney is dependent upon inductive interactions between epithelial and mesenchymal cells (Grobstein 1967). Development of the mature kidney is initiated with the outgrowth of an epithelial tube, termed the ureteric bud, which elongates and migrates into a population of mesenchyme, termed the metanephric mesenchyme (MM) beginning at embryonic (E) day 10.5. The ureteric cells send signals to the adjacent mesenchyme that instruct the MM to condense around the tips of the ureteric epithelium forming a population of induced nephron progenitors. These nephron progenitors undergo a mesenchymal-to-epithelial transition and progress through a series of molecular and morphological changes to form the nephron, the filtering units of the kidney. In reciprocal fashion the MM cells signal to the ureteric epithelial cells to promote growth and reiterative branching of the ureteric epithelial cells to form the collecting system of the kidney (Little and McMahon 2012), (Costantini and Kopan 2010). By E11.5, two distinct cell populations are established within the MM, the nephrogenic progenitors and the renal stroma. The reciprocal signaling interactions between the nephrogenic progenitors and the ureteric epithelium during kidney development are well characterized. However, the role of the renal stroma and its interactions with the nephrogenic progenitors and epithelium are poorly understood during kidney development.

The renal stroma is a population of matrix-producing fibroblast cells (Hatini, Huh et al. 1996), (Kanwar, Carone et al. 1997). During kidney development the stromal population is initially observed after the ureteric epithelium invades the MM, as

evidenced by the expression of the earliest stromal differentiation marker Foxd1 (Hatini, Huh et al. 1996). At the initiation of kidney development, the Foxd1 positive cells are loosely packed cells positioned adjacent to the condensing mesenchyme (Hatini, Huh et al. 1996). As the ureteric epithelium continues to branch, the stromal cells are positioned around the maturing epithelium and newly forming nephrons. As the kidney develops beyond E14.5, the renal stroma subdivides into three distinct cell populations: the capsular, cortical and medullary stroma. The function of the renal stroma was originally thought to provide a supportive framework for the nephrons and collecting duct system (Ekblom and Weller 1991). However, deletion of Foxd1 in the developing kidney results in defects in branching morphogenesis and nephrogenesis, suggesting an essential role for the renal stroma in kidney development (Hatini, Huh et al. 1996). Recent studies demonstrated that a complete ablation of the renal stromal resulted in increased induced nephron progenitors and significantly disrupted branching morphogenesis (Das, Tanigawa et al. 2013), (Hum, Rymer et al. 2014). Moreover, the renal stroma controls nephron differentiation by forming direct cell interactions with the nephrogenic progenitors (Das, Tanigawa et al. 2013). These studies highlight the importance of reciprocal interactions between stroma, mesenchyme, and epithelium. However the stromal factors that guide these interactions are poorly defined.

β -catenin is a multi-functional protein involved in cell adhesion and the regulation of gene transcription. In the cell, β -catenin localizes to the cell membrane, cytoplasm, and nucleus where it performs different cellular functions. At the cell membrane β -catenin is involved in the formation, maintenance, and function of adherens junctions by linking

cadherins to the actin cytoskeleton (Gumbiner 2000). In the cytoplasm, β -catenin is involved in cell signal transduction by translocating to the nucleus in response to extracellular stimuli. In the nucleus β -catenin acts as a co-transcriptional activator by forming complexes with DNA bound transcription factors to regulate gene transcription (Logan and Nusse 2004). During kidney development, β -catenin is expressed in the ureteric epithelium and plays essential roles in branching morphogenesis and in the differentiation of ureteric epithelial cells through the regulation of key genetic targets (Bridgewater, Cox et al. 2008, Marose, Merkel et al. 2008). β -catenin expression in the mesenchyme is essential for nephron formation by mediating signals necessary for the induction of nephron progenitors (Park, Valerius et al. 2007). Previously a role for β -catenin mediated signaling was demonstrated in the medullary stroma. In response to Wnt7b, secreted by ureteric epithelial cells, the medullary stroma activates a β -catenin-mediated canonical signaling pathway to control proper patterning of the cortico-medullary axis and elongation of epithelial structures (Yu, Carroll et al. 2009). However, the expression of β -catenin in stromal cells and the molecular mechanism by which stromally expressed β -catenin controls kidney development is not known.

In this study, we investigated the role of stromally expressed β -catenin in kidney development. We show β -catenin expression in distinctive intracellular patterns in the capsular, cortical, and medullary renal stroma. To understand the significance of stromally expressed β -catenin we generated a conditional knockout mouse in which β -catenin is specifically deleted in the renal stroma cell lineage (β -cat^{st/-}). These mutant mice demonstrate marked kidney abnormalities, most notably reductions in the

condensing mesenchyme. Using in situ hybridization and real-time quantitative PCR (qRT-PCR), we demonstrated *Wnt9b*, the key signal for the induction of nephron progenitors, was markedly reduced in ureteric epithelial cells in $\beta\text{-cat}^{\text{S-/-}}$. Consistent with reduced levels of *Wnt9b*, we demonstrated a significant down regulation of Wnt9b-dependent genes, while Wnt9b-independent genes remained unchanged in nephron progenitors. Moreover mice overexpressing β -catenin exclusively in the renal stroma demonstrated massive increases in induced nephron progenitors and *Wnt9b*. Together these data support a model in which β -catenin in the renal stroma communicates with the ureteric epithelium to modulate a genetic program that is required for the induction of nephron progenitors during mammalian kidney development.

MATERIALS AND METHODS

Mice strains and genotyping

Foxd1EGFPCre mice were crossed with mice containing LoxP sites flanking exons 2 through 6 ($\beta\text{-cat}^{A2-6/A2-6}$) (Brault, Moore et al. 2001) of the β -catenin allele. The *Foxd1-Cre*; $\beta\text{-cat}^{+/-}$ males were then crossed with $\beta\text{-cat}^{A2-6/A2-6}$ to generate homozygous β -catenin loss-of-function mutants in the renal stroma (termed $\beta\text{-cat}^{S-/-}$). β -catenin gain-of-function mice were generated by crossing *Foxd1EGFPCre* mice with mice containing LoxP site flanking exon 3 of the β -catenin allele ($\beta\text{-cat}^{A3/A3}$). Tail genomic DNA was isolated and PCR was used to detect the mutants using *Foxd1EGFPCre* primers 5'-GCGGCATGGTGCAAGTTGAAT-3' and 5'-CGTTCACCGGCATCAACGTTT-3'. Primers used to identify the β -catenin mutants are previously described (Brault, Moore et al. 2001). To validate the spatial pattern of *Foxd1EGFPCre* recombinase activity the *Foxd1EGFPCre* mice were crossed with *Gt(ROSA)26Sor(ROSA)* mice. All animal studies were performed in accordance with animal care and guidelines put forth by the Canadian Council for Animal Care and McMaster's Animal Research Ethics Board (AREB) (Animal Utilization Protocol #100855) and approved the project described in this manuscript.

Histology and Immunofluorescence

Whole kidney tissue was fixed in 4% paraformaldehyde for 24 hours at 4 °C. Kidneys were paraffin-embedded, sectioned to 5 μ m, and mounted on SuperfrostTM Plus slides (Thermo Fisher Scientific, Waltham, MA) and incubated overnight at 37°C.

Sections were deparaffinized using xylene washes and rehydrated using graded ethanol washes (100%, 95%, 75%, 50%, H₂O) and stained with hematoxylin and eosin (Sigma, St. Louis, MO). For immunofluorescence, tissue was prepared as described above and antigen retrieval was performed for 5 minutes in 10mM sodium citrate solution pH 6.0 in a pressure cooker, followed by blocking with serum-free protein block (Dako Corporation, Carpinteria, CA). Sections were incubated with primary antibodies to β -catenin (BD Transduction, Lexington, KY; 1:200), Pbx1 (Cell Signaling, Beverly, MA; 1:250 dilution), Pax2 (Covance, Montreal, QC; 1:200 dilution), Six2 (Proteintech Group, Chicago, IL; 1:250), Cited1 (Thermo Scientific, Fremont, CA, 1:200), Foxd1 (Santa Cruz, 1:200), Meis1/2 (Santa Cruz, 1:200), TN-C (AbCam, Cambridge, MA, 1:200), Amph (Proteintech Group, Chicago, IL, 1:250), Ncam (Sigma, St. Louis, MO, 1:250), Jag1 (Santa Cruz, CA, 1:200), Wt-1 (Santa Cruz, CA, 1:200), Cytokeratin (Sigma, St. Louis, MO, 1:200), Aquaporin-3 (Novus Biologicals, Oakville, ON, 1:200), overnight at 4°C. Tissue sections were washed in PBS pH 7.4, incubated with secondary antibodies Alexafluor 488 or 568 (Invitrogen, Carlsbad, CA; 1:1000 dilution) for 1 hour at room temperature and stained with Dapi (Sigma, St. Louis, MO; 1:1000 dilution) for 5 minutes and cover-slipped using Fluoromount (Sigma, St. Louis, MO) and photographed on a Nikon 90i-eclipse upright microscope.

Analysis of cell proliferation and apoptosis

Cell proliferation was assayed in paraffin-embedded kidney tissue by incorporation of 5-bromo-2-deoxyuridine (Roche Molecular Biochemicals, Mannheim, Germany), as previously described (Cano-Gauci, Song et al. 1999). Pregnant mice

received an intraperitoneal injection of BrdU (100 mg/g of body weight) 2 h prior to sacrifice. BrdU-positive cells were identified using an anti-BrdU peroxidase-conjugated antibody (Roche Molecular Biochemicals, Mannheim). Immunoreactivity was visualized using Aminoethyl Carbazole horseradish peroxidase chromogen/substrate solution (Vector, USA). Apoptosis was assessed in paraffin-embedded kidney tissue using the cell death detection kit (Roche Molecular Biochemicals, Mannheim, Germany) and visualized using 3,3'-Diaminobenzidine (DAB) substrate solution (Vector, USA).

Real-time reverse transcriptase-PCR

Real-time PCR was performed using the Applied Biosystems 7900HT fast RT-PCR system (Applied Biosystems, Burlington, ON). cDNA was generated using first strand cDNA synthesis (Invitrogen Carlsbad, CA) from total RNA. Real-time PCR reaction mix contained 12.5ng/ul of each cDNA sample, SYBR green PCR Master Mix (Applied Biosystems, Burlington, ON) and 300nM of each primer to a total volume of 25 μ l. Primers for *Cited1*, *Six2*, *Pax2*, *Wnt9b*, *Amph*, *Tafa5*, *Eya1*, *Ret*, *Wnt11* were designed using the Primer 3 software (<http://bioinfo.ut.ee/primer3-0.4.0/>) and verified using the UCSC genome bioinformatics website (genome.ucsc.edu). Relative levels of mRNA expression were determined using the $2^{(-\Delta\Delta Ct)}$ method. Individual expression values were normalized by comparison to β -2-microglobin.

In Situ Hybridization

Frozen blocks were sectioned at a thickness of 20 μ m. Non-radioactive In situ hybridization was performed as described (Yu, Carroll et al. 2009) using 1.2 μ g of either

Wnt9b, *Ret*, or *Wnt11* digoxigenin-labeled (DIG) riboprobes overnight at 68°C. Sections were treated with 2µg/ml RNase for 15 minutes at 37°C and incubated in anti-DIG-AP antibody (1:2000, Roche) at 4°C overnight and incubated with BM purple at room temperature to visualize signals. Sections were fixed in 4% PFA, mounted in glycerol mounting media (Vector, Burlingame, CA). In Situ Hybridization for *Wnt4* was performed using the Affymetrix QuantiGene ViewRNA assay. Briefly, paraffin blocks were sectioned at a thickness of 5 µm, deparaffinized, boiled in pre-treatment solution (Affymetrix, Santa Clara, CA) and digested with proteinase K. Sections were incubated with a custom designed QuantiGene ViewRNA *Wnt4* probe for 2 hrs at 40°C. Signal was amplified with Pre-Amp and Amp solutions and then developed Fast-Red Substrate. Slides were counterstained with DAPI, mounted with Fluoromount (Sigma, St. Louis, MO) and photographed on a Nikon 90i-eclipse upright microscope.

Statistical Analysis

The qRT-PCR, apoptosis, and proliferation data was analyzed using a two-tailed Student's t-test using GraphPad Prism software, version 5.0c (Graphpad, La Jolla, CA). $P < 0.05$ indicates statistical significance.

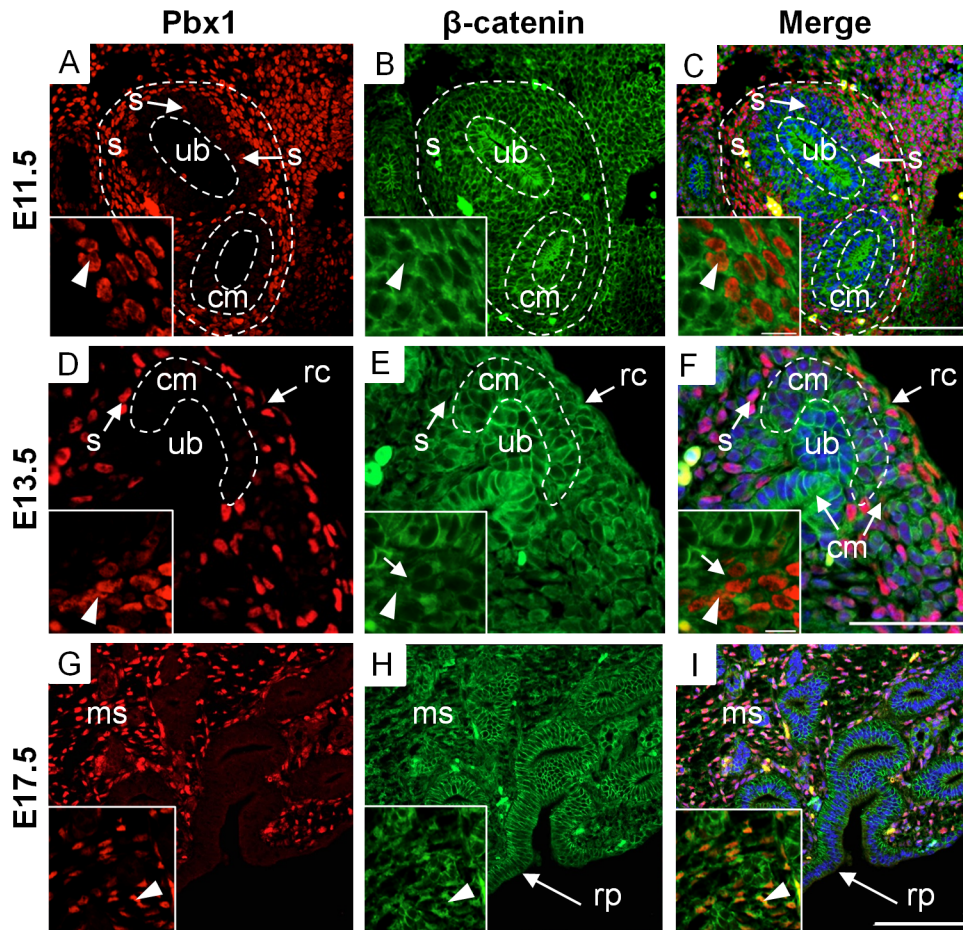
Ethics Statement

All animal studies were performed in accordance with animal care and institutional guidelines at McMaster University (Animal Utilization Protocol #100855).

RESULTS / DISCUSSION **β -catenin is expressed in distinctive patterns in the renal stroma**

To establish the expression pattern of β -catenin in the renal stroma we performed co-immunofluorescence using antibodies to β -catenin and the renal stromal nuclear marker Pbx1. We utilized a β -catenin antibody that recognizes all forms of the β -catenin protein (cadherin-bound, active, and inactive), and localizes to the membrane, cytoplasm and nucleus (Eger, Stockinger et al. 2000). The renal stroma is initially observed at E11.5 after the ureteric epithelium invades the mesenchyme (Hatini, Huh et al. 1996). At E11.5 Pbx1, a marker of all stromal cells (Supplemental Figure 3.1), is expressed in stromal cells surrounding the condensed mesenchyme and is primarily absent from the condensed mesenchyme itself (Figure 3.1A). We confirmed our previous findings that β -catenin is expressed in the condensed mesenchyme and ureteric epithelium (Bridgewater, Cox et al. 2008)(Figure 3.1B) and here we further demonstrate β -catenin co-localizes with stromal marker Pbx1 (Figure 3.1C). At E11.5, the intracellular distribution of β -catenin in Pbx1 positive cells is primarily cytoplasmic, and virtually absent from the nucleus (Figure 3.1B and C inset). Interestingly, some Pbx1 positive cells are found within the condensed mesenchyme population in close proximity to the ureteric epithelium (Figure 3.1A and C - arrow). Stromal-epithelial interactions have been shown to be essential in prostate and mammary branching morphogenesis (Cunha, Bigsby et al. 1985, Howard and Lu 2014). Therefore, the close proximity between the stroma and the ureteric epithelium may suggest possible cell-cell interactions between the renal stroma and ureteric epithelial cells.

Figure 3.1 – β -catenin is expressed in distinctive patterns in the renal stroma

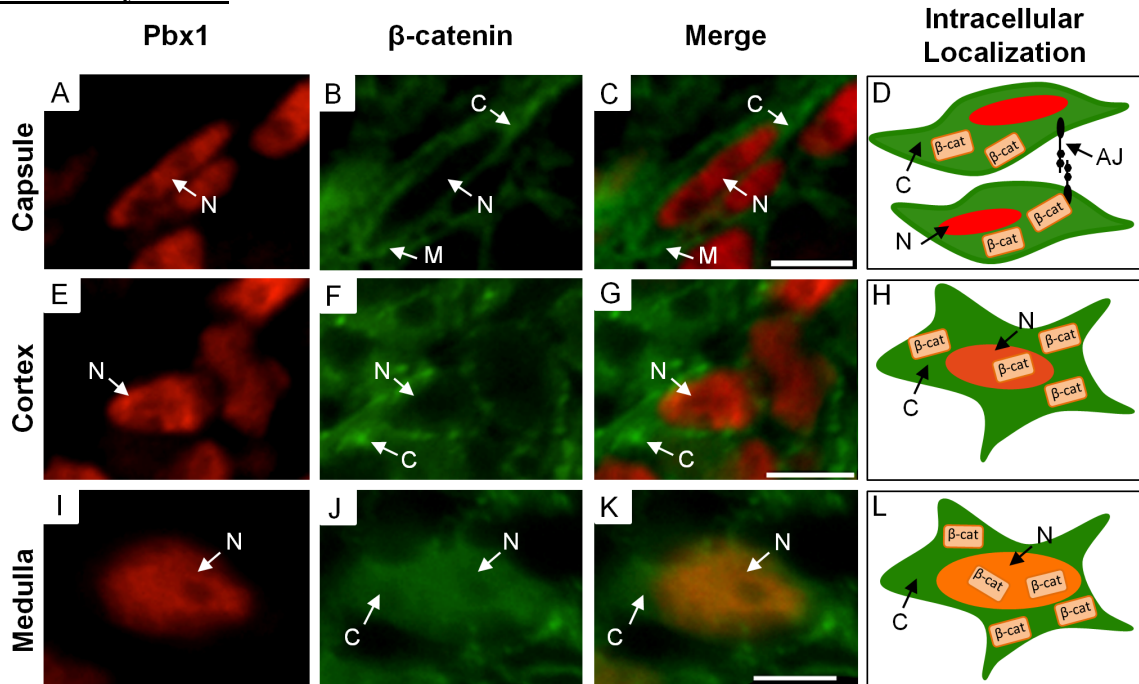


β -catenin is expressed in distinctive patterns in the renal stroma: (A-I) Immunofluorescence demonstrating β -catenin spatial and temporal expression in stromal cells. (A) At E11.5 Pbx1 is expressed in the nucleus of stromal cells (arrow head-inset) surrounding the condensing mesenchyme. Some Pbx1 positive stromal cells locate within the condensing mesenchyme, directly adjacent to epithelial cells (arrows). (B,C) At E11.5 β -catenin is expressed in the condensing mesenchyme and ureteric epithelium, and co-localizes with Pbx1 demonstrating expression in the renal stroma. At E11.5, some Pbx1 cells co-localize with β -catenin in the nuclear compartment of stromal cells (arrowhead-inset). (D) At E13.5, Pbx1 is expressed in capsular and cortical stroma surrounding the condensing mesenchyme. (E, F) At E13.5, β -catenin co-localizes in the cytoplasm of capsular stromal cells. The stromal cells located between developing nephrons express β -catenin in the cytoplasmic (arrow-inset) and nuclear compartment (arrowhead-inset). (G) At E17.5, Pbx1 marks the capsular, cortical, and medullary stroma. (H-I) β -catenin is expressed in the medullary stroma and co-localizes strongly with Pbx1 in the nuclear compartment (arrowhead-inset). (scale bar = 100 μ m, s=stroma, cm=condensing mesenchyme, ub=ureteric epithelium, rc=renal capsule, ms=medullary stroma, rp=renal pelvis).

At E13.5, the Pbx1 positive renal stroma cells are located between adjacent condensed mesenchymal populations and also form the renal capsule (Levinson, Batourina et al. 2005)(Figure 3.1D). β -catenin is expressed in both the capsular stromal cells and stromal cells located between the condensed mesenchyme (Figure 3.1 E, F). The cortical-medullary axis is established at E14.5, and after this time point (Li, Hartwig et al. 2014) the renal stroma is divided into the capsular, cortical, and medullary stroma. We observed β -catenin expression at E17.5 in cortical and capsular stroma in a pattern identical to that observed at E13.5. Further at E17.5 β -catenin is expressed in the medullary stroma (Figure 3.1G-I). Our temporal analysis reveals that β -catenin is expressed at the onset of stromal cell formation and is maintained in the different stromal cell populations throughout kidney development.

During our analysis of β -catenin expression, we observed that the intracellular distribution of β -catenin varied between the capsular, cortical, and medullary stromal compartments. In the capsular stroma, the intracellular distribution of β -catenin is primarily in the cytoplasm and membrane and virtually absent from the nucleus (Figure 3.2A-D), indicating a more prominent role in cell adhesion. In the population of cortical stroma, β -catenin is cytoplasmic and low levels are observed in the nucleus (Figure 3.2E-H). This intracellular pattern suggests an important role in cell adhesion with a more minor role in signaling and gene transcription. In contrast, within the medullary stroma, β -catenin is most highly expressed in the nuclei with lower levels in the cytoplasm (Figure 3.2I-L), suggesting a prominent role in the regulation of gene transcription. This intracellular distribution of β -catenin within these stromal compartments was maintained

throughout kidney development. These results demonstrate that each stromal cell population has a unique intracellular distribution of β -catenin suggesting unique functional roles during kidney development.

Figure 3.2 - Intracellular localization of β -catenin in capsular, cortical, and medullary stroma

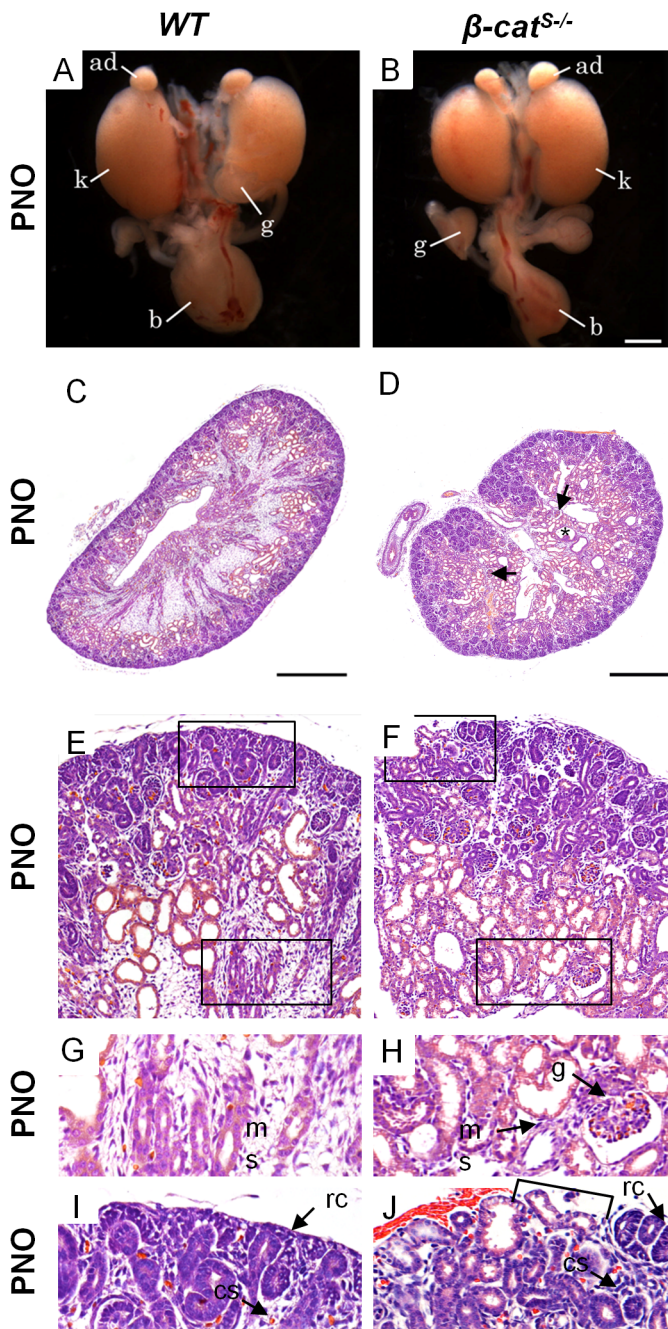
Intracellular localization of β -catenin in capsular, cortical, and medullary stroma: (A-L) Immunofluorescence showing β -catenin intracellular distribution in the capsular, cortical, and medullary stroma. (A-C) In the capsular stroma, β -catenin localizes in a membrane and cytoplasmic pattern and does not co-localize with nuclear stromal factor Pbx1. (D) Schematic diagram of the intracellular β -catenin localization and a suggested role in cell-cell adhesion via adherens junctions. (E-G) β -catenin weakly co-localizes with Pbx1 in the nuclear compartment but is primarily cytoplasmic. (H) Schematic diagram of the intracellular β -catenin localization showing possible roles in the cytoplasm and nucleus. (I-K) In the medulla, β -catenin co-localizes with Pbx1 primarily to the nuclear compartment but some cytoplasmic β -catenin expression is observed. (L) Schematic diagram of the intracellular β -catenin localization showing a more prominent role in the nucleus. (scale bar = 5 μ m, M = membrane, C=cytoplasm, N=nuclear, AJ=Adherens junctions).

Ablation of β -catenin in stromal cells leads to multiple kidney abnormalities

To investigate the role of stromally expressed β -catenin in kidney development we generated a conditional knockout mouse model whereby β -catenin was specifically deleted in the renal stroma cell lineage. We utilized a *Foxd1-Cre* transgenic mouse line (Humphreys, Lin et al. 2010) that expresses the Cre recombinase protein exclusively in the renal stroma (Das, Tanigawa et al. 2013), (Hum, Rymer et al. 2014). We crossed the *Foxd1-Cre* mice with transgenic mice containing *LoxP* sites flanking exons 2-6 of the β -catenin allele (Brault, Moore et al. 2001) resulting in the generation of mice with a genetic deletion of β -catenin from renal stromal cells (termed β -cat^{S/-}). We performed immunofluorescence using Pbx1 and β -catenin antibodies to confirm the absence of β -catenin within all stromal cells in β -cat^{S/-} mutant kidneys (Supplemental Figure 3.2). Our results demonstrate β -catenin expression was maintained in the condensed mesenchyme and ureteric epithelium but completely absent in Pbx1 positive cells during embryonic kidney development and at post-natal day 0 (PN0) in the cortex and medulla (Supplemental Figure 3.2).

β -cat^{S/-} mice died within hours after birth and kidney tissue was immediately isolated for gross and histological analysis. Analysis of the gross anatomy of kidneys from 7 different β -cat^{S/-} mutants at PN0 revealed 6 mutants with normal to slightly smaller kidneys when compared to wild-type (*WT*) (Figure 3.3A and B). One mutant demonstrated kidneys that were 50% smaller than *WT* littermates (data not shown). We then performed a histological analysis of β -cat^{S/-} kidneys. In contrast to *WT* (Figure 3.3C), β -cat^{S/-} mutant kidneys were lobular and contained numerous large ureteric epithelial derived cysts

(Supplemental Figure 3.3) in the medulla and cortex (Figure 3.3D). In addition, we observed glomeruli abnormally located in the medulla (Figure 3.3E-H) and tubules were inappropriately located just beneath the renal capsule (Figure 3.3E, F, I, J). $\beta\text{-cat}^{S/-}$ mutant kidneys demonstrate a phenotype that is consistent with previous reports by Yu et al (Yu, Carroll et al. 2009). Yu et al demonstrated that the loss of β -catenin from the medullary stroma cells resulted in the cystic transformation of collecting ducts (Yu, Carroll et al. 2009). Their study concluded that ureteric epithelial cells secrete Wnt7b which activates the canonical Wnt pathway in medullary stroma resulting in elongation and maintenance of loops of Henle and collecting ducts (Yu, Carroll et al. 2009).

Figure 3.3 – β -cat^{S/-} mutants demonstrate multiple kidney abnormalities

(A,B) Gross anatomy of PNO *WT* and β -cat^{S/-} kidneys show comparable size and shape. (C-J) In contrast to *WT*, histological analysis of β -cat^{S/-} mutant kidneys demonstrate numerous kidney abnormalities. (C,D) As compared to *WT*, β -cat^{S/-} mutant kidneys were lobular, lacked a distinct boarder, contained numerous cysts in the medulla and cortex (star), with an ill-defined cortical medullary axis and misplaced glomeruli (arrow). (E-J)

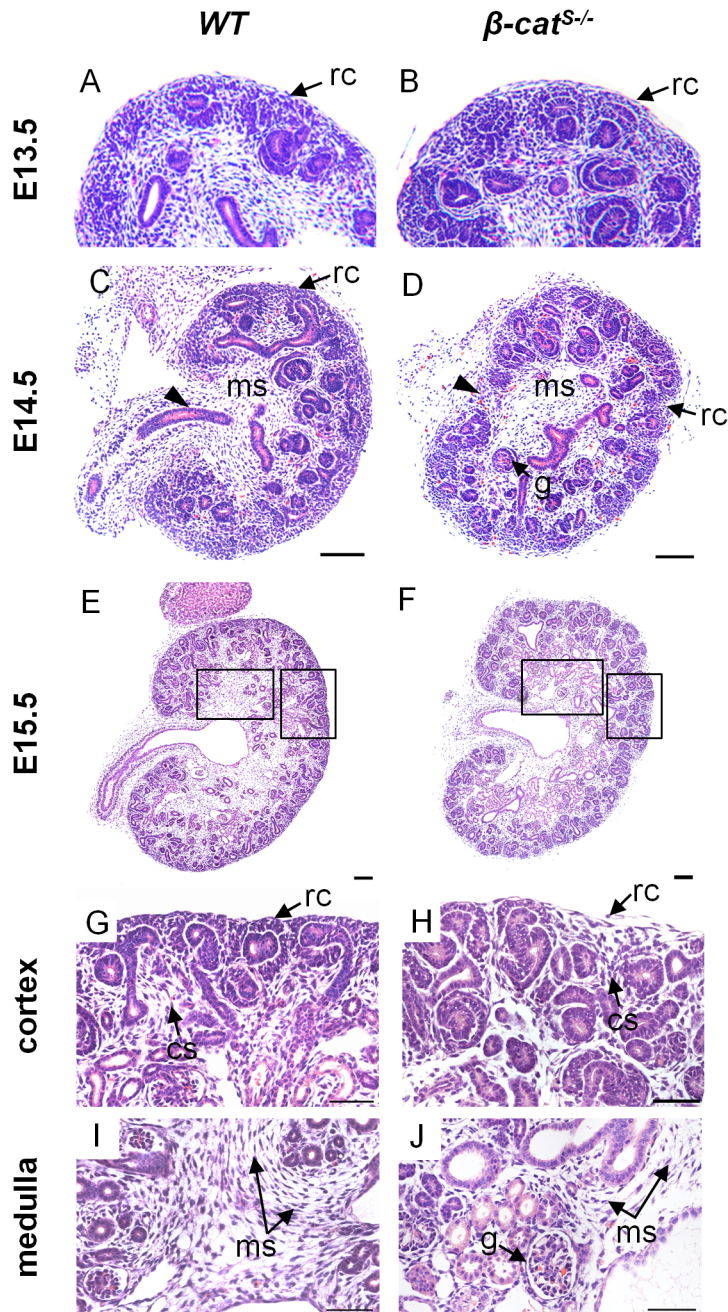
In contrast to *WT*, high magnification of $\beta\text{-cat}^{S/-}$ kidneys at PN0 revealed a non-adherent sporadic renal capsule (F and J), misplaced tubules just under the renal capsule (F and J), glomeruli in the medulla (H) and a marked reduction in medullary stroma (H). (A, B scale bar = 1mm, C, D scale bar = 100 μ m, ad=adrenal gland, k=kidney, b=bladder, rc=renal capsule, cs=cortical stroma, ms=medullary stroma, g=glomerulus).

In addition, β -cat^{S/-} kidneys revealed a paucity of renal capsule and sporadic non-adherent capsular cells (Figure 3.3I,J). This data combined with our expression analysis in which β -catenin primarily localizes to the cell membrane of the capsular stroma suggest a primary role in cell-cell adhesion. However, there are regions where the renal capsule remains intact and this could be due to the compensatory role of γ -catenin (plakoglobin) as previously described (Zhurinsky, Shtutman et al. 2000).

To determine when the mutant phenotype is initially established, we performed a histological analysis of β -cat^{S/-} kidneys at various embryonic time points including E13.5, E14.5, and E15.5. β -cat^{S/-} kidneys at E13.5 were indistinguishable from *WT* littermates (Figure 3.4A, B). By E14.5, β -cat^{S/-} kidneys revealed glomeruli in the medulla and a loosely adherent renal capsule (Figure 3.4C, D). At E15.5, β -cat^{S/-} kidneys displayed sparse, loosely packed cortical stroma between the adjacent condensed mesenchymal populations, glomeruli in the medulla, sparse medullary stroma, and the non-adherent renal capsule phenotype persisted (Figure 3.4E-J). We also analyzed branching morphogenesis and nephrogenesis and observed no overt changes in branch generation or nephrogenesis in β -cat^{S/-} kidneys (Supplemental Figure 3.4). We next analyzed the renal stroma cell population using various stromal markers Meis1/2, Foxd1, Tenascin C, and Pbx1 (Figure 3.5A-L). While the capsular, cortical, and medullary stroma were present we noted a reduction in the medullary stromal cell population (Figure 3.5C,D,G,H). To determine if apoptosis was a contributing factor to the reduced medullary stroma we performed a TUNEL analysis. Indeed the analysis showed increases in apoptosis within the medullary stroma at E15.5 (Figure 3.5M,N). Combined, these studies highlight the

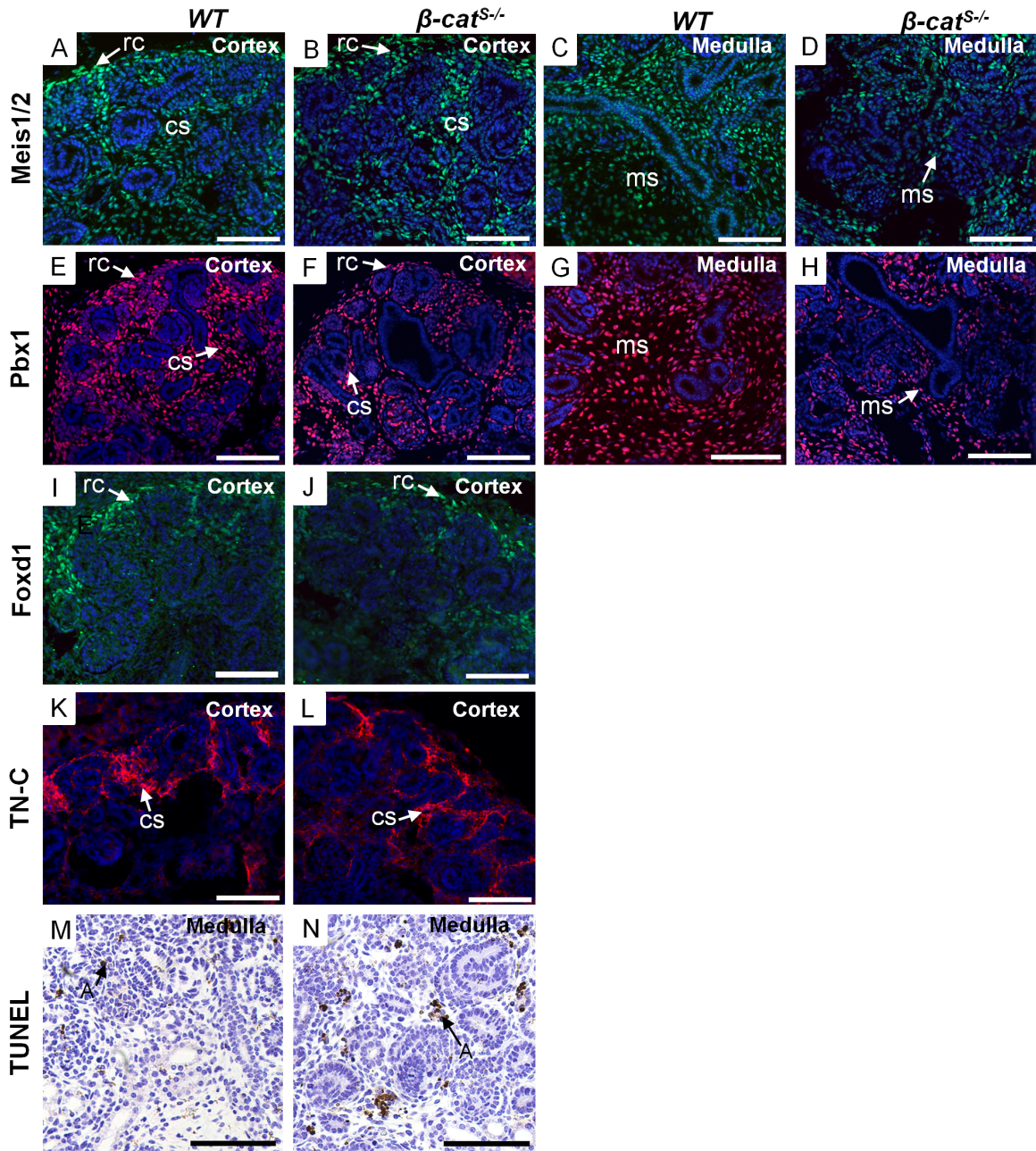
role of stromally expressed β -catenin in the proper formation of the distinct stromal compartments.

Figure 3.4 – Temporal analysis of the embryonic kidney phenotype in β -cat^{S/-} mutant



Temporal analysis of the embryonic kidney phenotype in β -cat^{S/-} mutants: (A, B) Histological analysis of *WT* and β -cat^{S/-} embryonic kidneys at E13.5 demonstrates no abnormalities in the stromal population, developing nephrons, or kidney patterning. (C, D) In contrast to *WT* at E14.5, β -cat^{S/-} kidneys demonstrate abnormally located glomeruli, and a non-adherent irregular patterned renal capsule. (E-J) In contrast to *WT* at E15.5, the non-adherent capsular phenotype persists in β -cat^{S/-} kidneys (H) and the cortical stroma is reduced and loosely packed (H). Similarly, the medullary stroma in β -cat^{S/-} kidneys is markedly reduced compared to *WT* (J) and glomeruli are also abnormally located within the medulla (rc= renal capsule, cs = cortical stroma, ms=medullary stroma, g=glomerulus, arrowhead = ureter). Scale Bar C-F =100 μ m, G-J=50 μ m

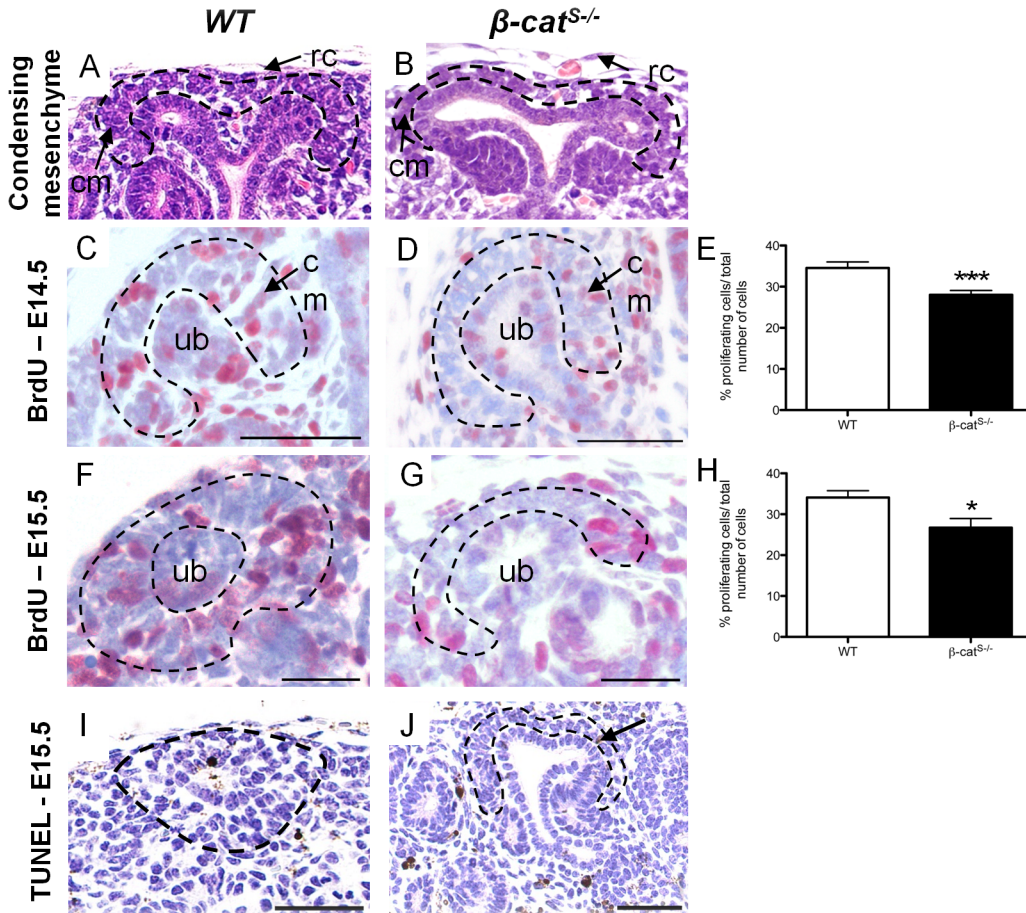
Figure 3.5 – Investigation of the renal stroma in β -cat^{S-/-} mutant kidneys



Investigation of the renal stroma in β -cat^{S/-} mutant kidneys :(A-L) Analysis of the renal stroma using stromal markers; Meis1/2, Pbx1, Foxd1, and TN-C at E15.5. As compared to *WT*, no overt changes were observed in the cortical stroma with respect to Meis1/2 (A, B), Pbx1 (E, F), Foxd1 (I, J), and TN-C (K, L). However, a reduction of Meis1/2 (C, D) and Pbx1 (G, H) was observed in the medullary region in β -cat^{S/-} kidneys. (M, N) TUNEL assay at E15.5 reveals an increase in apoptosis in the medullary stroma of β -cat^{S/-} kidneys compared to *WT*. (rc= renal capsule, cs = cortical stroma, ms=medullary stroma, A=apoptosis). Scale Bar =50 μ m

Stromally expressed β -catenin modulates Wnt9b expression in the ureteric epithelium

During kidney development the ureteric epithelial tips induce the mesenchyme population to tightly cluster around the ureteric epithelium tips and form a 3-4 cell-layer thick population of condensed mesenchymal cells (Little and McMahon 2012). Notably, the condensed mesenchyme population surrounding the ureteric epithelial tips in β -cat^{S/-} mutant kidneys was reduced to a single loosely packed layer of condensed mesenchymal cells when compared to *WT* (Figure 3.6 A, B). This finding suggests an important role for stromally expressed β -catenin in the induction of mesenchyme progenitors during kidney development. Signals from the ureteric epithelium promote proliferation of these mesenchyme progenitors (Carroll, Park et al. 2005, Karner, Das et al. 2011). We next examined whether the reduction in the condensed mesenchymal population in β -cat^{S/-} kidneys resulted from changes in cell proliferation. We quantified the percentage of proliferating cells at E14.5 and E15.5 specifically in the condensed mesenchyme using BrdU labeling. The percentage of proliferating condensing mesenchyme cells was reduced in β -cat^{S/-} mutant kidneys at E14.5 (WT: 34.56% versus β -cat^{S/-}: 28.02%) and at E15.5 (WT: 34.09% versus β -cat^{S/-}: 26.73%) (Figure 3.6C-H). In contrast, we observed virtually no apoptosis within the condensing mesenchyme population in either β -cat^{S/-} mutants or *WT* littermates (Figure 3.6I,J). This data demonstrates the reduction in the condensed mesenchyme in β -cat^{S/-} is most likely caused by reduced proliferation of the progenitor cell population.

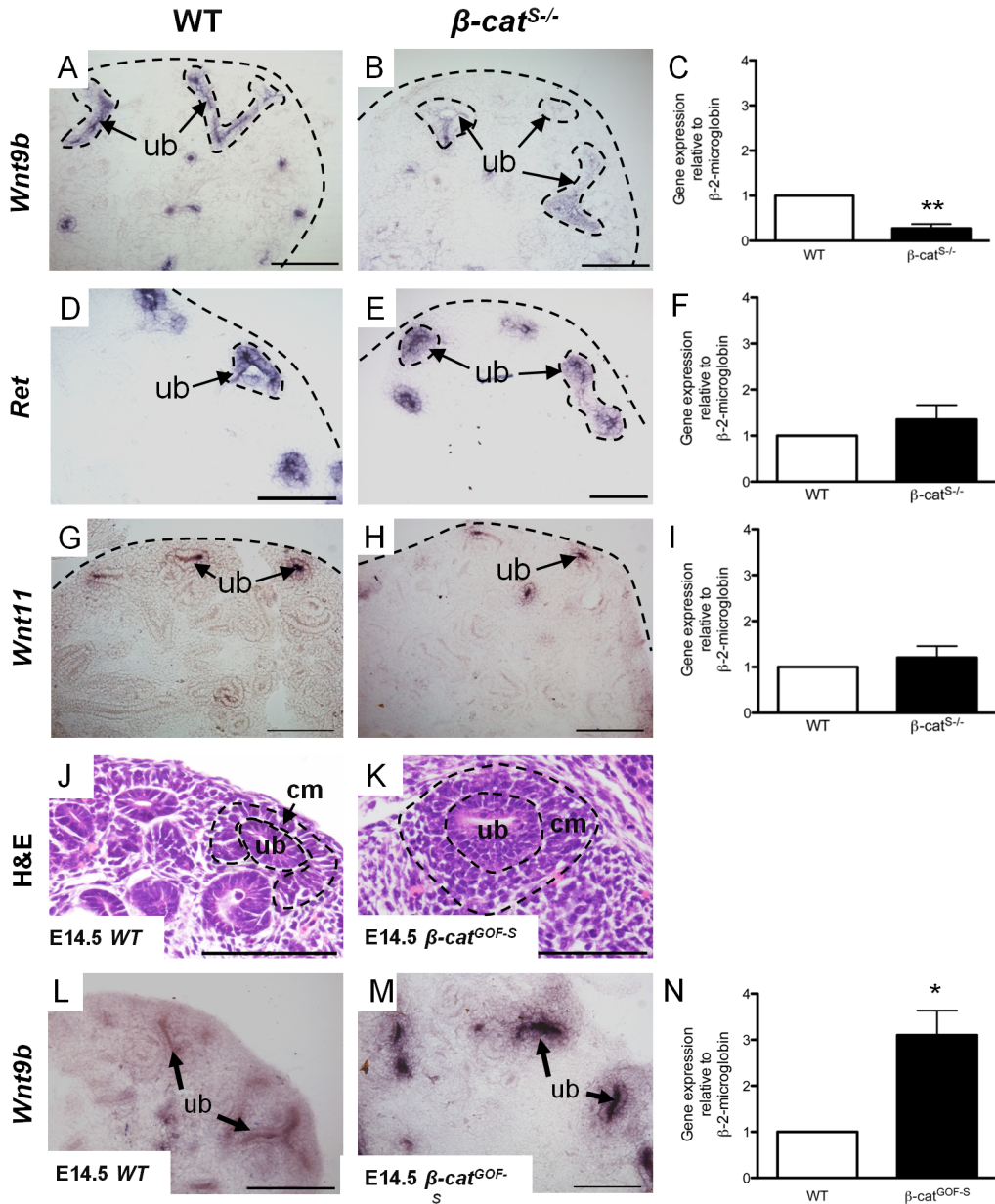
Figure 3.6 – The condensing mesenchyme cell population is reduced in β -cat^{S/-} mutant kidneys

The condensing mesenchyme cell population is reduced in β -cat^{S/-} mutant kidneys: (A,B) As compared to *WT*, which demonstrates 3-4 cell layers of aggregated condensing mesenchyme, β -cat^{S/-} kidneys display a reduced, single cell layer of loosely aggregated condensing mesenchyme. (C-H) Analysis of cell proliferation in the condensing mesenchyme was performed using BrdU cell proliferation assay. (C-E) As compared to *WT*, β -cat^{S/-} mutants demonstrated a 6.46% reduction in condensing mesenchyme cell proliferation at E14.5 (*WT*, 34.56% \pm 1.45, n=28 versus β -cat^{S/-}, 28.02% \pm 1.05, n=27, p=0.0006). (F-G) At E15.5 β -cat^{S/-} mutants demonstrated a 7.35% reduction in condensing mesenchyme cell proliferation when compared to *WT* (*WT*, 34.09% \pm 1.65, n=17 versus β -cat^{S/-}, 26.73% \pm 2.21, n=15, p=0.01). (I,J) A TUNEL assay at E15.5 did not reveal any changes in apoptosis in the condensing mesenchyme between *WT* and β -cat^{S/-}. Scale Bar = 50 μ m

Wnt9b is the key signaling factor secreted by the ureteric epithelium and controls the proliferation of progenitors and the induction of mesenchymal-to-epithelial transition of the nephrogenic progenitor population (Karner, Das et al. 2011). Therefore we analyzed *Wnt9b* expression by section in situ hybridization. We observed a marked reduction in *Wnt9b* mRNA expression in the majority of ureteric epithelial cells in $\beta\text{-cat}^{S-/-}$ kidneys (Figure 3.7A,B). We performed qRT-PCR in $\beta\text{-cat}^{S-/-}$ kidneys using 5 mutant kidneys from 3 separate litters, and confirmed a 72% reduction in *Wnt9b* mRNA levels in $\beta\text{-cat}^{S-/-}$ kidneys (Figure 3.7C). In support of these findings Wnt9b hypomorphs display a similar phenotype to our $\beta\text{-cat}^{S-/-}$ mutants (Karner, Chirumamilla et al. 2009, Das, Tanigawa et al. 2013). These results demonstrate a loss of β -catenin in stromal cells leads to reduced *Wnt9b* levels in the ureteric epithelium. To ensure the reductions in *Wnt9b* expression were not caused by a general disruption in the ureteric epithelium integrity, we analyzed *Ret* and *Wnt 11*, two other essential ureteric epithelial markers, and show no changes in their mRNA expression by in situ hybridization and qRT-PCR (Figure 3.7D-I). These results led us to hypothesize that stromally expressed β -catenin modulates *Wnt9b* expression in the ureteric epithelium. To support this hypothesis, we generated a second mutant mouse model in which β -catenin was overexpressed exclusively in kidney stromal cells ($\beta\text{-cat}^{GOF-S}$). The histological analysis of $\beta\text{-cat}^{GOF-S}$ kidneys revealed a marked increase in the progenitor population at E14.5 (Figure 3.7J,K). We next performed in situ hybridization and observed marked increases in *Wnt9b* expression at E14.5 (Figure 3.7L,M). We confirmed these changes by qRT-PCR and demonstrated a 310% increase in *Wnt9b* expression in $\beta\text{-cat}^{GOF-S}$ (Figure 3.7N). Taken together, analysis

of $\beta\text{-cat}^{S/-}$ and $\beta\text{-cat}^{GOF-S}$ mutants implicate stromally expressed β -catenin in the modulation of *Wnt9b* expression in the ureteric epithelium.

Figure 3.7 – β -catenin in the renal stroma modulates *Wnt9b* expression in ureteric epithelial cells



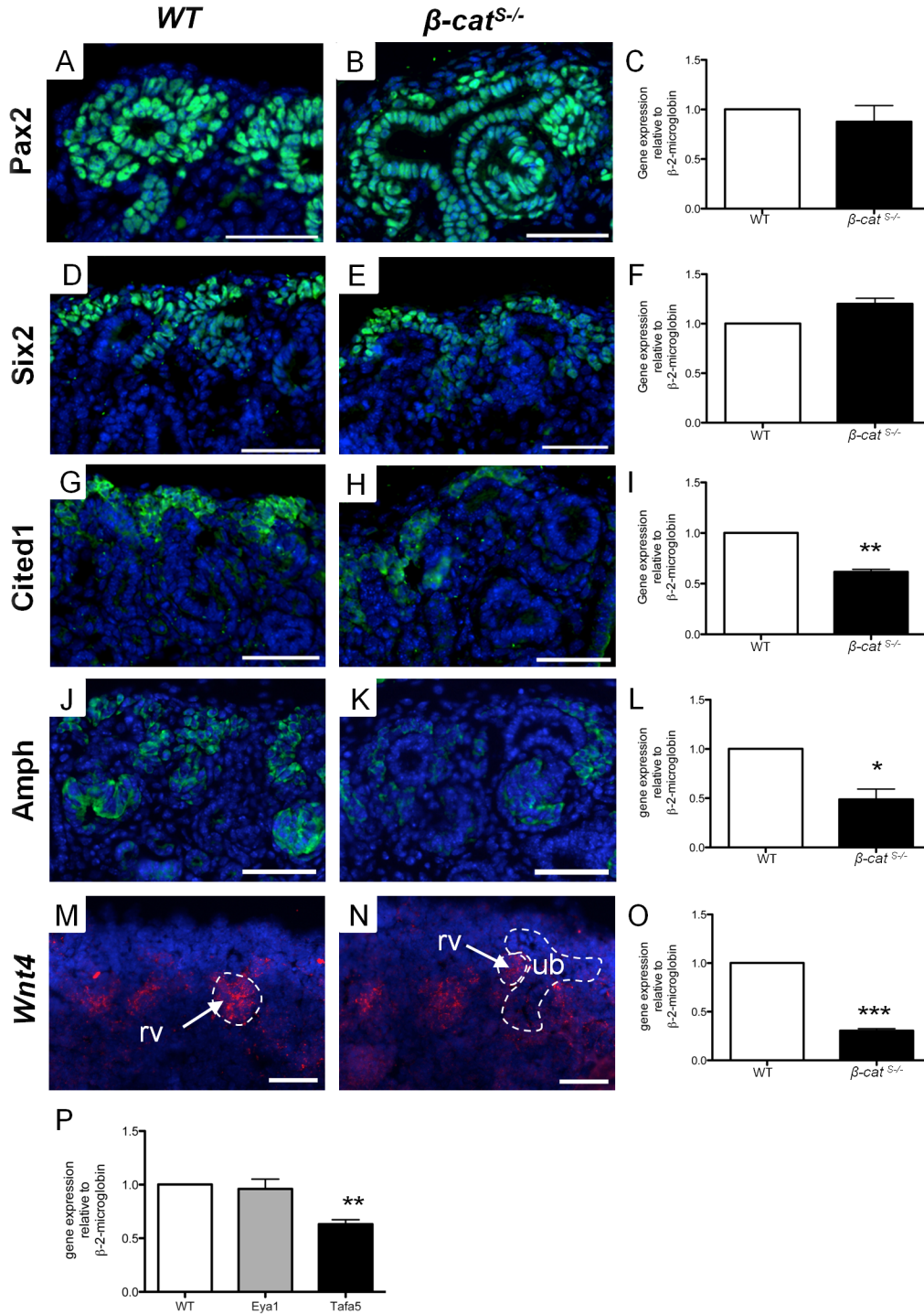
β -catenin in the renal stroma modulates *Wnt9b* expression in ureteric epithelial cells: (A-C) When compared to *WT*, In situ hybridization and real-time quantitative PCR for *Wnt9b* demonstrates *Wnt9b* mRNA expression is significantly reduced (1.00 versus 0.29, $p=0.008$) in E14.5 β -cat^{S-/} kidneys. (D-I) In situ hybridization and Real-time quantitative PCR for *Ret* and *Wnt11* demonstrated no differences in mRNA expression between *WT* and β -cat^{S-/} at E14.5. (J-K) Histological analysis of β -cat^{GOF-S} mutant kidneys demonstrate a marked increase in condensing mesenchyme population when compared to *WT* at E14.5. (L-N) In situ hybridization and quantitative PCR demonstrate *Wnt9b* expression in β -cat^{GOF-S} kidneys was significantly increased (1.02 versus 3.102, $p=0.021$) as compared to *WT* at E14.5. (scale bar = 50 μ m, rc=renal capsule, cm=condensing mesenchyme, ub = ureteric epithelium).

Deletion of β -catenin in stromal cells impairs Wnt9b signaling to the nephrogenic progenitors

Wnt9b signaling controls genes in the condensed mesenchyme which promote nephron formation through the β -catenin mediated canonical Wnt pathway (Karner, Das et al. 2011). To determine whether the reduction in *Wnt9b* expression disrupted Wnt9b downstream signaling, we analyzed the expression of known Wnt9b-independent and -dependent targets in β -cat^{S/-} mutants. We first analyzed the expression of Wnt9b independent genes, *Pax2*, *Six2*, and *Eya1*, which are all necessary for the proper induction of the nephrogenic progenitors (Mugford, Sipila et al. 2008). First, we performed immunofluorescence for Pax2 and Six2 on *WT* and β -cat^{S/-} mutant kidneys at E15.5. The number of Pax2 positive cells surrounding the ureteric epithelium was markedly reduced compared to *WT*, which is consistent with our finding of decreased induced nephrogenic progenitors (Figure 3.8A,B). Using qRT-PCR at E14.5, a time point prior to the reduced progenitor population, we demonstrated no significant change in *Pax2* mRNA expression in β -cat^{S/-} mutant kidneys when compared to *WT* (Figure 3.8C). Similarly, immunofluorescence analysis of Six2 revealed a modest decrease in the number of Six2 induced nephrogenic cells (Figure 3.8D, E) while qRT-PCR showed the levels of *Six2* expression were not changed in β -cat^{S/-} kidneys (Figure 3.8F). We also analyzed *Eya1*, a third Wnt9b independent gene (Gong, Yallowitz et al. 2007), which demonstrated no significant alterations in expression in β -cat^{S/-} kidneys (Figure 3.8P). Taken together, this analysis confirms the reduction in the number of nephrogenic progenitor cells in β -cat^{S/-} kidneys but does not affect the expression levels of these

Wnt9b-independent genes. Therefore Pax2, Six2, and Eya1 are not likely contributing to the reduction of the induced nephrogenic progenitors.

Figure 3.8 - β -cat^{S/-} mutants demonstrate altered Wnt9b signaling to the condensing mesenchyme



β -cat^{S/-} mutants demonstrate altered Wnt9b signaling to the condensing mesenchyme - (A-P) Analysis of Wnt9b dependent and independent gene targets by immunofluorescence and real-time quantitative PCR at E15.5 and E14.5 respectively. (A-F) In contrast to *WT* at E15.5, the number of Pax2 and Six2 positive cells in the condensing mesenchyme was reduced in β -cat^{S/-} kidneys. No changes were observed in the *Pax2* and *Six2* mRNA expression levels at E14.5 by qRT-PCR. (G-I) Both the number of Cited 1 positive cells and *Cited 1* mRNA expression levels were reduced (1.00 versus 0.62, p=0.003) in β -cat^{S/-} kidneys. (J-L) The levels of Amphiphysin were significantly reduced in the condensing mesenchyme at both the protein and mRNA levels in β -cat^{S/-} kidneys (1.01 versus 0.48, p=0.025) (M-O) In situ hybridization and qRT-PCR analysis of *Wnt4* demonstrates a reduction in *Wnt4* mRNA levels in E14.5 β -cat^{S/-} kidneys (1.00 versus 0.30, p=0.0007). (P) QRT-PCR of Wnt9b-independent gene *Eyal* demonstrates no changes in mRNA expression levels in β -cat^{S/-} kidneys. In contrast, Wnt9b-dependent gene *Tafa5* (1.00 versus 0.42, p=0.003) was significantly decreased in β -cat^{S/-} kidneys (scale bar = 50 μ m) (rv=renal vesicle, ub=ureteric bud).

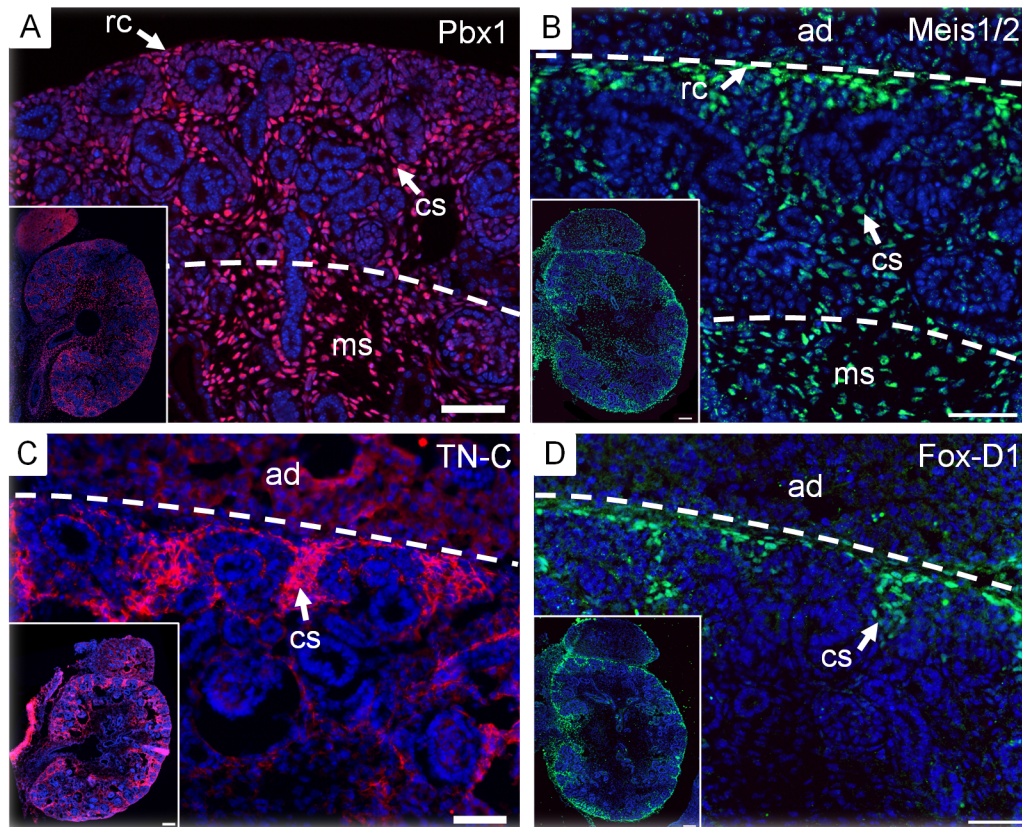
To determine if the reduction in *Wnt9b* translates to decreased Wnt9b-dependent downstream targets in the nephrogenic progenitors, we analyzed *Cited1*, *Amph*, *Tafa5* and *Wnt4* (Karner, Das et al. 2011). First, we performed immunofluorescence for Cited1 and Amph at E15.5. β -cat^{S/-} mutants demonstrated reduced Cited1 and Amph nephrogenic progenitors. The cells that expressed Cited1 and Amph demonstrated decreased protein expression levels when compared to *WT* (Figure 3.8G,H,J,K). We confirmed a 38% and 47% reduction in *Cited 1* and *Amph* mRNA respectively at E14.5 in β -cat^{S/-} kidneys using qRT-PCR (Figure 3.8F, I). In addition, Wnt9b dependent targets *Wnt4* and *Tafa5* also demonstrated reduced mRNA expression levels (Figure 3.8M-P). Our results are consistent with previous reports in *Wnt9b* hypomorph mice and Wnt9b null mice (Karner, Chirumamilla et al. 2009, Karner, Das et al. 2011), and strongly support a role for stromally expressed β -catenin in the regulation of *Wnt9b* expression and its downstream signaling to the condensing mesenchyme.

β -catenin is expressed in distinctive intracellular patterns within the capsular, cortical, and medullary renal stroma. However the role of stromally expressed β -catenin in the regulation of kidney development is not described. Ablation of β -catenin in stromal cells results in numerous kidney abnormalities, most notably a reduction in the condensing mesenchyme. *Wnt9b* expression in the ureteric epithelium and Wnt9b-dependent genes in the nephron progenitors were markedly reduced in β -cat^{S/-} mutants. Our findings support a model by which stromally expressed β -catenin regulates the expression of *Wnt9b* and its downstream targets, thereby regulating the induction of nephrogenic progenitors. The molecular mechanisms by which stromal cells control

Wnt9b expression in the ureteric epithelium remain to be determined. We propose three possible mechanisms by which stromally expressed β -catenin modulates *Wnt9b* expression in the ureteric epithelium. First, previous studies have shown stromal cells secrete factors that affect gene expression in epithelial cells in other model systems (Cullen-McEwen, Caruana et al. 2005, Li, Hartwig et al. 2014). The localization of β -catenin to the nucleus in the cortical and medullary stroma suggests β -catenin may control the expression of secreted factors that signal to the adjacent ureteric epithelium to control *Wnt9b* expression. These potential secreted factors are the focus of our future studies. Second, stromal-epithelial cell interactions have been shown to regulate the development of other organ systems (Cunha, Bigsby et al. 1985, Howard and Lu 2014). Therefore, it is possible that stromal cells directly interact with the ureteric epithelial population in the kidney. We and others have demonstrated that the renal stroma is directly adjacent to the ureteric epithelium and therefore is ideally located to form direct cell-cell interactions with ureteric epithelial cells to affect cellular processes. Third, recent studies have shown that the renal stromal and condensed mesenchyme form direct cell interactions through stromally expressed proto-cadherin Fat4 (Das, Tanigawa et al. 2013). Thus, it is possible that stromal cells, via the mesenchyme cell population, modulate Wnt9b expression in epithelial cells. Taken together our studies highlight that the renal stroma communicates with the ureteric epithelium to modulate gene expression and control kidney development.

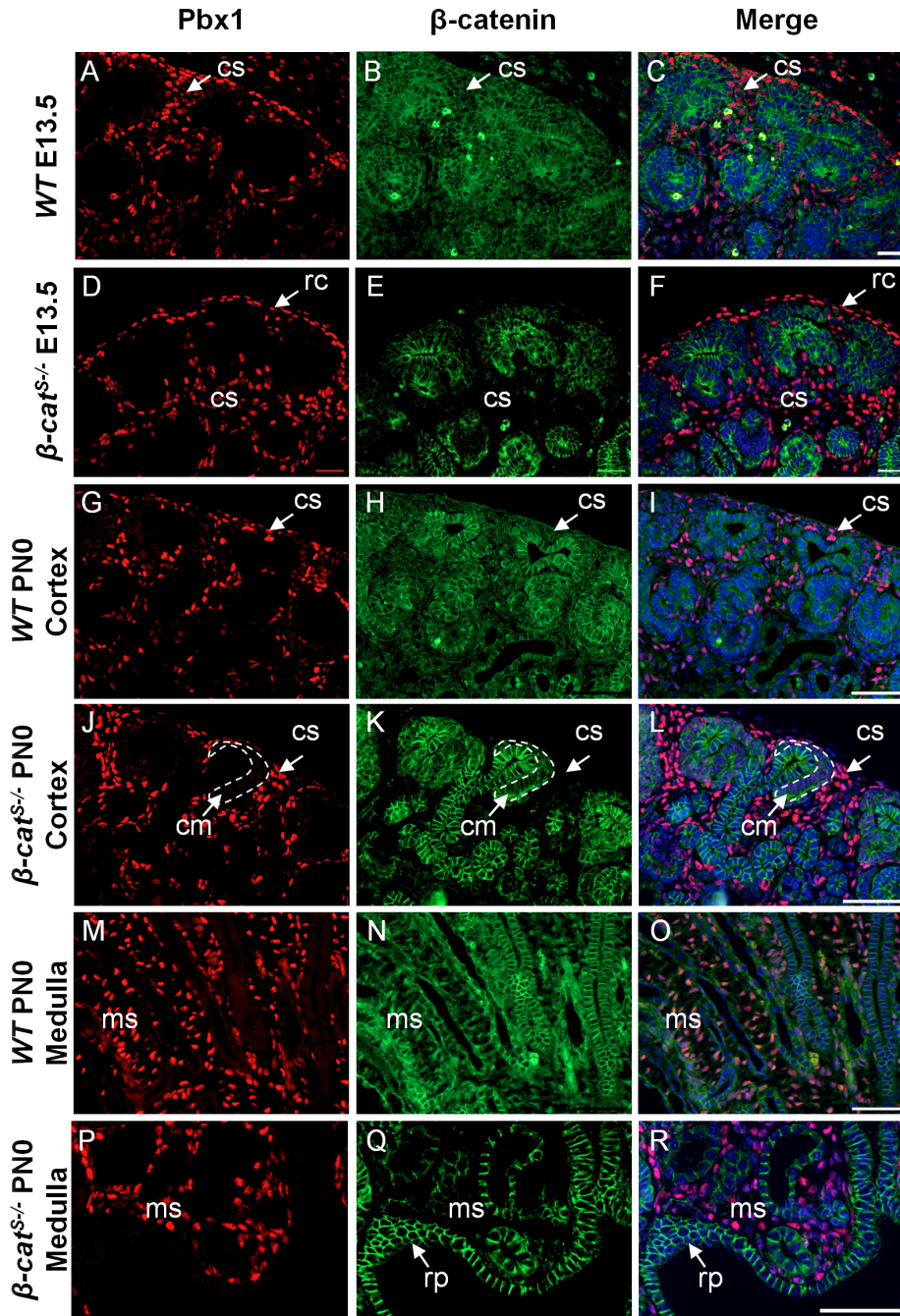
ACKNOWLEDGMENTS

We would like to thank Dr. Bradley Doble and Dr. Judith West-Mays for their helpful discussions and Michael Romaniuk for the artistic contributions in Fig 2. This study was funded by the Kidney Foundation of Canada (DB) and the National Sciences and Engineering Research Council (NSERC).

SUPPLEMENTARY MATERIAL**Supplemental Figure 3.1 - The Pbx1 antibody targets the capsular, cortical, and medullary stroma**

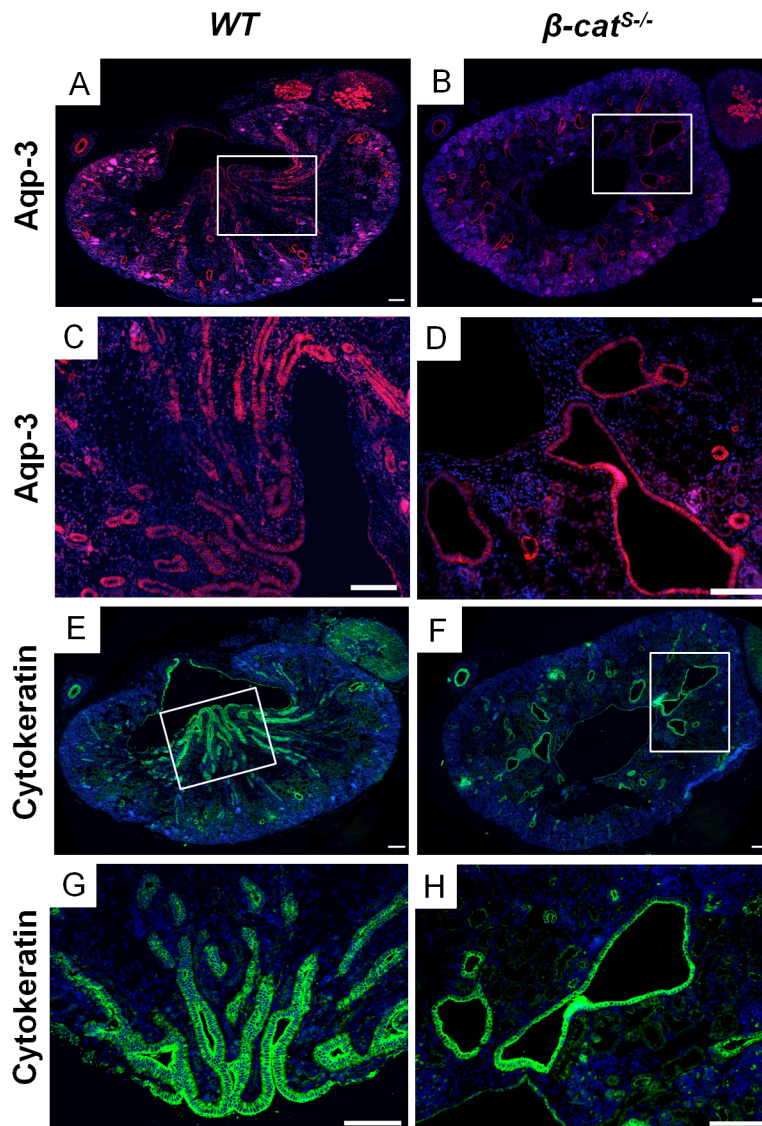
The Pbx1 antibody targets the capsular, cortical, and medullary stroma: (A-D) Immunofluorescence analysis of Pbx1, Meis1/2, TN-C, and Foxd1 in *WT* kidneys at E15.5. Pbx1 (A) and Meis1/2 (B) mark the capsular (rc), cortical (cs), and medullary stroma (ms), whereas TN-C (C) and Foxd1 (D) expression is restricted to the capsular and cortical stroma between the developing nephrons. The insets demonstrate the expression pattern of each marker in the whole kidney (scale bar = 50 μm, ad= adrenal gland, cs = cortical stroma, ms = medullary stroma, rc = renal capsule).

Supplemental Figure 3.2 - Generation of mutant mice with stroma specific deletion of β -catenin.



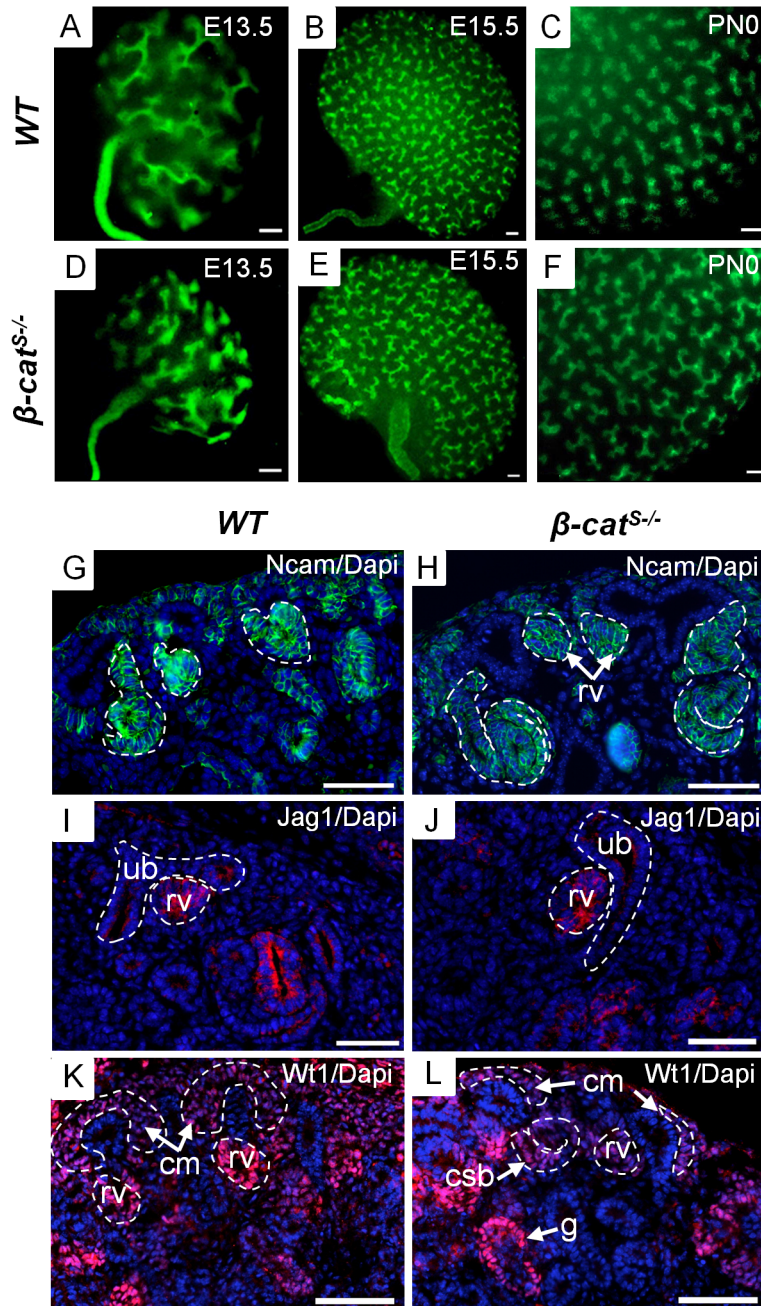
Generation of mutant mice with stroma specific deletion of β -catenin: (A-R)

Pbx1 and β -catenin immunofluorescence demonstrating the loss of β -catenin from stromal cells in β -cat^{S/-} kidneys. (A-F) At E13.5 in β -cat^{S/-} kidneys, β -catenin is not expressed in Pbx1 positive stromal cells. β -catenin expression is maintained in the ureteric epithelium and mesenchyme populations. (G-R) In β -cat^{S/-} kidneys at PN0 β -catenin is not expressed in capsular, cortical or medullary stroma. β -catenin expression persists in the ureteric epithelium and mesenchyme populations. (scale bar = 50 μ m, ub=ureteric epithelium, cm=condensing mesenchyme, s=stroma, cs=cortical stroma, ms=medullary stroma, rp=renal papilla, rc=renal capsule).

Supplemental Figure 3.3 – Characterization of cyst origin in β -cat^{S/-}

Characterization of cyst origin in β -cat^{S/-}: (A-H) Expression analysis of collecting duct markers Aquaporin-3 (A-D) and Cytokeratin (E-H) in *WT* and β -cat^{S/-} kidneys at PN0. All cysts observed in β -cat^{S/-} kidneys originated from the ureteric epithelium. No cysts were found in the tubules or loops of Henle.

Supplemental Figure 3.4 – Branching morphogenesis and Nephrogenesis are not disrupted in β -cat^{S/-} kidneys



Branching morphogenesis and Nephrogenesis are not disrupted in β -cat^{S/-} kidneys: (A-F) Whole-mount branching analysis using the ureteric epithelium marker cytokeratin at E13.5 (A,D), E15.5 (B,E), and PN0 (C,F). No overt changes were observed between *WT* and β -cat^{S/-} kidneys. (G-L) Immunofluorescence analysis of nephrogenic markers

Ncam (G,H), Jag1 (I,J), and Wt-1 (K,L) in *WT* and β -*cat*^{S/-} kidneys at E15.5. Despite the reduction in condensing mesenchyme, β -*cat*^{S/-} kidneys undergo nephrogenesis and form mature nephrons (glomerulus in L). (scale bars A-F = 100 μ m, G-L=50 μ m) (rv=renal vesicles, ub= ureteric bud, csb=comma-shaped body, cm= condensing mesenchyme, g= glomerulus).

CHAPTER 4

Stromally expressed β -catenin controls medullary stromal development via regulation of cell survival

Authors: Felix J Boivin, Janice Lim, Darren Bridgewater

Corresponding Author: Darren Bridgewater, Pathology and Molecular Medicine, McMaster University Medical Centre, 1200 Main St. West, Hamilton, Ontario, Canada L8N 3Z5. Phone (905) 525-9140 ext. 20754, Fax (905)-546-1129, Email: Bridgew@mcmaster.ca

Citation: In preparation for submission to *Developmental Biology*

PREFACE***Significance to thesis***

In chapter 3 we demonstrated that a loss of stromal β -catenin resulted in defects in the renal capsule, the renal cortex, and the medulla. A histological analysis of stromal β -catenin deficient kidneys revealed non-adherent capsular stromal cells, a reduction of nephrogenic progenitors in the renal cortex, and a lack of medulla. This suggests distinct roles for β -catenin in the different stromal compartments. The study presented in chapter 3 focused on the role of stromal β -catenin in the regulation of the nephrogenic progenitors in the renal cortex. However, the role of β -catenin in the regulation of medulla formation is not clear. Additionally, the mechanisms that control the development, maintenance, and differentiation of the stromal populations are poorly defined. Therefore, in chapter 4 we explore the role of β -catenin in medullary stroma development.

Authors' contribution

Felix J. Boivin conceived and designed the study, performed and supervised all experiments, performed and supervised all data analysis, wrote the original draft of the manuscript.

Janice Lim assisted in experiments and analysis.

Darren Bridgewater contributed to the design of the study, assisted in the interpretation of the data, contributed to refining the original draft of the manuscript.

ABSTRACT

The renal stroma is a population of matrix-producing fibroblast cells essential for kidney development by modulating branching morphogenesis and nephrogenesis. Yet the development, differentiation, and maintenance of the stroma are not well defined. The transcriptional co-activator β -catenin is essential for the formation of the cortico-medullary axis and the development of the medullary compartment. While a deletion of β -catenin specifically in stromal cells results in a lack of medulla, the role of β -catenin in medullary development is not clear. Here we demonstrate that the defects in the cortico-medullary axis and the lack of medullary compartment are primarily due to a reduction in the medullary stroma. We demonstrate that a loss of stromal β -catenin primarily affects the differentiation between cortical and medullary stroma and results in increased stromal apoptosis at the cortico-medullary junction. Our results indicate β -catenin controls stromal cell survival by modulating the levels of anti-apoptotic genes. This regulation possibly results from the formation of a new transcriptional complex that binds to the promoter region of anti-apoptotic genes to regulate the differentiation between cortical and medullary stroma.

Key words: Renal stroma, β -catenin, Apoptosis, Bcl2l1, Medullary development

INTRODUCTION

Stromal cells are a population of matrix-producing fibroblast cells found within the kidney parenchyma that provide a supportive framework for the nephrons and collecting ducts and regulate interstitial pressure within the kidney (Garcia-Estan and Roman 1989, Ekblom and Weller 1991). Recent studies have demonstrated that stromal cells also play essential roles in the developing kidney. Stromal cells modulate nephrogenesis by forming direct cell-cell interactions with the nephron progenitors of the condensed mesenchyme to control the balance between proliferation and differentiation (Das, Tanigawa et al. 2013, Bagherie-Lachidan, Reginensi et al. 2015). Similarly, stromal factors such as *Raldh2*, *Ecm1*, and *Pigf1* modulate communication between the stroma and the ureteric epithelium for proper branching and elongation of the collecting duct system (Mendelsohn, Batourina et al. 1999, Batourina, Gim et al. 2001, Zhang, Palmer et al. 2003, Paroly, Wang et al. 2013). The ablation of all stromal progenitors results in delayed branching of the epithelium and an expansion of the nephron progenitors (Das, Tanigawa et al. 2013, Hum, Rymer et al. 2014). In the progression of chronic kidney disease, stromal-derived pericytes promote fibrosis development by undergoing myofibroblast transdifferentiation and increasing production of extra-cellular matrix proteins (Humphreys, Lin et al. 2010). Similarly, acute kidney injury promotes proliferation of medullary interstitial fibroblasts and myofibroblast transdifferentiation via the Wnt/ β -catenin pathway, suggesting a recapitulation of developmental pathways post injury. Although studies have highlighted important roles for the renal stroma during

kidney development and disease, the mechanisms that control their development, differentiation, and survival are poorly understood.

We recently demonstrated an essential role for β -catenin in the differentiation and specification of the renal stroma. The overexpression of stromal β -catenin results in disruptions in stromal cell identity and ectopic expression of factors, such as Wnt4 and Bmp4, essential for vascular morphogenesis (Boivin, Sarin et al. 2016). Conversely, the deletion of stromal β -catenin results in abnormal medullary formation and reductions in medullary stroma (Yu, Carroll et al. 2009, Boivin, Sarin et al. 2015). A functional role for β -catenin in medullary stromal cells has been demonstrated in medullary extension of the nephrogenic tubules, growth of the loop of Henle, and elongation of the collecting ducts (Yu, Carroll et al. 2009). Wnt7b, which is expressed and secreted by the ureteric stalk epithelial cells, activates β -catenin in the adjacent medullary stromal cells and promotes p57Kip2 expression, a cyclin-dependent kinase inhibitor. However, the contributions of p57Kip2 to renal medulla morphogenesis are not clear, as no changes in cell proliferation are observed in stromal β -catenin and p57Kip2 deficient kidneys (Zhang, Liegeois et al. 1997, Yu, Carroll et al. 2009). This suggests β -catenin regulates other genes essential for medullary stroma development. However, the mechanisms and genes regulated by β -catenin in medullary stroma are poorly defined.

In this study, we demonstrate that a loss of β -catenin expression in stromal cells from the onset of kidney development does not affect the cortical stroma population demonstrating β -catenin does not modulate the formation of cortical stromal progenitors. Instead, the loss of β -catenin results in reduced medullary stroma caused by an increase in

apoptosis in the stromal cells that are located deeper into the kidney. Our data provide evidence that β -catenin ensures proper medullary stromal cell differentiation by regulating stromal cell survival via the expression of anti-apoptotic genes. This regulation results from a novel transcriptional complex that binds to the promoter region of anti-apoptotic genes to control the development of the medullary stroma compartment.

METHODS

Mice strains and genotyping

To generate β -catenin deficient mice, termed β -cat^{S/-}, we first crossed FoxD1eGFPCre males (Humphreys, Lin et al. 2010) with mice containing loxP sites flanking exons 2-6 (β -cat ^{Δ 2-6/ Δ 2-6}) of the β -catenin allele (Brault, Moore et al. 2001). The *Foxd1-Cre*; β -cat^{+/-} males were then crossed with β -cat ^{Δ 2-6/ Δ 2-6} females to generate homozygous β -catenin loss-of-function mutants in the renal stroma. FoxD1eGFPCre mice were maintained on a CD1 genetic background, while β -cat ^{Δ 2-6/ Δ 2-6} mice were maintained on a C57BL/6J genetic background. Mice were genotyped using the following primers specific to the FoxD1eGFPCre allele: Forward 5'-GCGGCATGGTGCAAGTTGAAT-3' and Reverse 5'-CGTTCACCGGCATCAACGTTT-3', and Forward 5'-AAGGTAGAGTGATGAAAGTTGTT-3' and Reverse 5'-CACCATGTCCTCTGTCTATTC-3' for the floxed β -catenin allele. All animal studies were performed in accordance with animal care and guidelines put forth by the Canadian Council for Animal Care and McMaster's Animal Research Ethics Board (AREB) (Animal Utilization Protocol #100855) and approved the project described in this manuscript.

Histology and Immunofluorescence

Whole kidney tissue was fixed in 4% paraformaldehyde for 24 hours at 4 °C. Kidneys were paraffin-embedded, sectioned to 5 μ m, and mounted on Superfrost™ Plus slides (Thermo Fisher Scientific, Waltham, MA) and incubated overnight at 37°C. Sections were deparaffinized using xylene washes and rehydrated using graded ethanol washes

(100%, 95%, 75%, 50%, H₂O) and stained with hematoxylin and eosin (Sigma, St. Louis, MO). For immunofluorescence, tissue was prepared as described above and antigen retrieval was performed for 5 minutes in 10mM sodium citrate solution pH 6.0 in a pressure cooker, followed by blocking with serum-free protein block (Dako Corporation, Carpinteria, CA). Sections were incubated with primary antibodies to Pbx1 (Cell Signaling, Beverly, MA; 1:250 dilution) and Foxd1 (Santa Cruz, 1:200) overnight at 4°C. Tissue sections were washed in PBS pH 7.4, incubated with secondary antibodies Alexafluor 488 or 568 (Invitrogen, Carlsbad, CA; 1:1000 dilution) for 1 hour at room temperature and stained with Dapi (Sigma, St. Louis, MO; 1:1000 dilution) for 5 minutes and cover-slipped using Fluoromount (Sigma, St. Louis, MO) and photographed on a Nikon 90i-eclipse upright microscope.

In Situ Hybridization

In Situ Hybridization for Pod1 was performed using the Affymetrix QuantiGene ViewRNA assay. Briefly, paraffin-embedded *WT* and *β-cat^{S-/-}* kidneys were sectioned at a thickness of 5 μm, deparaffinized, boiled in pre-treatment solution (Affymetrix, Santa Clara, CA) and digested with proteinase K. Sections were incubated with a custom designed QuantiGene ViewRNA probe for 2 hrs at 40°C. Signal was amplified with Pre-Amp and Amp solutions and then developed Fast-Red or Fast-blue Substrate. Slides were counter-stained with DAPI, mounted with Fluoromount (Sigma, St. Louis, MO) and photographed on a Nikon 90i-eclipse upright microscope.

Real-time reverse transcriptase-PCR

Real-time PCR was performed using the Applied Biosystems 7900HT fast RT-PCR

system (Applied Biosystems, Burlington, ON). cDNA was generated using first strand cDNA synthesis (Invitrogen Carlsbad, CA) from total RNA. Real-time PCR reaction mix contained 2.5ng of each cDNA sample, SYBR green PCR Master Mix (Applied Biosystems, Burlington, ON) and 300nM of each primer to a total volume of 25 μ l. Primers for *FoxD1*, *Pod1*, *Vegfa*, *Birc5*, *Bcl2l1*, *Mybl2*, *Bag3*, *Esr1*, *Kcnp1*, *Pbx1*, *Pax2*, *Ret* were designed using the Primer 3 software (<http://bioinfo.ut.ee/primer3-0.4.0/>) and verified using the UCSC genome bioinformatics website (genome.ucsc.edu). Relative levels of mRNA expression were determined using the $2^{(-\Delta\Delta Ct)}$ method. Individual expression values were normalized by comparison to β -2-microglobulin.

Analysis of cell proliferation and apoptosis

Cell proliferation was assayed in paraffin-embedded kidney tissue by incorporation of 5-bromo-2-deoxyuridine (Roche Molecular Biochemicals, Mannheim, Germany), as previously described (Cano-Gauci, Song et al. 1999). Pregnant mice received an intra-peritoneal (IP) injection of BrdU (100 mg/g of body weight) 2 h prior to sacrifice. BrdU-positive cells in the stroma were identified by co-labeling with the anti-BrdU antibody (Abcam, Cambridge, ab8152, 1:250) and Pbx1 antibody (Cell Signaling, Beverly, MA; 1:250). Apoptosis was assessed in paraffin-embedded kidney tissue using the cell death detection kit (Roche Molecular Biochemicals, Mannheim, Germany) and visualized using 3,3'-Diaminobenzidine (DAB) substrate solution (Vector, USA).

Immunoblotting and Co-Immunoprecipitation

Whole kidney tissue was homogenizing in TENT++ buffer [0.1M Tris-Cl (pH 8.0), 0.01M EDTA (pH 8.0), 1M NaCl, 0.2% Triton-X 100, protease inhibitor, phosphatase

inhibitor]. Protein concentration was determined by Bradford protein assay according to the manufacturer's instructions (Bio-Rad). For immunoblotting, 20 µg was loaded on an SDS-PAGE and probed with Bcl-XL (Cell Signaling, Beverly, MA). For immunoprecipitations, lysates were incubated with a 1:40 dilution of β-catenin antibody (BD Transduction, Lexington, KY), YAP1 (Novus Biologicals, Oakville, ON), or TBX5 (Abcam, Cambridge, MA) and immunoprecipitation matrix (ImmunoCruz, SantaCruzBiotech, Dallas, TX) at 4°C overnight on a rotator. Immunoprecipitates were pelleted, resuspended in SDS-PAGE sample buffer, and immunoblotting performed by incubating for 1 hr at RT with primary antibodies β-catenin (BD Transduction Laboratories, Mississauga, ON), YAP1 (Novus Biologicals, Oakville, ON), and TBX5 (Abcam Inc, Cambridge, MA) and horseradish peroxidase-conjugated secondary antibodies. The reaction was visualized using an Enhanced Chemiluminescence Detection system (Pierce Thermo Scientific, IL).

Chromatin Immunoprecipitation (ChIP)

Kidney tissue was dissected and cross-linked in 4 % formaldehyde. Cross-linked tissue was homogenized in lysis buffer (1%SDS, 10mM EDTA, 50mM Tris pH 8.0) and sonicated to generate DNA fragments of 200-1000bp. Soluble chromatin was precleared by Protein G agarose /salmon sperm DNA beads (Millipore, Billerica, MA). Immunoprecipitation was performed using 2µg of mouse anti-β-catenin antibody (BD, Franklin Lakes, NJ), anti-YAP antibody (Novus Biologicals, Oakville, ON) or isotype specific IgG (negative control) was added to every 100µl of soluble chromatin to immunoprecipitate β-catenin and YAP-binding DNA. Immune complexes were separated

with G agarose /salmon sperm DNA beads followed by a series of washing buffer with protein inhibitors. Crosslinked protein-DNA compound was disassociated by incubation with DNase-free proteinase K and RNA residual was removed by RNase A. DNA purified with Zymo ChIP DNA clean & concentrated kit (Zymo Research, Irvine, CA). Fragments containing the Tbx5 binding sites identified via in silico using MULAN were examined by PCR. A fragment within the Bcl2l1 coding region was used as a negative control. All primers were designed with Primer 3 software.

RT² Profiler PCR Array

RNA from whole kidneys was extracted using the Qiagen RNeasy micro Kit (Qiagen, Hilden, Germany). cDNA was generated using the RT² First Strand Kit (Qiagen, Hilden, Germany). Quantitative PCR was performed using the RT² Profiler PCR Array plates (PAMM-212Z, Qiagen). The cDNA samples were mixed with RT² MasterMix and added to the PCR array plates. The plates were run on the Applied Biosystems StepOne Real-Time PCR machine and analyzed using the PCR array Data analysis software provided by Qiagen.

Statistical Analysis

The RT-qPCR, stromal cell count, apoptosis, and cell proliferation were analyzed using a two-tailed Student's t-test using GraphPad Prism software, version 5.0c. $P < 0.05$ indicates statistical significance.

Ethics Statement

All studies were performed in accordance with animal care and guidelines put forth by the Canadian Council for Animal Care and McMaster's Animal Research Ethics

Ph.D. Thesis – Felix Boivin-Laframboise McMaster University – Medical Sciences
Board (AREB) (Animal Utilization Protocol #100855) and approved the project described
in this study.

RESULTS

The ablation of stromal β -catenin results in reduced medullary stroma

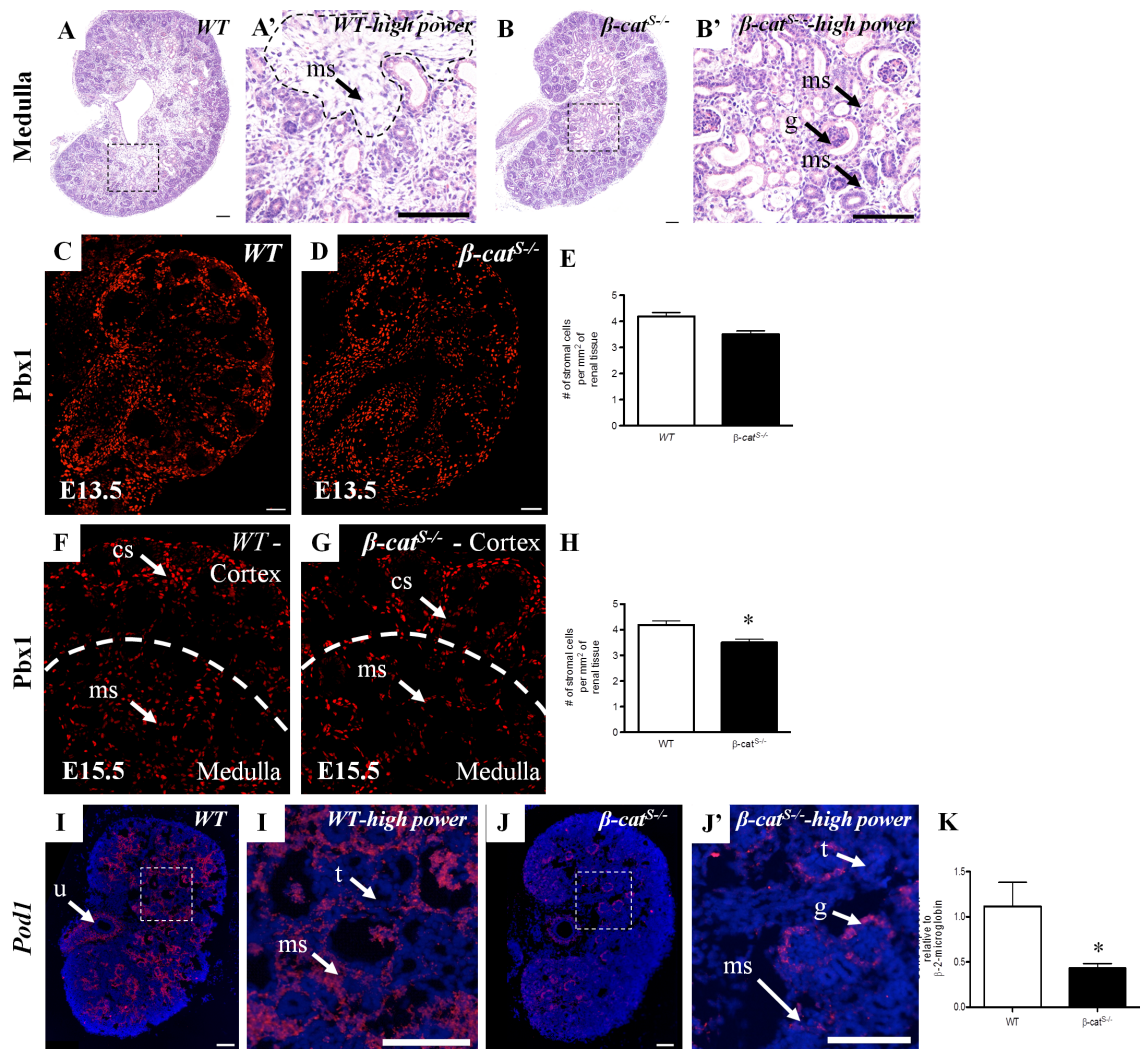
The genetic ablation of β -catenin specifically in the renal stroma cells from embryonic day (E) 11.5 results in multiple developmental renal abnormalities (Boivin, Sarin et al. 2015). Initially, kidney development appears phenotypically normal between E11.5 and E13.5. However, by E14.5, the stromal β -catenin deficient kidneys exhibit cortico-medullary patterning defects with glomeruli ectopically located within the medullary compartment and a sporadic loosely adherent renal capsule surrounding the kidney. By E15.5, the nephrogenic progenitor population surrounding the ureteric epithelium is reduced compared to *WT* littermates. At birth, there are numerous ureteric epithelial derived cysts in the cortex and medulla, indicating that β -cat^{S-/-} kidneys are not functioning properly (Boivin et al, 2015). Since stromal cells modulate proliferation of the nephron progenitors (Das, Tanigawa et al. 2013, Hum, Rymer et al. 2014) and control formation of the cortico-medullary axis (Yu, Carroll et al. 2009), we suspected these abnormalities were associated with defects in the stromal population.

Our previous histological analysis of β -cat^{S-/-} kidneys suggested no overt changes in the cortical stroma. At E15.5, the cortical stroma appeared loosely packed surrounding the condensed mesenchyme and developing nephrons. Furthermore, our analysis of cortical stromal markers, such as FoxD1 and Tenacin-C, demonstrated no changes in the amount and organization of the cortical stroma at E15.5 (Boivin, Sarin et al. 2015). In contrast, a close histological analysis of the medullary compartment revealed very few stromal cells surrounding the maturing collecting ducts and nephrogenic tubules in β -cat^{S-}

^{-/-} kidneys (Figure 1A-B). The medullary stromal cells in *WT* controls form a large population of stellate-shaped cells (Figure 1A') compared to the very few medullary stromal cells surrounding the nephrogenic tubules in β -*cat*^{S-/-} kidneys (Figure 1B'). Additionally, the medullary stromal cells in β -*cat*^{S-/-} kidneys appear more rounded compared to *WT* medullary stroma. The severe reduction in medullary stromal cells could explain the cortico-medullary axis defects (as evidenced by the presence of glomeruli (g) in the medulla (Figure 1B') previously reported in β -*cat*^{S-/-} kidneys (Yu, Carroll et al. 2009, Boivin, Sarin et al. 2015).

Our previous characterization of the renal stroma using general markers of all stromal cells, such as Pbx1 and Meis1/2, revealed a markedly reduced medullary stroma compartment (Boivin, Sarin et al. 2015). However, due to the lack of specific antibodies that detect the medullary stroma, we were not able to directly count the number of medullary stromal cells. Therefore, to determine whether a loss of stromal β -catenin resulted in reduced medullary stroma, we first quantitated the overall number of stromal cells using a nuclear marker of all stromal cells (Pbx1) and then quantified the levels and expression pattern of *Podl*, a known medullary stromal marker (Quaggin, Schwartz et al. 1999), by *In Situ* hybridization (ISH) and qPCR. Combining these two quantification methods allows us to specifically determine if the amount of medullary stroma is reduced since we established there are no changes in the cortical stroma. Analysis of Pbx1 at E13.5, a time point where no abnormalities are observed (Figure 1C-D), did not reveal any significant changes in the number of stromal cells (4.32 cells/mm² in *WT* vs 4.33 cells/mm² in β -*cat*^{S-/-}, p=0.97) (Figure 1E). At E15.5, a time point when the medulla is

established in *WT* mice, the number of all stromal cells was reduced in the regions consistent with the medulla (below dotted line) in $\beta\text{-cat}^{S/-}$ compared to *WT* littermate kidneys (Figure 1F-G). We observed a 16.67% reduction in the number of Pbx1+ cells in $\beta\text{-cat}^{S/-}$ compared to *WT* littermate kidneys in all stromal cells. (4.20 cells/mm² in *WT* vs 3.50 cells/mm² in $\beta\text{-cat}^{S/-}$, p=0.0025) (Figure 1H). To confirm the reduction in medullary stromal markers, we quantified the levels and analyzed the expression pattern of *Pod1* in $\beta\text{-cat}^{S/-}$ kidneys. In *WT* littermates, *Pod1* expression was observed surrounding the nephrogenic tubules and ureter in the medulla (Figure 1I-I'). In contrast, *Pod1* expression was virtually absent in the medulla in $\beta\text{-cat}^{S/-}$ kidneys and was observed at very low levels in a few medullary stromal cells surrounding the glomeruli and tubules (Figure 1J). Expression was maintained in the glomeruli (Figure 1J'). Quantification of *Pod1* expression by qPCR confirmed a significant reduction in $\beta\text{-cat}^{S/-}$ compared to *WT* littermates (1.11 vs 0.42, p=0.02)(Fig. 1K). Combined with our previous findings, this analysis of the renal stroma demonstrates that a loss of β -catenin in stromal cells does not affect the cortical stroma cell population but specifically affects the development of the medullary stroma.

Figure 4.1 - The ablation of stromal β -catenin results in reduced medullary stroma

The ablation of stromal β -catenin results in reduced medullary stroma: (A-B) H&E stain of *WT* littermates and β -cat^{S/S-} kidneys at E15.5. The medullary stroma is markedly reduced between the nephrogenic tubules in β -cat^{S/S-} kidneys (B') compared to *WT* (A'). (C-D) Pbx1 expression in *WT* control littermates and β -cat^{S/S-} kidneys at E13.5. (E) Number of stromal cells per mm² of renal tissue at E13.5. The overall number of stromal cells is not significantly reduced in β -cat^{S/S-} kidneys (4.32 cells/mm² in *WT* vs 4.33 cells/mm² in β -cat^{S/S-}, p=0.97). (F-G) Pbx1 expression in *WT* control littermates and β -cat^{S/S-} kidneys at E15.5. (H) Number of stromal cells per mm² of renal tissue at E15.5. The overall number of stromal cells is significantly reduced in β -cat^{S/S-} kidneys (4.20 cells/mm² in *WT* vs 3.50 cells/mm² in β -cat^{S/S-}, p=0.0025). (I-J) *Pod1* In Situ hybridization in *WT* littermates and β -cat^{S/S-} kidneys at E15.5. *Pod1* expression is observed in all medullary stromal cells (ms) surrounding the tubules (t) and ureter in *WT* littermates (I'). In β -cat^{S/S-} kidneys, *Pod1* expression is observed in glomeruli and at low

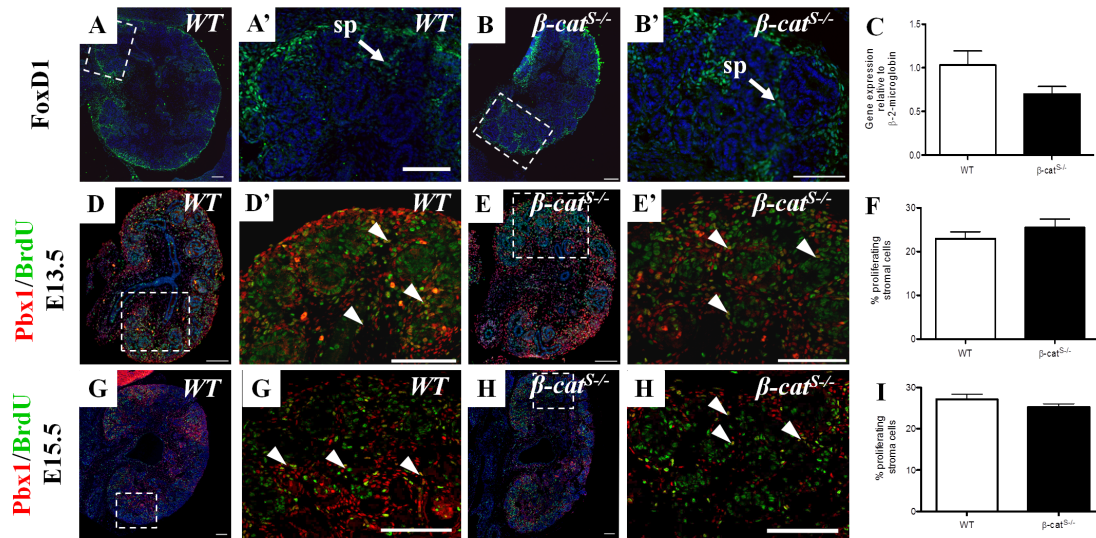
levels in a few medullary stromal cells (ms) (J'). (K) *Pod1* expression is significantly decreased in β -*cat*^{S/-} kidneys, (1.11 vs 0.42, p=0.02). (cs=cortical stroma, g=glomeruli, ms=medullary stroma, t=tubule, u=ureter. Scale bars = 100 μ m)

β -catenin is not required for the development of stromal progenitors

Next, we wanted to determine the cellular events that contribute to the reduction in medullary stroma. The kidney develops in a circumferential manner (Cebrian, Borodo et al. 2004). In this regard, the youngest developing structures are found in the outermost region of the kidney cortex. In contrast the more mature nephrogenic structures are located deeper in the nephrogenic zone farthest from the outside of the kidney (Cebrian, Borodo et al. 2004). As kidney development progresses, the progenitor cells in the outer region of the kidney that will form the stroma express high levels of FoxD1. These Foxd1 progenitors will differentiate into distinct stromal populations: 1) the capsular and cortical stroma in the cortex, and 2) the medullary stroma in the medulla (Kobayashi, Mugford et al. 2014). A close examination of the FoxD1+ cell population did not reveal any major changes in the overall organization of the stromal progenitors between β -cat^{S/-} and *WT* littermates (Figure 2A-B). In both *WT* and β -cat^{S/-}, FoxD1+ cells were found surrounding the condensed mesenchyme in the nephrogenic zone. However, in contrast to *WT* littermates (Figure 2A'), a few FoxD1+ cells were found deeper into the cortex, below the nephrogenic zone (Figure 2B'). Quantification of FoxD1 expression between *WT* and β -cat^{S/-} kidneys did not reveal any alterations (1.029 vs 0.69, p=0.112)(Figure 2C). Combined, these data demonstrate that the loss of stromal β -catenin from the onset of kidney development does not affect the ability of stromal progenitors to form properly and does not affect the differentiation state of these cells.

We next analyzed the proliferation rate of the stromal cells by pulse-labeling with BrdU to determine whether the reduction in medullary stroma was caused by a reduction

in stromal proliferation. We analyzed BrdU incorporation in stromal cells using an anti-BrdU antibody co-localized with the general stromal marker Pbx1 (the yellow cells represent the co-localization of BrdU and Pbx1). We demonstrate no changes in the overall proliferation rate at E13.5, prior to the onset of medullary development (22.95 vs. 25.44, $p=0.38$) (arrowhead, Figure 2D-F). Additionally, we demonstrate no changes at E15.5, once medullary stroma is established (27.17 vs. 25.30, $p=0.1945$) (Figure 2G-I) in β -cat^{S/-} kidneys compared to *WT* littermates. This demonstrates that a loss of stromal β -catenin does not affect proliferation of the renal stroma and that the reduction in medullary stroma is not caused by reduced proliferation of stromal cells.

Figure 4.2 - β -catenin is not essential for cortical stroma development

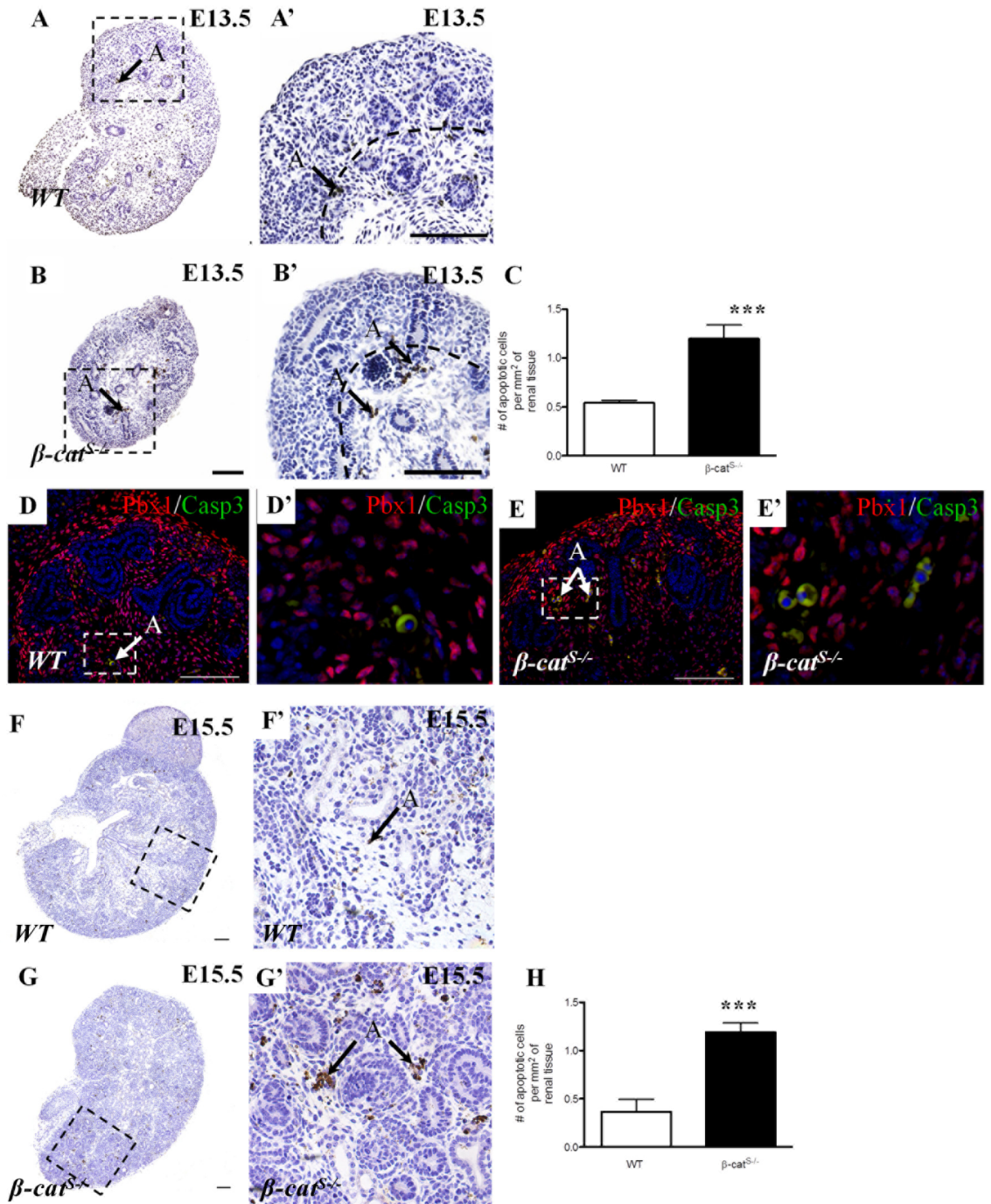
β -catenin is not essential for cortical stroma development: (A-B) FoxD1 expression in the cortical stroma progenitors is unchanged in β -cat^{S/S-/-} kidneys (B) compared to *WT* littermates (A). (C) FoxD1 mRNA expression is not significantly different in β -cat^{S/S-/-} (1.029 vs 0.69, p=0.112). (D-E) Proliferation assay in β -cat^{S/S-/-} and *WT* littermate kidneys at E13.5. Arrowheads indicate proliferating cells. They co-express Pbx1 and BrdU (F) Proliferation rate is not significantly different in β -cat^{S/S-/-} kidneys at E13.5, (22.95 vs. 25.44, p=0.38). (G-H) Proliferation assay at E15.5. (I) Proliferation rate is not significantly different in β -cat^{S/S-/-} kidneys at E15.5, (27.17 vs. 25.30, p=0.1945). (scale bar = 100 μ m, sp=stromal progenitors)

The loss of stromal β -catenin results in increased apoptosis of stromal cells

Since apoptosis eliminates cells via programmed cell death, we next analyzed whether medullary stromal cells were undergoing apoptosis. To analyze this, we performed a TUNEL (Terminal deoxynucleotidyl transferase dUTP Nick End Labeling) assay and identified numerous brown TUNEL+ cells located in the stromal compartment in the β -cat^{S/-} kidneys compared to *WT* (0.54 vs 1.2 cells/mm², p<0.05)(Figure 3A-C) as early as E13.5. The cells undergoing cell death were found in clusters deep within the renal tissue and displayed dense and round nuclei, which is a hallmark of apoptotic chromatin shrinkage (Elmore 2007). These apoptotic cells were never found within the outer regions of the nephrogenic zone (above dotted line in the images) (Figure 3B') and few apoptotic cells were observed in *WT* littermates (Figure 3A'). Since TUNEL staining identifies double stranded DNA breaks, which is a feature of both necrosis and apoptosis, we also performed immunofluorescence at E13.5 for activated Caspase-3, a marker of apoptosis. We co-localized the Caspase-3 expression with the stromal marker Pbx1, to determine whether the Caspase-3+ cells were stromal cells. The Caspase-3 cells are marked in green and the Pbx1 stromal cells are marked in red, which means that the cells co-expressing both Caspase-3 and Pbx1 appear yellow. We demonstrated that Caspase-3 and Pbx1 co-localized in β -cat^{S/-} kidneys, which confirmed that the TUNEL+ cells were undergoing apoptosis and were of stromal origin (Figure 3D-E). Similar to TUNEL+ cells, Casp-3+ cells were found in clusters just below the nephrogenic zone in β -cat^{S/-} kidneys (Figure 3E'). To determine whether these apoptotic cells were always found in clusters at the cortico-medullary junction as kidney development progresses, we

quantitated the number of TUNEL+ cells and analyzed their expression pattern at E15.5. We confirmed a significant increase in the number of apoptotic cells in the stromal compartment (0.36 vs 1.19 cells/mm²) (Figure 3H) at the junction between the cortex and medulla. This expression pattern was identical to that observed at E13.5 in β -cat^{S/-} kidneys. Similarly, no cell death was observed in the outer cortex (Figure 3F-G). Additionally, the analysis of *WT* littermates revealed no apoptotic cells were in the cortico-medullary region (Figure 3F'). Together, these findings demonstrate that a loss of stromal β -catenin results in increased apoptosis predominantly around the region where the cortico-medullary junction is established.

Figure 4.3 - β -catenin deficiency increases apoptosis in the medullary stroma



β -catenin deficiency increases apoptosis in the medullary stroma: (A-C) TUNEL assay at E13.5. Apoptotic clusters are observed in the stroma in β -cat^{S-/-} kidneys below the developing nephrons. Apoptosis is significantly increased in β -cat^{S-/-} kidneys compared to *WT* littermates, (0.54 vs 1.2 cells/mm², p<0.05)(C). (D-E) Double immunofluorescence using active caspase3 and stromal marker Pbx1 in β -cat^{S-/-} and *WT* littermate kidneys. Stromal cells are undergoing apoptosis. (F-G) TUNEL assay at E15.5. Apoptotic clusters are observed in the renal stroma between the cortex and medulla in β -cat^{S-/-} kidneys. (H) Apoptosis is significantly increased in β -cat^{S-/-} kidneys compared to *WT* littermates (0.36 vs 1.19 cells/mm²). A=apoptosis, cs= cortical stroma, scale bars = 100 μ m.

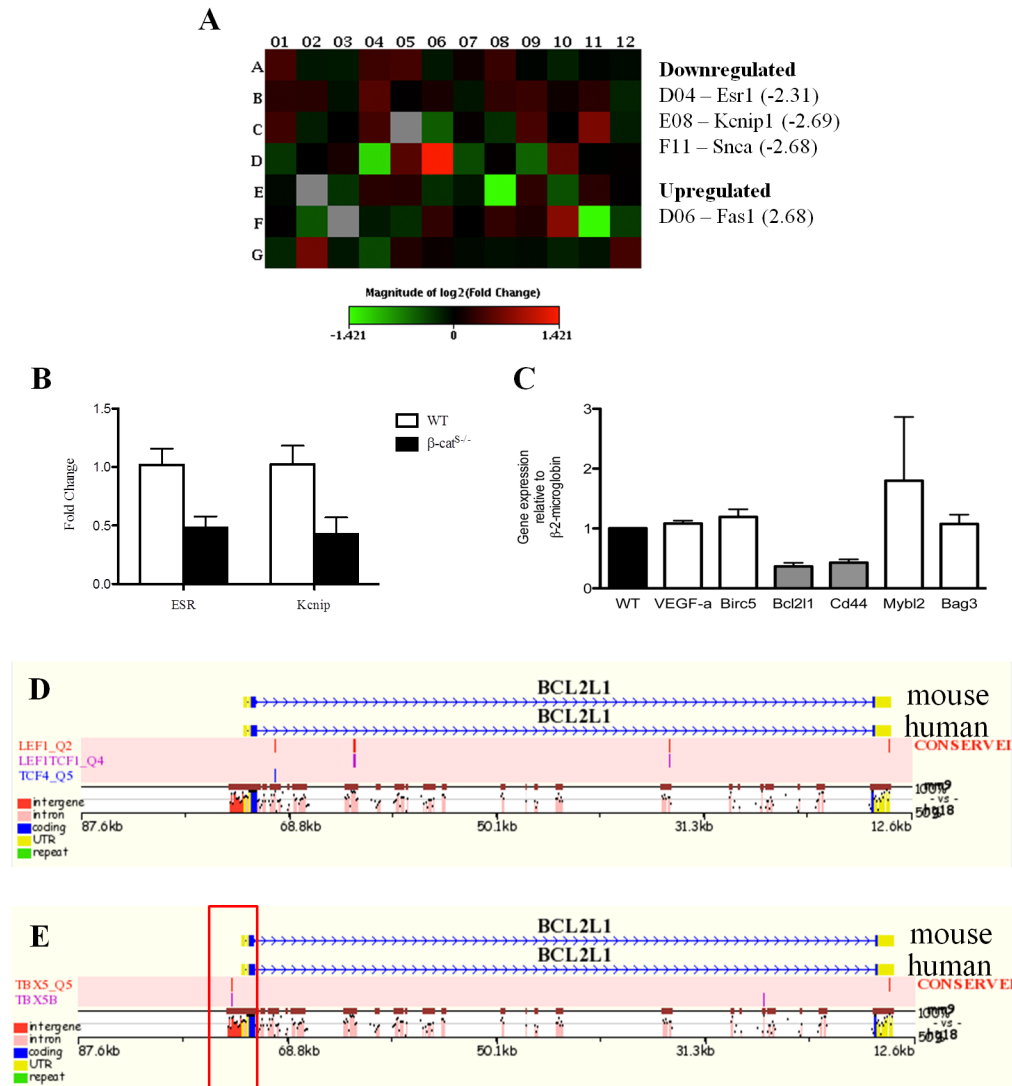
Stromal β -catenin modulates the expression of anti-apoptotic genes

The Wnt/ β -catenin pathway modulates apoptosis via regulation of anti-apoptotic genes (Ille and Sommer 2005, Huang, Wang et al. 2006) in various cell types, such as endothelial cells and vascular smooth muscle cells (Holnthoner, Pillinger et al. 2002, Wang, Xiao et al. 2002). Additionally, in models of acute kidney injury, β -catenin inhibits apoptosis by modulating the levels of Bax, a pro-apoptotic factor, via the regulation of *Akt1* expression in proximal tubular epithelial cells (Wang, Havasi et al. 2009, Zhou, Li et al. 2012). Therefore, we hypothesized that β -catenin in the renal stroma regulates the expression of genes involved in protecting cells from apoptosis. We searched for known anti-apoptotic genes that are regulated by β -catenin and expressed in the developing kidney. This analysis identified candidates *Birc5* (Schwab, Patterson et al. 2003, Rosenbluh, Nijhawan et al. 2012), *CD44* (Fanni, Fanos et al. 2013), *Bcl2l1* (Gonzalez-Garcia, Perez-Ballesteros et al. 1994, Xie, Huang et al. 2005, Rosenbluh, Nijhawan et al. 2012), *Mybl2* (Huang, Wang et al. 2006), *Bag3* (Huang, Wang et al. 2006), and *Vegf-a* (Kim and Goligorsky 2003, Clifford, Deacon et al. 2008). Furthermore, to identify novel apoptotic genes regulated by β -catenin, we also performed a quantitative assay using a Qiagen profiler array. This profiler array allows the investigation of 84 central genes associated with mechanisms of programmed cell death, such as shrinkage, fragmentation, and activation of the caspase cascade. Both pro- and anti-apoptotic genes are included in this array, which allows us to identify indirect pro-apoptotic targets of β -catenin that may contribute to apoptosis in *β -cat^{S-/}* kidneys. The Qiagen profiler assay relies on a qPCR

approach using 96-well plates where 84 genes are quantified simultaneously along with housekeeping genes and negative controls. We performed the quantitative analysis on at least 3 *WT* littermates and 3 β -*cat*^{S/-} kidneys using mRNA from whole kidneys at E12.5, a day prior to the changes in apoptosis to see if changes in apoptotic genes were promoting the increase in apoptosis observed at E13.5. A heatmap was generated where green squares represent underexpressed genes and red squares represent overexpressed genes (Figure 4A). This analysis demonstrated 3 genes were downregulated (*Esr1*, *Kcnp1*, and *Snca*) and 1 gene was upregulated (*Fasl*) (Figure 4A). Specifically, anti-apoptotic genes *Esr1* (54% reduction, 1.01 vs 0.47, p=0.03) and *Kcnp1* (59% reduction, 1.02 vs 0.43, p=0.04) were significantly reduced in β -*cat*^{S/-} kidneys (Figure 4B). In addition, we observed a 66% reduction (1.079 vs 0.41, p=0.08) in anti-apoptotic gene and a 182% increase (1 vs 2.82, p=0.54) in pro-apoptotic gene *Fasl*. However, these two genes were not statistically significant. Additionally by qPCR, anti-apoptotic genes *Bcl2l1* was reduced 64% (1 vs 0.36, p=0.0035) and *Cd44* was reduced by 57% (1 vs 0.43, p=0.0092) (Figure 4C).

Since *Bcl2l1* expression in β -*cat*^{S/-} was markedly lower than the other anti-apoptotic genes and has been shown to be involved in the regulation of apoptosis during murine organogenesis (Gonzalez-Garcia, Perez-Ballester et al. 1994) and the development of β -catenin-driven renal cancers, such as Wilms' tumour (Ghanem, Van der Kwast et al. 2001), we focused on *Bcl2l1* to determine if β -catenin has the potential to regulate its transcription. Since β -catenin regulates gene transcription by forming a complex with the Tcf/Lef family of DNA-bound transcription factors (MacDonald, Tamai

et al. 2009) we analyzed the *Bcl2l1* promoter region for conserved Tcf/Lef binding sites. Surprisingly, this analysis did not reveal any conserved Tcf/Lef binding sites suggesting *Bcl2l1* transcription is not likely regulated by an interaction between β -catenin and the Tcf/Lef complex (Figure 4D). However, β -catenin can regulate the expression of *Bcl2l1* by forming a complex with the transcriptional co-activators Yes1-associated protein (Yap) and Yes1, and the transcriptional factor Tbx5 in colon cancer cell lines (Rosenbluh, Nijhawan et al. 2012). Therefore, we investigated the *Bcl2l1* promoter for Tbx5 binding sites in the 5' proximal promoter region and found a highly conserved Tbx5 binding site 1.2 kb upstream of the *Bcl2l1* start site. (Figure 4E).

Figure 4.4 – Stromal β -catenin regulates the expression of anti-apoptotic genes

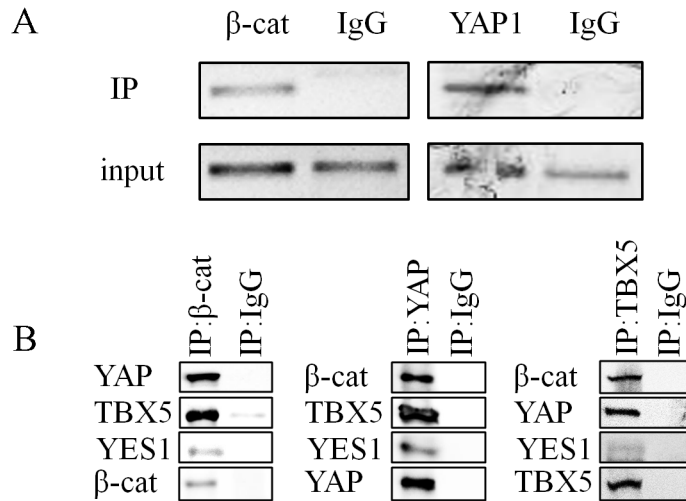
Stromal β -catenin regulates the expression of anti-apoptotic genes: (A) Quantitative analysis of anti-apoptotic genes using a Qiagen profiler assay. A heatmap was generated to identify the genes that are upregulated and downregulated using whole kidney lysate. (B) *Esr1* and *Kcnip1* were significantly downregulated in β -cat^{S/S-} kidneys compared to *WT* littermates. (C) qRT-PCR of anti-apoptotic genes in whole kidneys at E12.5. *Bcl2l1* (1 vs 0.36, $p=0.0035$) and *CD44* (1 vs 0.43, $p=0.0092$) are significantly reduced compared to *WT* littermates. (D) *In Silico* analysis of the *Bcl2l1* for Tcf/Lef conserved binding sites. No Tcf/Lef binding sites were observed in the *Bcl2l1* promoter region. (E) *In Silico* analysis of *Bcl2l1* for Tbx5 conserved binding sites. There is a highly conserved binding site 1.2Kb upstream of the *Bcl2l1* transcription start site.

To determine whether this complex formed at the Tbx5 site in the *Bcl2l1* promoter in the developing kidney, we performed chromatin immunoprecipitation on E13.5 whole kidney tissue lysates. We performed these experiments on whole kidney lysates, since using isolated stroma cells did not yield enough protein. We demonstrated that β -catenin and Yap associated with the Tbx5 binding site in the *Bcl2l1* promoter 1.2kb upstream of the *Bcl2l1* transcription start site (Figure 5A). The protein/chromatin complex was immunoprecipitated using antibodies specific to either β -catenin or Yap. We then utilized primers designed specifically to target the Tbx5 binding site in the *Bcl2l1* promoter region to determine, via PCR amplification, whether this DNA fragment associated with β -catenin and Yap. We used a non-specific IgG as a negative control and demonstrated no amplification at the same Tbx5 site. This demonstrates that β -catenin and Yap independently associate with the Tbx5 binding site in the *Bcl2l1* promoter, and suggests that *Bcl2l1* is a direct target of β -catenin in the developing kidney. These results are consistent with previous findings demonstrating association of β -catenin and Yap with the Tbx5 site in *Bcl2l1* promoter (Rosenbluh, Nijhawan et al. 2012). While we do not show the functional contribution to this complex, Rosenbluh et al demonstrated using a luciferase assay that the association of Yap and β -catenin at the Tbx5 site in the *Bcl2l1* promoter is sufficient to promote transcription of *Bcl2l1*.

While β -catenin does not physically interact with chromatin (MacDonald, Tamai et al. 2009) Rosenbluh et al demonstrated these proteins work in a complex to modulate *Bcl2l1* expression in various cancer cells (Rosenbluh, Nijhawan et al. 2012), to demonstrate whether the presence of this complex in the developing kidney, we next

performed a series of immunoprecipitation assays with β -catenin, Yap, and Tbx5 (Figure 5B). This analysis was performed on whole kidney lysates since we were unable to extract a sufficient amount of protein from isolated stromal cells. We first pulled down β -catenin and demonstrated strong association of Yap and Tbx5 by immunoblotting, demonstrating an interaction with β -catenin. We confirmed all three proteins interacted together by also performing pull down assays with Yap and Tbx5 (Figure 5C). Studies have demonstrated that interaction with Yes1, a Yap binding partner, is essential for formation and activation of this complex (Rosenbluh, Nijhawan et al. 2012). We confirmed the presence of Yes1 in the complex and, as expected, demonstrated stronger interaction with the Yap protein than with β -catenin and Tbx5 (Figure 4G). Together, this analysis confirms the presence of a β -catenin/Yap/Tbx5 in the developing kidneys, and demonstrates that *Bcl2l1* is most likely a direct target, as evidenced by other studies (Rosenbluh, Nijhawan et al. 2012).

Figure 4.5 – β -catenin forms a complex with Tbx5 and Yap, which binds to the promoter region of *Bcl2l1*



β -catenin forms a complex with Tbx5 and Yap, which binds to the promoter region of *Bcl2l1*: (A) Chromatin Immunoprecipitation demonstrating amplification of the Tbx5 binding site when immunoprecipitated with β -catenin and YAP. (B) Co-immunoprecipitation for β -catenin, Yap, and Tbx5 in whole kidney lysates.

DISCUSSION

The processes that control the formation of the renal stroma cell lineage are poorly understood. Here, we demonstrate that β -catenin is an important player in the maintenance of the medullary stroma. The generation of a mouse model with an ablation of β -catenin in all Foxd1+ stromal progenitors leads to reduced medullary stroma resulting from an increase in stromal cell apoptosis. This apoptosis was strictly localized at the junction between the renal cortex and medulla. Our results suggest that β -catenin may regulate stromal cell survival through the modulation of anti-apoptotic gene expression. Additionally, we provide evidence that a novel transcriptional complex consisting of β -catenin, Tbx5, Yap, and Yes exists in the developing kidney and binds to the promoter region of the anti-apoptotic gene *Bcl2l1*. Together, our findings demonstrate that stromal β -catenin is central to proper medullary stroma formation by modulating stromal cell survival possibly through a novel transcriptional complex that regulates the anti-apoptotic gene *Bcl2l1*.

β -catenin controls medullary stroma development

Lineage tracing studies have defined a population of FoxD1+ cells located in the renal cortex as stromal progenitors that give rise to all stromal cell types. Throughout kidney development, the stromal progenitors in the renal cortex ultimately differentiate into mature stromal cells that integrate the cortex and medulla (Kobayashi, Mugford et al. 2014). The factors that control the differentiation of these stromal progenitors are not well established. Interestingly, while the FoxD1 transcription factor defines the stromal progenitors, studies have shown it is dispensable for the differentiation of stromal lineage

and that cortical and medullary stromal cells form despite the ablation of FoxD1 (Fetting, Guay et al. 2014, Kobayashi, Mugford et al. 2014). This suggests other factors are acting independently of FoxD1 to regulate stromal cell specification. Our results demonstrate that the ablation of stromal β -catenin results in reduced medullary stroma without affecting the initial Foxd1 stromal progenitor population or the cortical stroma. Therefore, these results demonstrate β -catenin is not essential for the specification and maintenance of the cortical stroma, but instead controls the process of medullary stroma formation.

How does β -catenin control medullary stroma formation? In the developing kidney, β -catenin plays important roles in cell fate determination. In ureteric epithelial cells, β -catenin controls the expression of genes essential for ureteric bud tip cell identity, such as *c-Ret* (Bridgewater, Cox et al. 2008). Similarly, in the condensed mesenchyme β -catenin controls the expression of genes essential for mesenchymal-to-epithelial differentiation, such as *Wnt4* and *Fgf8* (Park, Valerius et al. 2007). Our results support a similar role for β -catenin in the regulation of medullary stroma development. However, it is not clear whether β -catenin directly regulates the expression of genes essential for medullary stroma formation. We demonstrated a virtual absence of *Pod1*, which is a known regulator of medullary formation and is expressed in fully differentiated medullary stromal cells. A loss of *Pod1* results primarily in a severe reduction in medullary stroma (Quaggin, Schwartz et al. 1999, Cui, Schwartz et al. 2003) similar to that observed in β -*cat*^{S/-} kidneys. Additionally, other reports have identified p57Kip2, a cyclin-dependent kinase inhibitor essential for medulla development (Zhang, Liegeois et al. 1997), as a β -

catenin target in the medullary stroma (Yu, Carroll et al. 2009). Together, this suggests β -catenin controls the expression of factors essential for medullary stroma differentiation.

β -catenin regulates cell survival in the renal stroma

We have demonstrated increased apoptosis in stromal cells specifically at the junction between the renal cortex and medulla in β -cat^{S-/-} kidneys, demonstrating stromal cells fated to integrate the medulla are eliminated via a cell death program. However, it is not clear whether this process is directly regulated by β -catenin. Two scenarios could explain the increase in programmed cell death.

First, we propose a mechanism whereby programmed cell death is triggered in stromal cells that fail to differentiate properly. Studies have shown the repression of β -catenin in mammary gland epithelial cells leads to differentiation defects and results in increased apoptosis in various organs throughout development (Hsu, Shakya et al. 2001). Additionally, mice deficient for p57Kip2, which is essential for medulla formation (Zhang, Liegeois et al. 1997), exhibit delayed differentiation and increased apoptosis (Yan, Frisen et al. 1997), suggesting programmed cell death is triggered as a mechanism to eliminate improperly differentiating stromal cells. Further research is required to determine whether the misregulation of medullary factors results in programmed cell death.

Alternatively, we have demonstrated that a loss of stromal β -catenin results in reduced expression of anti-apoptotic genes. Additionally, our analysis of the anti-apoptotic gene *Bcl2l1* demonstrates that β -catenin can target the promoter region of anti-apoptotic genes by forming a complex with Yap and Tbx5. Therefore, it is possible that

β -catenin modulates the expression of anti-apoptotic genes to promote survival of differentiating medullary stromal cells. Studies performed in embryonic stem cells have demonstrated that high levels of anti-apoptotic genes, such as *Bcl2l1* and *Bcl2*, are activated in properly differentiating stem cells (Duval, Malaise et al. 2004). This suggests anti-apoptotic genes confer protective properties in differentiating stem cells by preventing apoptosis. We propose that multipotent stromal progenitors fated to differentiate into medullary stromal cells are protected from apoptosis via the regulation of anti-apoptotic genes. Since our analysis of anti-apoptotic genes was performed using whole kidney lysates, we cannot confirm the changes in gene expression were specific to the renal stroma. Therefore, further investigation is required to determine whether the changes in anti-apoptotic genes observed in β -cat^{S/-} kidneys are specific to the renal stroma. Additionally, the functional contribution of the Tbx5/Yap/ β -catenin complex to the regulation of stromal survival in the developing kidney is not clear. While we did not demonstrate the expression of this complex specifically in stromal cells, microarray analysis of laser captured renal medullary interstitial cells at E15.5 along with *In Situ hybridization* of whole mount kidneys demonstrates strong expression of Tbx5 in medullary stromal cells (www.gudmap.com). Furthermore, the Yap co-activator, which acts as a nuclear effector in the Hippo signaling pathway, strongly localizes to the nuclei of medullary stromal cells in the developing kidney (Bagherie-Lachidan, Reginensi et al. 2015). Combined with our expression analysis of β -catenin during kidney development (Boivin, Sarin et al. 2015), the expression of these factors in stromal cells suggests this complex is capable medullary stromal cells. Potentially, the loss of β -catenin

in those medullary stromal cells would prevent the formation of this complex and prevent the expression of *Bcl2l1*. Further research is required to determine whether this complex forms specifically in stromal cells.

In summary, we demonstrate here that β -catenin is essential for proper differentiation and survival of medullary stromal cells. Our findings are consistent with the work of others with respect to the medullary defects (Yu, Carroll et al. 2009) and provide further insight into the role for β -catenin in medulla formation. However, we were unable to demonstrate changes in anti-apoptotic genes specifically in stroma cells, which limits our interpretation of β -catenin's role in stromal cell survival. Therefore, we are currently working on characterizing isolated β -catenin-deficient stromal cells to identify direct targets of β -catenin and gain a better appreciation of the its role in medullary stromal cell differentiation.

CHAPTER 5

Technical Report: Isolation of Renal Stromal Cells From *WT* AND β -*cat*^{-/-} Mouse Strains

Authors: Felix J Boivin, Darren Bridgewater

PREFACE***Significance to thesis***

By generating transgenic mouse models where the levels of β -catenin are specifically altered in stromal cells, we have demonstrated that β -catenin controls factors essential for proper communication with neighbouring cells. Additionally, our findings suggest β -catenin controls mechanisms that regulate the differentiation and survival of the medullary stroma. However, since the developing kidney comprises various cell types, it is difficult to investigate the role of β -catenin in a cell-specific manner. In chapter 5 we describe a protocol to isolate renal stromal cells from *WT* and β -catenin-deficient mice and explore downstream applications that facilitate the study of β -catenin specifically in the renal stroma.

Authors' contribution

Felix J. Boivin designed the study, performed all experiments, performed all data analysis, and wrote the original draft of the manuscript.

Darren Bridgewater contributed to the design of the study, assisted in the interpretation of the data, and contributed to refining the original draft of the manuscript.

ABSTRACT

Our studies have demonstrated the important role of stromal cells in the developing kidney. The renal stroma provides a structural framework for the developing nephrons and collecting ducts by producing extracellular matrix components, but is also essential for regulating communication between the condensed mesenchyme and ureteric epithelium. The developing kidney comprises several cell types, and therefore it is difficult to study the intrinsic cellular mechanisms that regulate the development, differentiation, and survival of the stromal population. Also, while some studies have reported successful culture of primary stromal cells, they are difficult to manipulate in culture. Furthermore, there are no immortalized renal stromal cell lines available to perform *in vitro* assays, such as transfection. In the context of our studies, we have generated genetically altered mouse models that manipulate the levels of β -catenin exclusively in the renal stroma. These mouse models exhibit developmental defects that highlight stromal factors in the regulation of neighboring cells, but these factors are poorly understood. To investigate this further, I developed a protocol that allows the isolation of stromal cells from *WT* and genetically altered mutant mice. Additionally, I demonstrate potential downstream applications for these cells, such as qPCR, microarray analysis, and RNA-seq. This method does not involve making further mouse crosses and allows us to investigate stromal cells in a cell-specific manner to investigate their role in kidney development and determine the cell-autonomous role of β -catenin in the specification and maintenance of the renal stroma.

INTRODUCTION

Previous studies have suggested a role for stromal β -catenin in the formation of the cortico-medullary axis in the developing kidney (Yu, Carroll et al. 2009). Additionally, the analysis of β -catenin/TCF reporter mice, which help to identify the pattern of Wnt/ β -catenin activity, demonstrates high levels of β -catenin activity in stromal cells during kidney development. However, the direct targets of β -catenin in stromal cells are poorly characterized. My thesis is focused on studying the role of β -catenin in the renal stroma population during kidney development. Specifically, I am interested in identifying direct transcriptional targets of β -catenin in stromal cells. To do so, I generated a genetically altered mouse model where the levels of β -catenin are deleted exclusively in the renal stroma. Our characterization of this stromal β -catenin deficient model demonstrates a mis-regulation of anti-apoptotic genes, such as *Bcl2l1* (Boivin and Bridgewater 2014), *CD44*, *Esr1*, and *Kcni1*. Additionally, we have demonstrated using the same model that stromal β -catenin modulates the levels of Wnt9b expression in the ureteric epithelium (Boivin, Sarin et al. 2015). These findings suggest that stromal β -catenin controls the expression of genes important for proper stromal development and communication with adjacent cell populations in the developing kidney.

Our analysis of whole *WT* and *β -cat^{S/-}* kidneys allowed us to identify mis-regulated genes that are potentially regulated by stromal β -catenin. However, since the developing kidney involves up to 20 distinct cell types depending on the embryonic time point (Quaggin 2016), it is difficult to determine whether the misregulated genes we identified in our mouse models are directly controlled by stromal β -catenin. Furthermore,

while some studies have been able to culture primary stroma cells (Sims-Lucas, Schaefer et al. 2013), there are no immortalized stromal cell lines available that can be easily transfected. Therefore, we have developed a protocol that specifically allows us to study the stromal population via Fluorescence Activated Cell Sorting (FACS). In this technical report, we describe the steps used to isolate and confirm the identity of stromal cells from *FoxD1-eGFPCre*, *FoxD1-eGFPCre;β-cat^{+/-}*, and *FoxD1-eGFPCre;β-cat^{-/-}* kidneys and demonstrate the potential downstream applications for these stromal cells, such as RT-qPCR, microarray, and RNA-seq. In addition to identifying novel targets of β-catenin, the isolation of stromal cells will allow us to better understand the contribution of β-catenin to the development and survival of the renal stroma in a cell-specific manner.

METHODS

Mouse strains and genotyping

To generate β -catenin deficient mice, termed β -cat^{S-/-}, we first crossed *FoxD1eGFPCre* males (Humphreys, Lin et al. 2010) with mice containing loxP sites flanking exons 2-6 (β -cat ^{Δ 2-6/ Δ 2-6}) of the β -catenin allele (Brault, Moore et al. 2001). The *Foxd1-Cre*; β -cat^{+/-} males were then crossed with β -cat ^{Δ 2-6/ Δ 2-6} females to generate homozygous β -catenin loss-of-function mutants in the renal stroma. *FoxD1eGFPCre* mice were maintained on a CD1 genetic background, while β -cat ^{Δ 2-6/ Δ 2-6} mice were maintained on a C57BL/6J genetic background. Mice were genotyped using the following primers specific to the *FoxD1eGFPCre* allele: Forward 5'-GCGGCATGGTGCAAGTTGAAT-3' and Reverse 5'-CGTTCACCGGCATCAACGTTT-3', and Forward 5'-AAGGTAGAGTGATGAAAGTTGTT-3' and Reverse 5'-CACCATGTCCTCTGTCTATTC-3' for the floxed β -catenin allele. All animal studies were performed in accordance with animal care and guidelines put forth by the Canadian Council for Animal Care and McMaster's Animal Research Ethics Board (AREB) (Animal Utilization Protocol #100855) and approved the project described in this manuscript.

Immunohistochemistry

Whole kidney tissue was fixed in 4% paraformaldehyde for 24 hours at 4 °C. Kidneys were paraffin-embedded, sectioned to 5 μ m, and mounted on Superfrost™ Plus slides (Thermo Fisher Scientific, Waltham, MA) and incubated overnight at 37°C. Sections were deparaffinized using xylene washes and rehydrated using graded ethanol washes

(100%, 95%, 75%, 50%, H₂O). Antigen retrieval was performed for 5 minutes in 10mM sodium citrate solution pH 6.0 in a pressure cooker. Endogenous peroxidase activity was blocked with 3%H₂O₂ for 15 mi. Sections were then blocked with 5% Horse serum for 1hr followed by a Biotin and Avidin block for 15min each. Slides were then incubated with a GFP antibody (AbCam, Cambridge, MA; 1200 dilution) overnight at 4°C. Tissue sections were washed in PBS and incubated with a biotinylated horse anti-goat secondary antibody (Vector, 1:1000 dilution) for 1 hour at room temperature. Signal was amplified using the ABC amplification Kit (Vector Lab) for 30 minutes and signal was developed using a DAB peroxidase (HRP) substrate kit (Vector Lab) until desired staining was achieved. Slides were dehydrated through a series of ethanol washes followed by three Xylene washes. Slides were mounted using the VectaMount permanent mounting medium (Vector Lab) and photographed on a Nikon 90i-eclipse upright microscope.

Real-time reverse transcriptase-PCR

Real-time PCR was performed using the Applied Biosystems 7900HT fast RT-PCR system (Applied Biosystems, Burlington, ON). cDNA was generated using first strand cDNA synthesis (Invitrogen Carlsbad, CA) from total RNA. Real-time PCR reaction mix contained 2.5ng of each cDNA sample, SYBR green PCR Master Mix (Applied Biosystems, Burlington, ON) and 300nM of each primer to a total volume of 25 µl. Primers for *Pbx1*, *Pax2*, *Ret*, *Pod1*, *Sfrp1*, *FoxD1* and *B2M* were designed using the Primer 3 software (<http://bioinfo.ut.ee/primer3-0.4.0/>) and verified using the UCSC genome bioinformatics website (genome.ucsc.edu). Relative levels of mRNA expression were determined using the $2^{(-\Delta\Delta Ct)}$ method. Individual expression values were normalized

by comparison to *β -2-microglobulin*.

Fluorescent-Activated Cell Sorting

For FACS experiments, renal tissue was dissected, washed in PBS, and then dissociated using 0.3% Collagenase (Sigma, St Louis, MO) for 10min at 37°C. Kidneys were then triturated through a 25-gauge needle to make a single-cell suspension, and then washed 3 times in iced cold PBS supplemented with 2%FBS. Before sorting, cells were run through a 40 μ m strainer (FisherScientific, Nepean, ON). Cells were either sorted into PBS or directly into Qiagen's RLT Lysis Buffer.

Statistical Analysis

The RT-qPCR quantification was analyzed using a two-tailed Student's t-test with the GraphPad Prism software, version 5.0c. $P < 0.05$ indicates statistical significance.

Ethics Statement

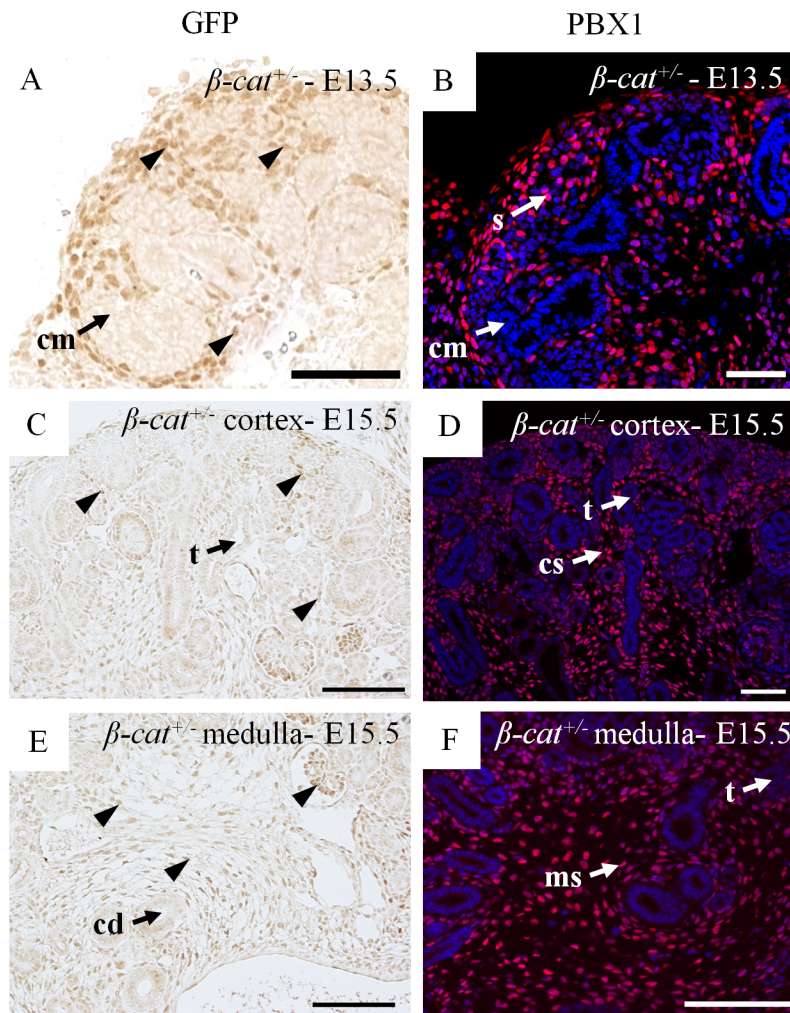
All studies were performed in accordance with animal care and guidelines put forth by the Canadian Council for Animal Care and McMaster's Animal Research Ethics Board (AREB) (Animal Utilization Protocol #100855) and approved the project described in this study.

RESULTS

Isolation of renal stromal cells from *WT* and β -*cat*^{S/-} mice

In previous studies, we demonstrated that a loss of stromal β -catenin results in a downregulation of several anti-apoptotic genes. However, since the developing kidney is comprised of several different cell types (Quaggin 2016), we were unable to confirm changes in those anti-apoptotic genes specifically in the renal stroma. Therefore, in order to perform a gene expression analysis specifically in the renal stroma, we developed a protocol to specifically isolate the stromal population. To develop our model system, we utilized a cre-lox recombination system. The Cre-expressing mice used in our study express the Green Fluorescent Protein (GFP) reporter and a promoter fragment that specifically drives Cre recombinase in FoxD1+ stromal progenitors. Theoretically, the dual expression of Cre and GFP in stromal cells allows us to specifically isolate stroma cells via Fluorescence-Activated-Cell-Sorting (FACS). However, studies have reported weak eGFP expression in *FoxD1eGFP*Cre mice (Sims-Lucas, Schaefer et al. 2013), resulting in low yields during the cell isolation procedure, which prevents the use in downstream applications. To circumvent this problem, Sims-Lucas et al crossed the *FoxD1eGFP*Cre mice with tdTomato-ROSA mice, which allow the expression of a brighter fluorescent marker (red fluorescent protein) specifically in Cre expressing cells (stroma in this case). However, crossing the dtTomato-ROSA to generate our mutant mice would require extensive breeding of multiple colonies and would require a phenotypic analysis of the new crosses, as dtTomato mice are on a different genetic background. Therefore, we determined whether the eGFP reporter gene in

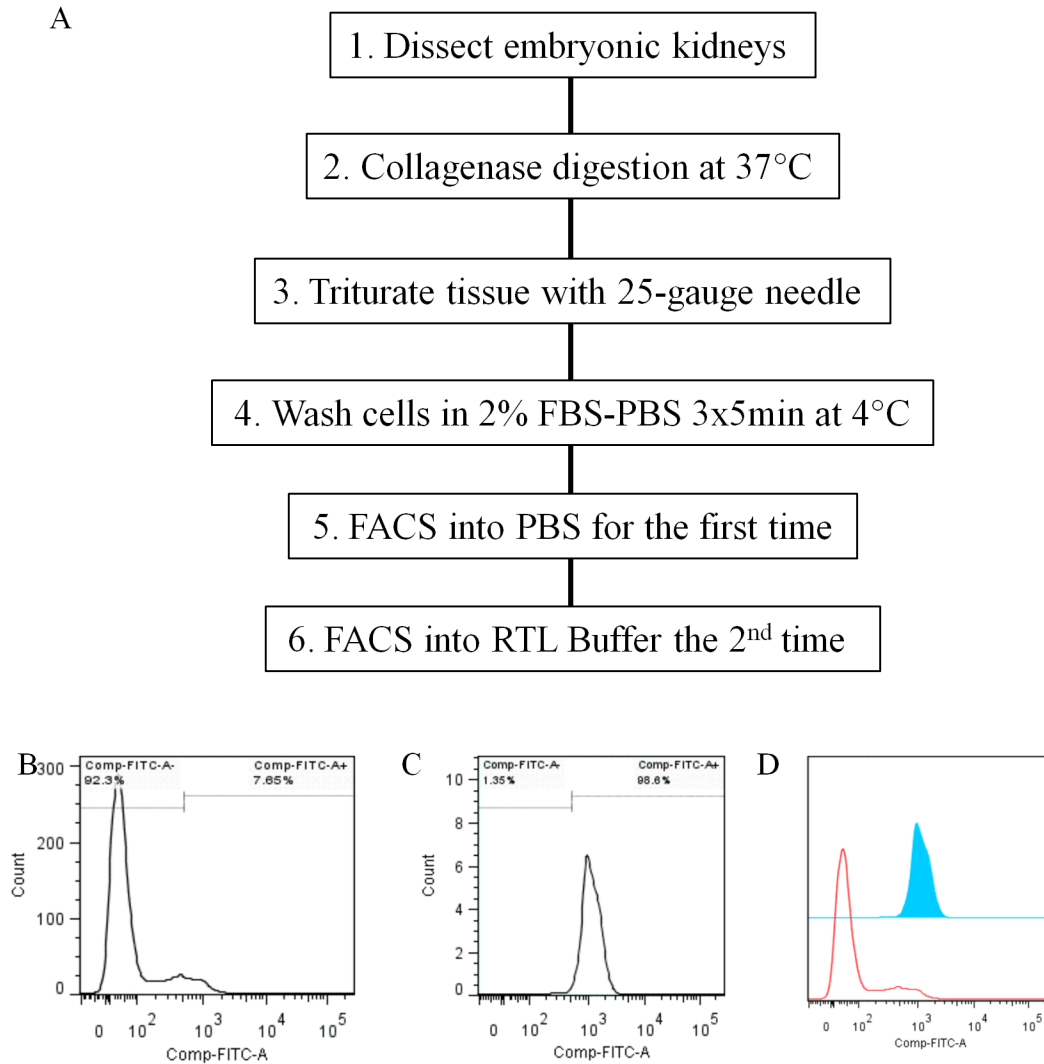
FoxD1eGFPCre mice could yield sufficient stromal cells for downstream applications such as qPCR, microarray, and RNA-seq. Since the eGFP reporter is expressed in FoxD1+ stromal progenitors and we are interested in isolating all stromal from the cortex and medulla, we first performed an immunohistochemistry stain in both *FoxD1eGFPCre;β-cat^{Δ2-6/+}* (WT littermates) and *FoxD1eGFPCre;β-cat^{Δ2-6/Δ2-6}* (*β-cat^{S/-}*) kidneys to confirm eGFP expression in all the stromal populations. We compared the eGFP expression pattern to an immunofluorescence stain for Pbx1, which marks all stromal cells (Boivin, Sarin et al. 2015). At E13.5, GFP+ cells are found the condensed mesenchyme and ureteric epithelium in a pattern identical to stromal cells, as evidenced by the Pbx1 expression (Figure 1A-B). In addition, the GFP+ cells adopt morphology identical to Pbx1 stromal cells (Figure 1B). At E15.5, a time point when the cortex and medulla are clearly established, GFP+ cells are found surrounding the collecting ducts, condensed mesenchyme and developing nephrons (Figure 1C) in a pattern identical to that of Pbx1+ cells (Figure 1D). In the medulla, GFP is expressed in the cells surrounding the collecting ducts and nephrogenic tubules, consistent with the Pbx1 expression pattern (Figure 1E-F). GFP expression is also observed in the glomeruli (Figure 1D, arrow), which was previously reported in previous lineage tracing studies that demonstrated stromal cells give rise to mesangial cells in the glomeruli, and that FoxD1 is also highly expressed mature podocytes (Kobayashi, Kwan et al. 2005, Kobayashi, Mugford et al. 2014). Together, this analysis confirms the presence of the eGFP reporter in all stromal populations.

Figure 5.1 – Lineage tracing analysis in *FoxD1-eGFPCre* kidneys

Lineage tracing analysis in *FoxD1-eGFPCre* kidneys - (A,C,E) GFP expression in *FoxD1-eGFPCre* kidneys at E13.5 (arrowheads)(A) and E15.5 in the cortex (C) and medulla (E). In the cortex, GFP (A,C) is expressed in a pattern identical to that of *Pbx1* (B, D), a general stromal marker, around the condensed mesenchyme (cm) at E13.5 (A-B) and E15.5 (C-D). In the medulla, GFP is expressed in cells surrounding the mature nephrogenic tubules (t) and collecting ducts (cd)(E) consistent with the *Pbx1* expression in medullary stromal cells (F). (cd = collecting duct, cm = condensed mesenchyme, cs = cortical stroma, ms = medullary stroma, t = tubule, scale bar = 100 μ m).

Now that we have established that the GFP expression is limited to the stroma population at E13.5, we next investigated whether we could isolate the stromal cell population via FACS sorting. Kidneys from *WT* and our mutant mice were dissected at E13.5. Four *WT* and four $\beta\text{-cat}^{S/-}$ kidneys were used. The kidneys were dissociated and triturated in 0.3% collagenase and subsequently washed in ice-cold PBS supplemented with 2% Fetal Bovine Serum (FBS). To ensure high specificity of the GFP+ cell population, we sorted one of the samples twice (in this case we sorted the $\beta\text{-cat}^{S/-}$ twice). The GFP+ cells were initially sorted into PBS. From the first sorting event, we demonstrated that 7.65% of the cells were GFP+ (24,915 cells)(Figure 2B). The GFP+ cells were sorted a second time and we confirmed 98.6% of the cells were GFP+ (24,566 cells)(Figure 2C-D). The second time the cells were sorted directly into RTL Qiagen Lysis buffer to prevent RNA degradation. We FACS sorted 24,566 cells from four $\beta\text{-cat}^{S/-}$ kidneys (2 embryos), and 19,836 cells from four *WT* littermate kidneys (2 embryos). *WT* kidneys from a separate litter (*FoxD1eGFPCre* x CD1) were also used to further isolate *WT* stromal cells. However, cells isolated from *FoxD1eGFPCre* mice cannot be used as littermate controls since the kidneys are not isolated at the same time and the post-coital time point might differ for two different pregnant mice. However, using these mice allows us to compare *WT* stroma cells on different genetic backgrounds (CD1 vs C57;Bl/6J), which provides further insight into stromal cells from different mouse strains. We sorted 38,000 cells from six *WT FoxD1eGFPCre* kidneys. Taken together, this demonstrates that we can isolate approximately 5,800 cells per kidney without having to cross these mice with a dtTomato reporter to increase the signal to permit increased

isolation efficiency. These FACS isolations demonstrate that we can isolate GFP⁺ cells with high efficiency from embryonic kidneys and confirms the low levels of contamination. However, the identity of these sorted cells should be confirmed in order to be used for downstream applications such as RNA-seq.

Figure 5.2 – Isolation of stromal cells using FACS

Isolation of stromal cells using FACS – (A) Steps to perform isolation of stromal cells via fluorescence-activated cell sorting (FACS). (B) – Cells were sorted a first time in PBS. We demonstrated that 7.65% were GFP+ cells. (C) – To reduce the level of contamination, we sorted the GFP+ cells a second time. We demonstrated 98.6% of the cells were GFP+. (D) Overlap of first and second sorting event. The blue population demonstrates the GFP+ cell population.

RNA extraction of FACS sorted stromal cells

Next, we determined whether these cells can be used for downstream applications. Since we first wanted to identify the types of cells present within the sorted population, we performed mRNA extraction using the RNeasy micro extraction kit, which is specifically designed for mRNA extraction of small cell samples. The sorted cells were directly sorted into lysis buffer and vortexed for about one minute to extract the RNA. Each sample was processed through a Qiagen column where RNA binds to the RNA binding membrane matrix. The column is then washed with ethanol and the RNA eluted into 14ul RNase free water (for a full protocol visit <https://www.qiagen.com/ca/shop/sample-technologies/rna/rna-preparation/rneasy-micro-kit>). We first quantified and assessed the quality of each sample. We analyzed the isolated RNA using a bioanalyzer, which provides an assessment of the quality and quantity of very small RNA samples (less than 1ng/ul) (performed by the Mobix DNA sequencing lab at McMaster University). The results from the bio analyzer demonstrated the isolation process yields high quality mRNA as indicated by the presence of undegraded ribosomal RNA (rRNA) bands at 2kb for 12S and 5kb for 28S in each sample (Figure 2A). Further quantitation of the isolated RNA demonstrated that for the *WT1* sample, which was composed of 6 kidneys (E13.5) and 38,000 cells, had a yield of 0.36ng/ul. The *WT2* sample, which was composed of 4 kidneys and 19,836 cells, had a yield of 2.182ng/ul. Finally, the β -*cat*^{S-/-} sample, which was composed of 4 kidneys and 24,566 cells, had a yield of 2.101 ng/ul (Figure 3A). While the RNA extraction appears somewhat variable using the Qiagen kit, our analysis demonstrates that approximately

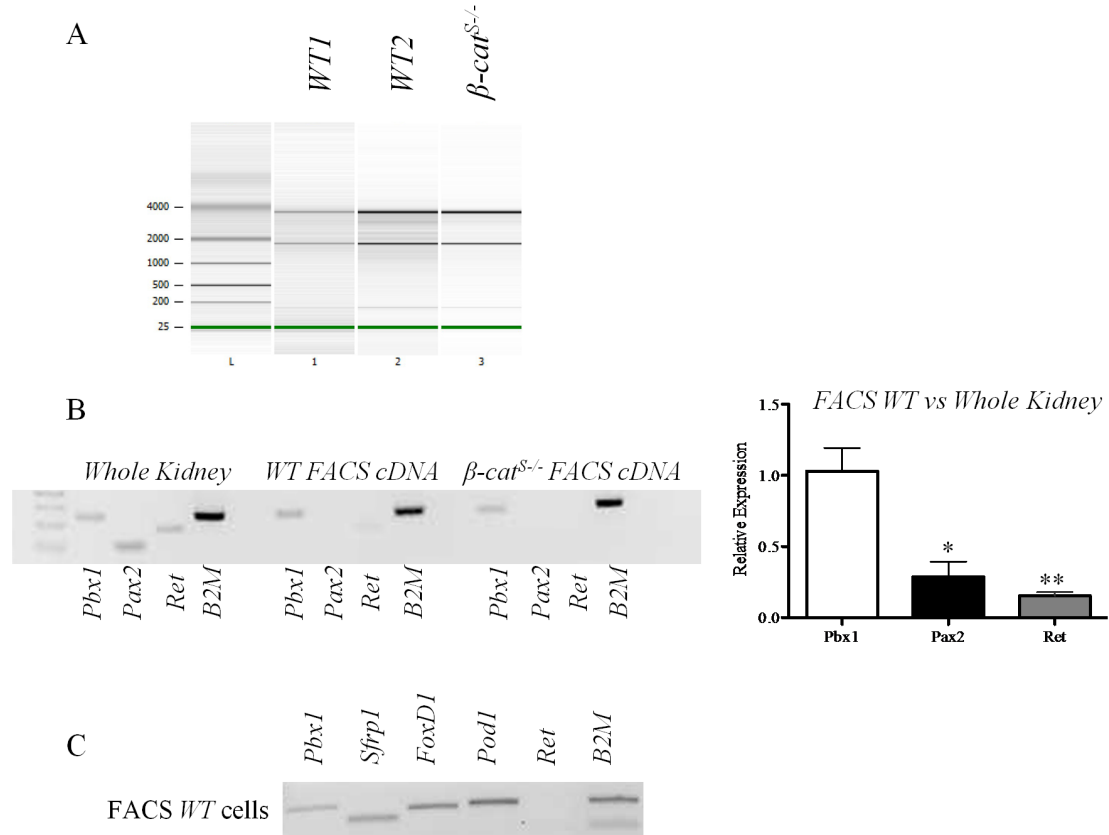
29ng of RNA (14ul x 2.1ng/ul) can be extracted from about 22,000 cells. According to the Qiagen RNeasy Micro kit, 500,000 cells should yield approximately 5000ng. This means that about 22,000 cells should yield around 220ng or a concentration of 15.71ng/ul when eluted in 14ul of water. Since the concentrations of our samples are relatively low we are currently working on optimizing the RNA extraction step using different kits designed for very small samples.

Identification of FACS sorted stromal cells

As early as E13.5, the kidney is composed multiple cell populations that originate from the stromal progenitors, the ureteric epithelial progenitors, and the nephrogenic progenitors (Little and McMahon 2012). Therefore, to ensure that the GFP+ cells we isolated were stromal cells, we utilized the RNA isolated above to perform RT-qPCR and assessed the expression level of factors specific to the three main cell populations in the kidney. First, we analyzed the expression of *Ret*, a marker of the ureteric epithelium, and demonstrated a virtual absence in *WT* and β -*cat*^{S/-} isolated cells compared to whole kidneys (1.03 vs 0.154, p=0.006)(Figure 3B). Similarly, *Pax2* expression, which is found both in the ureteric epithelium and nephrogenic progenitors, was also virtually absent in *WT* and β -*cat*^{S/-} cells compared to whole kidney lysate (1.03 vs 0.29, p=0.01)(Figure 3B). The presence of low *Pax2* and *Ret* expression in the *WT* sample demonstrates there is some level of epithelial and mesenchymal contamination. The expression of *Pbx1*, which is a marker of stromal cells, was strongly expressed in both *WT* and β -*cat*^{S/-} cells and in whole kidney lysates. This demonstrates that the isolated cells are stromal cells and there

is a very low level of contamination from nephrogenic or ureteric epithelial progenitors that are not likely to have significant effects on downstream applications.

Furthermore, to specifically determine which stromal cell populations were present within the isolated GFP+ cells, we analyzed markers from the capsular, cortical, and medullary stroma by performing PCR on cDNA from one of the *WT* samples. We detected the expression of *Pbx1* (*general stroma*), *Sfrp1* (*capsular*), *FoxD1* (*cortical*), and *Pod1* (*medullary*) markers in *WT* GFP+ cells. Ret expression (ureteric epithelium) was not detected in *WT* FACS cells (Figure 3C). Together, this analysis demonstrates that stromal cells from *FoxD1eGFPCre* (*WT1* sample on CD1 background), *FoxD1eGFPCre*;β-*cat*^{S+/-} (*WT2* sample) and *FoxD1eGFPCre*;β-*cat*^{S-/-} (β-*cat*^{S-/-} sample) kidneys can be isolated to extract sufficient amounts of stromal specific mRNA for gene expression analysis. This protocol will allow us to perform gene expression analysis as well as RNA-seq on FACS sorted cells to identify stromal specific β-catenin-targets. However, since the number of sorted cells per FACS experiment is still relatively low (around 5,800 cell/kidney), this protocol may not be suitable for protein assays, such as co-immunoprecipitation and chromatin immunoprecipitation. Therefore, we are currently optimizing a FACS protocol to determine whether crossing *FoxD1eGFPCre* and *FoxD1eGFPCre*;β-*cat*^{S-/-} mice with dtTomato-ROSA mice would allow us to extract sufficient protein yields.

Figure 5.3 – Identification of the stromal markers in FACS stromal cells

Identification of the stromal markers in FACS stromal cells – (A) RNA isolation from *WT* FACS cells (samples *WT1* and *WT2*) and β -*cat*^{S/S-} cells. (B) – qPCR quantification of stromal, mesenchymal, and epithelial markers in whole kidneys, *WT* FACS sorted cells and β -*cat*^{S/S-} sorted cells (1.03 vs 0.29, $p=0.01$ and 1.03 vs 0.154, $p=0.006$). Epithelial and mesenchymal markers are virtually absent in *WT* and β -*cat*^{S/S-} sorted cells. (C) Quantification of different stromal markers in FACS *WT* cells. We observed the presence of capsular (*Sfrp1*), cortical (*FoxD1*), and medullary (*Pod1*) markers in FACS *WT* cells. *Ret* expression was not observed in FACS *WT* cells.

CHAPTER 6 – DISCUSSION

At the onset of this thesis project, the contribution of the stromal population to kidney development and renal dysplasia was poorly understood. Additionally, the role of stromal β -catenin in kidney development and in the genesis of renal dysplasia was not known. This thesis identified important roles for β -catenin in the developing kidney. First, I demonstrated that a stabilization of β -catenin specifically in stromal cells contributes to the genesis of renal dysplasia by disrupting proper stromal cell differentiation. Secondly, I showed that stromal β -catenin regulates communication between the ureteric epithelium and the condensed mesenchyme via the Wnt9b signaling pathway. Thirdly, I demonstrated that β -catenin is essential for medullary stromal cell differentiation. Finally, I developed a protocol to isolate stromal cells from *WT* and stromal β -catenin deficient mice and investigated potential downstream applications to further our understanding of stromal β -catenin in the context of kidney development and disease. Combined, these studies advance our understanding of stromal β -catenin in the developing kidney and define its crucial role in the development of renal dysplasia.

The Role of Stromal β -catenin in Renal Dysplasia

The overexpression of stromal β -catenin was sufficient to mimic the histopathological features observed in renal dysplasia, including disrupted nephrogenesis, disrupted branching morphogenesis, and a notable expansion of the stromal-like cells. Prior to the work presented in chapter 2, this expanded population of fibroblast cells in renal dysplasia had always been described as stromal cells (Woolf, Price et al. 2004, Winyard and Chitty 2008, Goodyer 2009, Sarin, Boivin et al. 2014, Chen and Chang

2015). My work provides a better characterization and understanding of the molecular changes in this cell population and demonstrates that they are in fact not stromal cells. Instead, they are a population of cells that express high levels of chemo-attractants, which promote vascular defects. I have identified misregulated chemo-attractants both in β -*cat*^{GOF-S} kidneys and in human samples of renal dysplasia that are likely direct targets of β -catenin. Additionally, by comparing β -*cat*^{GOF-S} kidneys to human dysplastic tissues, I demonstrated that our model is suitable to study the molecular mechanisms involved in the pathogenesis of renal dysplasia. Moving forward with this project, it will be important to determine whether a downregulation of these chemo-attractants can rescue vascular morphogenesis defects, and possibly rescue the defects in stromal cell identity observed in β -*cat*^{GOF-S} kidneys. Combined, this work provides foundational knowledge for the development of better treatment strategies for patients with renal dysplasia.

The Functional Role of Stromal β -catenin in Kidney Development

Despite prior work hinting at a functional role for β -catenin in medullary stromal cells (Yu, Carroll et al. 2009), the expression and cellular localization of β -catenin in the different stromal populations was poorly defined when I started this thesis project. To gain a better understanding of its functional role in the distinct stromal lineages, I performed a careful analysis of β -catenin expression at different embryonic time points and demonstrated a dynamic expression pattern throughout development in capsular, cortical, and medullary stromal cells. This expression analysis advanced our understanding of the potential roles of β -catenin in the different stromal compartments

and expanded on previous studies that demonstrated Wnt/ β -catenin signaling activity in medullary stromal cells (Yu, Carroll et al. 2009).

In the renal capsule, the deletion of β -catenin resulted in several non-adherent capsular stromal cells, suggesting a role in cell adhesion. The contribution of these capsular defects to kidney development is not clear. Capsular stromal cells play an essential role in maintaining the high pressure within the kidney parenchyma (Garcia-Estan and Roman 1989) and regulating proper formation and communication with the underlying cortical stroma and condensed mesenchyme (Levinson, Batourina et al. 2005, Yallowitz, Hrycaj et al. 2011). β -cat^{S-/-} kidneys exhibited several misplaced tubules directly below the non-adherent capsular stromal cells. This suggests the defects in capsular stroma likely contribute to the abnormalities observed in the underlying nephrogenic zone. Further work is required to determine whether these defects are directly caused by the loss of β -catenin or caused by disruptions in renal capsule formation.

In the renal cortex, I demonstrated using both β -cat^{S-/-} and β -cat^{GOF-S} kidneys that stromal β -catenin modulates Wnt9b signaling between the ureteric epithelium and condensed mesenchyme. During the course of this thesis, several studies have advanced our understanding of the mechanisms that regulate the nephron progenitors. Stromal cells are ideally located directly adjacent to the nephron progenitors and ureteric epithelium to modulate cellular processes. Studies have shown that stromal factors, such as Fat4 (Das, Tanigawa et al. 2013) and Decorin (Fetting, Guay et al. 2014) communicate directly with the nephrogenic progenitors to modulate proliferation and differentiation of the

nephrogenic progenitors. My results support a similar mechanism whereby stromal cells modulate proliferation of the nephrogenic progenitors. However, unlike previous studies that focused mainly on direct interactions between the stroma and the nephrogenic progenitors, my findings demonstrate that β -catenin controls factors that modulate gene expression in epithelial cells to control proliferation of the nephrogenic progenitors. Interestingly, a study published at the same time as mine demonstrated that a stromal deletion of *Dicer1*, a protein essential for post-transcriptional processing of micro-RNAs, resulted primarily in a lack of β -catenin expression and reduced nephrogenic progenitors around the ureteric bud tip (Nakagawa, Xin et al. 2015). Surprisingly, these stromal *Dicer1* deficient kidneys are phenotypically similar to β -cat^{S-/-} kidneys with respect to cortico-medullary axis defects and reduced nephrogenic progenitors (Nakagawa, Xin et al. 2015). This study further supports a mechanism where a loss of stromal β -catenin results in reduced nephrogenic progenitors.

The molecular mechanism by which β -catenin in stromal cells controls the expression of *Wnt9b* in epithelial cells is not clear. Previous studies have demonstrated stromal cells secrete factors that signal to adjacent cell populations (Mendelsohn, Batourina et al. 1999, Batourina, Gim et al. 2001, Yang, Blum et al. 2002, Paroly, Wang et al. 2013). Since β -catenin localizes to the nucleus of cortical and medullary stromal cells, it likely controls the expression of secreted factors that signal to the epithelium to modulate *Wnt9b* expression. Alternatively, direct stromal-epithelial interactions have been shown to regulate proper development of other organs (Cunha, Bigsby et al. 1985, Howard and Lu 2014), suggesting β -catenin could regulate the expression of factors, such

as extracellular matrix components and cell surface factors, that signal directly to the epithelium via cell-cell interactions to modulate cellular processes. Further work is required to identify these stromal factors. In chapter 5, I demonstrated that sufficient mRNA could be isolated specifically from stromal cells in *WT* and β -*cat*^{S-/-} kidneys. Performing RNA-sequencing using stroma-specific mRNA from *WT* and β -*cat*^{S-/-} would allow us to identify stromal factors controlled by β -catenin that promote communication between the renal stroma and the epithelium to modulate Wnt9b signaling.

My studies have also identified an important role for β -catenin in the medullary stroma. A deletion of stromal β -catenin results primarily in a failure of medullary formation and cortico-medullary defects. Before I started this thesis project, previous studies had reported a mechanism where Wnt7b, expressed and secreted by the ureteric epithelial stalk cells, signals to the adjacent stromal cells to activate the Wnt/ β -catenin pathway and contribute to tubule elongation and medulla. The role of β -catenin in these medullary stromal cells however was not clear. The analysis of medullary stroma in β -*cat*^{S-/-} kidneys revealed a significant reduction in medullary genes essential for medullary stromal differentiation, such as Wnt4 (Yu, Carroll et al. 2009, Boivin, Sarin et al. 2015), and Pod1, demonstrating an important role for β -catenin in the development of the medullary stroma. However, further work will be required to determine whether β -catenin specifically regulates the expression of those medullary stromal genes.

In addition to a role in medullary stroma differentiation, I demonstrated that stromal β -catenin possibly plays a role in the regulation of stromal cells survival. However, the mechanism by which stromal β -catenin regulates cell survival is not clear.

One possibility is that the misdifferentiated stromal cells are simply discarded via programmed cell death. However, I demonstrated that β -catenin binds to Tbx5, Yap, and Yes to form a complex that interacts with the promoter region of *Bcl2l1*, which is significantly reduced in β -cat^{S-/-} kidneys. This complex has previously been shown to directly regulate the transcription of *Bcl2l1* (Rosenbluh, Nijhawan et al. 2012), suggesting a potential functional role in the kidney. Therefore, it is possible that stromal β -catenin controls survival of the development medullary stroma by regulating the expression of anti-apoptotic genes. Further research is required to determine whether this complex forms specifically in stromal cells and to determine if it regulates the expression of *Bcl2l1*. Interestingly, previous studies have demonstrated medullary stromal cell survival must be tightly regulated for proper medulla formation (Carev, Krnic et al. 2006, Ho 2014). My findings expand on a potential role for β -catenin in the regulation of apoptosis in the kidney and suggest cell survival must be tightly regulated for proper formation of the medullary stroma.

Limitations and Future Directions

The work presented in this thesis has allowed me to identify several misregulated genes in β -cat^{S-/-} kidneys. However, the quantification of these genes was performed using mRNA from whole kidneys. While this approach is appropriate for cell-specific genes, such as *Wnt9b* in ureteric epithelial cells (Carroll, Park et al. 2005), it is difficult to confirm changes in genes that are ubiquitously expressed in various cell types of the developing kidney, such as *Bcl2l1* (Gonzalez-Garcia, Perez-Ballesteros et al. 1994). In

order to address this limitation, I developed a protocol to isolate sufficient amounts of mRNA specifically from *WT* and $\beta\text{-cat}^{S/-}$ stromal cells. This approach will allow us to confirm changes in anti-apoptotic genes specifically in stromal cells. Furthermore, I suspect β -catenin controls genes in stromal cells that signal to the adjacent ureteric epithelium to regulate the expression of *Wnt9b*. Therefore, performing RNA-sequencing on *WT* and β -catenin deficient stromal cells will allow us to identify novel β -catenin targets involved in this mechanism and further our current understanding of stromal β -catenin in the kidney.

This thesis has established important roles for stromal β -catenin in the development of renal dysplasia and kidney formation. Most importantly, with the development of two novel mouse models, I have demonstrated that β -catenin must be tightly regulated in stromal cells for proper kidney formation. Increased levels of stromal β -catenin result in renal dysplasia by disrupting proper stromal cell identity and vascular morphogenesis. Conversely, a loss of β -catenin in stromal cells results in a failure of renal medulla formation and disrupted communication between adjacent epithelial and mesenchymal cells populations. These studies expand our understanding of stromally-expressed β -catenin in the kidney and provide significant foundational knowledge for the development of better treatment strategies for patients with renal dysplasia by identifying key mechanisms involved in the pathogenesis of kidney disease.

REFERENCES

Bagherie-Lachidan, M., A. Reginensi, Q. Pan, H. P. Zaveri, D. A. Scott, B. J. Blencowe, F. Helmbacher and H. McNeill (2015). "Stromal Fat4 acts non-autonomously with Dchs1/2 to restrict the nephron progenitor pool." *Development* **142**(15): 2564-2573.

Batourina, E., S. Gim, N. Bello, M. Shy, M. Clagett-Dame, S. Srinivas, F. Costantini and C. Mendelsohn (2001). "Vitamin A controls epithelial/mesenchymal interactions through Ret expression." *Nat Genet* **27**(1): 74-78.

Berthon, A., I. Sahut-Barnola, S. Lambert-Langlais, C. de Jossineau, C. Damon-Soubeyrand, E. Louiset, M. M. Taketo, F. Tissier, J. Bertherat, A. M. Lefrancois-Martinez, A. Martinez and P. Val (2010). "Constitutive beta-catenin activation induces adrenal hyperplasia and promotes adrenal cancer development." *Hum Mol Genet* **19**(8): 1561-1576.

Blank, U., M. L. Seto, D. C. Adams, D. M. Wojchowski, M. J. Karolak and L. Oxburgh (2008). "An in vivo reporter of BMP signaling in organogenesis reveals targets in the developing kidney." *BMC Dev Biol* **8**: 86.

Boivin, F. and D. Bridgewater (2014). " β -Catenin in the renal stroma regulates apoptosis via Bcl2l1 during kidney development (344.4)." *The FASEB Journal* **28**(1 Supplement).

Boivin, F. J., S. Sarin, P. Dabas, M. Karolak, L. Oxburgh and D. Bridgewater (2016). "Stromal beta-catenin overexpression contributes to the pathogenesis of renal dysplasia." *J Pathol*.

Boivin, F. J., S. Sarin, J. C. Evans and D. Bridgewater (2015). "The Good and Bad of beta-Catenin in Kidney Development and Renal Dysplasia." *Front Cell Dev Biol* **3**: 81.

Boivin, F. J., S. Sarin, J. Lim, A. Javidan, B. Svajger, H. Khalili and D. Bridgewater (2015). "Stromally expressed beta-catenin modulates Wnt9b signaling in the ureteric epithelium." *PLoS One* **10**(3): e0120347.

Boyle, S. C., Z. Liu and R. Kopan (2014). "Notch signaling is required for the formation of mesangial cells from a stromal mesenchyme precursor during kidney development." *Development* **141**(2): 346-354.

Brault, V., R. Moore, S. Kutsch, M. Ishibashi, D. H. Rowitch, A. P. McMahon, L. Sommer, O. Boussadia and R. Kemler (2001). "Inactivation of the beta-catenin gene by

Wnt1-Cre-mediated deletion results in dramatic brain malformation and failure of craniofacial development." *Development* **128**(8): 1253-1264.

Brenner, B. M., D. L. Garcia and S. Anderson (1988). "Glomeruli and blood pressure. Less of one, more the other?" *Am J Hypertens* **1**(4 Pt 1): 335-347.

Bridgewater, D., B. Cox, J. Cain, A. Lau, V. Athaide, P. S. Gill, S. Kuure, K. Sainio and N. D. Rosenblum (2008). "Canonical WNT/beta-catenin signaling is required for ureteric branching." *Dev Biol* **317**(1): 83-94.

Bridgewater, D., V. Di Giovanni, J. E. Cain, B. Cox, M. Jakobson, K. Sainio and N. D. Rosenblum (2011). "beta-catenin causes renal dysplasia via upregulation of Tgfbeta2 and Dkk1." *J Am Soc Nephrol* **22**(4): 718-731.

Bridgewater, D. and N. D. Rosenblum (2009). "Stimulatory and inhibitory signaling molecules that regulate renal branching morphogenesis." *Pediatr Nephrol* **24**(9): 1611-1619.

Brunskill, E. W., J. S. Park, E. Chung, F. Chen, B. Magella and S. S. Potter (2014). "Single cell dissection of early kidney development: multilineage priming." *Development* **141**(15): 3093-3101.

Cain, J. E., V. Di Giovanni, J. Smeeton and N. D. Rosenblum (2010). "Genetics of renal hypoplasia: insights into the mechanisms controlling nephron endowment." *Pediatr Res* **68**(2): 91-98.

Cano-Gauci, D. F., H. H. Song, H. Yang, C. McKerlie, B. Choo, W. Shi, R. Pullano, T. D. Piscione, S. Grisaru, S. Soon, L. Sedlackova, A. K. Tanswell, T. W. Mak, H. Yeger, G. A. Lockwood, N. D. Rosenblum and J. Filmus (1999). "Glypican-3-deficient mice exhibit developmental overgrowth and some of the abnormalities typical of Simpson-Golabi-Behmel syndrome." *J Cell Biol* **146**(1): 255-264.

Carev, D., D. Krnic, M. Saraga, D. Sapunar and M. Saraga-Babic (2006). "Role of mitotic, pro-apoptotic and anti-apoptotic factors in human kidney development." *Pediatr Nephrol* **21**(5): 627-636.

Carroll, T. J., J. S. Park, S. Hayashi, A. Majumdar and A. P. McMahon (2005). "Wnt9b plays a central role in the regulation of mesenchymal to epithelial transitions underlying organogenesis of the mammalian urogenital system." *Dev Cell* **9**(2): 283-292.

Cattelino, A., S. Liebner, R. Gallini, A. Zanetti, G. Balconi, A. Corsi, P. Bianco, H. Wolburg, R. Moore, B. Oreda, R. Kemler and E. Dejana (2003). "The conditional inactivation of the beta-catenin gene in endothelial cells causes a defective vascular pattern and increased vascular fragility." *J Cell Biol* **162**(6): 1111-1122.

Cebrian, C., K. Borodo, N. Charles and D. A. Herzlinger (2004). "Morphometric index of the developing murine kidney." *Dev Dyn* **231**(3): 601-608.

Chen, R. Y. and H. Chang (2015). "Renal dysplasia." *Arch Pathol Lab Med* **139**(4): 547-551.

Clevers, H. and R. Nusse (2012). "Wnt/beta-catenin signaling and disease." *Cell* **149**(6): 1192-1205.

Clifford, R. L., K. Deacon and A. J. Knox (2008). "Novel regulation of vascular endothelial growth factor-A (VEGF-A) by transforming growth factor (beta)1: requirement for Smads, (beta)-CATENIN, AND GSK3(beta)." *J Biol Chem* **283**(51): 35337-35353.

Collins, A. J., R. N. Foley, B. Chavers, D. Gilbertson, C. Herzog, K. Johansen, B. Kasiske, N. Kutner, J. Liu, W. St Peter, H. Guo, S. Gustafson, B. Heubner, K. Lamb, S. Li, S. Li, Y. Peng, Y. Qiu, T. Roberts, M. Skeans, J. Snyder, C. Solid, B. Thompson, C. Wang, E. Weinhandl, D. Zaun, C. Arko, S. C. Chen, F. Daniels, J. Ebben, E. Frazier, C. Hanzlik, R. Johnson, D. Sheets, X. Wang, B. Forrest, E. Constantini, S. Everson, P. Eggers and L. Agodoa (2012). "United States Renal Data System 2011 Annual Data Report: Atlas of chronic kidney disease & end-stage renal disease in the United States." *Am J Kidney Dis* **59**(1 Suppl 1): A7, e1-420.

Costantini, F. and R. Kopan (2010). "Patterning a complex organ: branching morphogenesis and nephron segmentation in kidney development." *Dev Cell* **18**(5): 698-712.

Cui, S., L. Schwartz and S. E. Quaggin (2003). "Pod1 is required in stromal cells for glomerulogenesis." *Dev Dyn* **226**(3): 512-522.

Cullen-McEwen, L. A., G. Caruana and J. F. Bertram (2005). "The where, what and why of the developing renal stroma." *Nephron Exp Nephrol* **99**(1): e1-8.

Cunha, G. R., R. M. Bigsby, P. S. Cooke and Y. Sugimura (1985). "Stromal-epithelial interactions in adult organs." *Cell Differ* **17**(3): 137-148.

Das, A., S. Tanigawa, C. M. Karner, M. Xin, L. Lum, C. Chen, E. N. Olson, A. O. Perantoni and T. J. Carroll (2013). "Stromal-epithelial crosstalk regulates kidney progenitor cell differentiation." *Nat Cell Biol* **15**(9): 1035-1044.

DiRocco, D. P., A. Kobayashi, M. M. Taketo, A. P. McMahon and B. D. Humphreys (2013). "Wnt4/beta-catenin signaling in medullary kidney myofibroblasts." *J Am Soc Nephrol* **24**(9): 1399-1412.

Dudley, A. T. and E. J. Robertson (1997). "Overlapping expression domains of bone morphogenetic protein family members potentially account for limited tissue defects in BMP7 deficient embryos." *Dev Dyn* **208**(3): 349-362.

Duval, D., M. Malaise, B. Reinhardt, C. Kedinger and H. Boeuf (2004). "A p38 inhibitor allows to dissociate differentiation and apoptotic processes triggered upon LIF withdrawal in mouse embryonic stem cells." *Cell Death Differ* **11**(3): 331-341.

Eberhart, C. G. and P. Argani (2001). "Wnt signaling in human development: beta-catenin nuclear translocation in fetal lung, kidney, placenta, capillaries, adrenal, and cartilage." *Pediatr Dev Pathol* **4**(4): 351-357.

Eger, A., A. Stockinger, B. Schaffhauser, H. Beug and R. Foisner (2000). "Epithelial mesenchymal transition by c-Fos estrogen receptor activation involves nuclear translocation of beta-catenin and upregulation of beta-catenin/lymphoid enhancer binding factor-1 transcriptional activity." *J Cell Biol* **148**(1): 173-188.

Ekblom, P. and A. Weller (1991). "Ontogeny of tubulointerstitial cells." *Kidney Int* **39**(3): 394-400.

El-Dahr, S. S., L. M. Harrison-Bernard, S. Dipp, I. V. Yosipiv and S. Meleg-Smith (2000). "Bradykinin B2 null mice are prone to renal dysplasia: gene-environment interactions in kidney development." *Physiol Genomics* **3**(3): 121-131.

Elmore, S. (2007). "Apoptosis: a review of programmed cell death." *Toxicol Pathol* **35**(4): 495-516.

Fanni, D., V. Fanos, C. Gerosa, G. Senes, A. Sanna, P. Van Eyken, N. Iacovidou, G. Monga and G. Faa (2013). "CD44 immunoreactivity in the developing human kidney: a marker of renal progenitor stem cells?" *Ren Fail* **35**(7): 967-970.

Fetting, J. L., J. A. Guay, M. J. Karolak, R. V. Iozzo, D. C. Adams, D. E. Maridas, A. C. Brown and L. Oxburgh (2014). "FOXD1 promotes nephron progenitor

differentiation by repressing decorin in the embryonic kidney." *Development* **141**(1): 17-27.

Garcia-Estan, J. and R. J. Roman (1989). "Role of renal interstitial hydrostatic pressure in the pressure diuresis response." *Am J Physiol* **256**(1 Pt 2): F63-70.

Ghanem, M. A., T. H. Van der Kwast, J. C. Den Hollander, M. K. Sudaryo, M. M. Van den Heuvel, M. A. Noordzij, R. J. Nijman, E. H. Soliman and G. J. van Steenbrugge (2001). "The prognostic significance of apoptosis-associated proteins BCL-2, BAX and BCL-X in clinical nephroblastoma." *Br J Cancer* **85**(10): 1557-1563.

Gong, K. Q., A. R. Yallowitz, H. Sun, G. R. Dressler and D. M. Wellik (2007). "A Hox-Eya-Pax complex regulates early kidney developmental gene expression." *Mol Cell Biol* **27**(21): 7661-7668.

Gonzalez-Garcia, M., R. Perez-Ballesterro, L. Ding, L. Duan, L. H. Boise, C. B. Thompson and G. Nunez (1994). "bcl-XL is the major bcl-x mRNA form expressed during murine development and its product localizes to mitochondria." *Development* **120**(10): 3033-3042.

Goodyer, P. (2009). *Renal Dysplasia/Hypoplasia*. Pediatric Nephrology. E. Avner, W. Harmon, P. Niaudet and N. Yoshikawa, Springer Berlin Heidelberg: 107-120.

Grobstein, C. (1967). "Mechanisms of organogenetic tissue interaction." *Natl Cancer Inst Monogr* **26**: 279-299.

Grote, D., S. K. Boualia, A. Souabni, C. Merkel, X. Chi, F. Costantini, T. Carroll and M. Bouchard (2008). "Gata3 acts downstream of beta-catenin signaling to prevent ectopic metanephric kidney induction." *PLoS Genet* **4**(12): e1000316.

Gujral, T. S., W. van Veelen, D. S. Richardson, S. M. Myers, J. A. Meens, D. S. Acton, M. Dunach, B. E. Elliott, J. W. Hoppener and L. M. Mulligan (2008). "A novel RET kinase-beta-catenin signaling pathway contributes to tumorigenesis in thyroid carcinoma." *Cancer Res* **68**(5): 1338-1346.

Gulati, S., S. Mittal, R. K. Sharma and A. Gupta (1999). "Etiology and outcome of chronic renal failure in Indian children." *Pediatr Nephrol* **13**(7): 594-596.

Gumbiner, B. M. (2000). "Regulation of cadherin adhesive activity." *J Cell Biol* **148**(3): 399-404.

Gumbiner, B. M. (2005). "Regulation of cadherin-mediated adhesion in morphogenesis." *Nat Rev Mol Cell Biol* **6**(8): 622-634.

Harada, N., Y. Tamai, T. Ishikawa, B. Sauer, K. Takaku, M. Oshima and M. M. Taketo (1999). "Intestinal polyposis in mice with a dominant stable mutation of the beta-catenin gene." *EMBO J* **18**(21): 5931-5942.

Hatini, V., S. O. Huh, D. Herzlinger, V. C. Soares and E. Lai (1996). "Essential role of stromal mesenchyme in kidney morphogenesis revealed by targeted disruption of Winged Helix transcription factor BF-2." *Genes Dev* **10**(12): 1467-1478.

Heallen, T., M. Zhang, J. Wang, M. Bonilla-Claudio, E. Klysik, R. L. Johnson and J. F. Martin (2011). "Hippo pathway inhibits Wnt signaling to restrain cardiomyocyte proliferation and heart size." *Science* **332**(6028): 458-461.

Heuberger, J. and W. Birchmeier (2010). "Interplay of cadherin-mediated cell adhesion and canonical Wnt signaling." *Cold Spring Harb Perspect Biol* **2**(2): a002915.

Ho, J. (2014). "The regulation of apoptosis in kidney development: implications for nephron number and pattern?" *Front Pediatr* **2**: 128.

Holnthoner, W., M. Pillinger, M. Groger, K. Wolff, A. W. Ashton, C. Albanese, P. Neumeister, R. G. Pestell and P. Petzelbauer (2002). "Fibroblast growth factor-2 induces Lef/Tcf-dependent transcription in human endothelial cells." *J Biol Chem* **277**(48): 45847-45853.

Howard, B. A. and P. Lu (2014). "Stromal regulation of embryonic and postnatal mammary epithelial development and differentiation." *Semin Cell Dev Biol* **25-26**: 43-51.

Hoy, W. E., M. D. Hughson, J. F. Bertram, R. Douglas-Denton and K. Amann (2005). "Nephron number, hypertension, renal disease, and renal failure." *J Am Soc Nephrol* **16**(9): 2557-2564.

Hsu, W., R. Shakya and F. Costantini (2001). "Impaired mammary gland and lymphoid development caused by inducible expression of Axin in transgenic mice." *J Cell Biol* **155**(6): 1055-1064.

Hu, M. C., T. D. Piscione and N. D. Rosenblum (2003). "Elevated SMAD1/beta-catenin molecular complexes and renal medullary cystic dysplasia in ALK3 transgenic mice." *Development* **130**(12): 2753-2766.

Hu, M. C. and N. D. Rosenblum (2005). "Smad1, beta-catenin and Tcf4 associate in a molecular complex with the Myc promoter in dysplastic renal tissue and cooperate to control Myc transcription." *Development* **132**(1): 215-225.

Huang, M., Y. Wang, D. Sun, H. Zhu, Y. Yin, W. Zhang, S. Yang, L. Quan, J. Bai, S. Wang, Q. Chen, S. Li and N. Xu (2006). "Identification of genes regulated by Wnt/beta-catenin pathway and involved in apoptosis via microarray analysis." *BMC Cancer* **6**: 221.

Hum, S., C. Rymer, C. Schaefer, D. Bushnell and S. Sims-Lucas (2014). "Ablation of the renal stroma defines its critical role in nephron progenitor and vasculature patterning." *PLoS One* **9**(2): e88400.

Humphreys, B. D., S. L. Lin, A. Kobayashi, T. E. Hudson, B. T. Nowlin, J. V. Bonventre, M. T. Valerius, A. P. McMahon and J. S. Duffield (2010). "Fate tracing reveals the pericyte and not epithelial origin of myofibroblasts in kidney fibrosis." *Am J Pathol* **176**(1): 85-97.

Hussein, S. M., E. K. Duff and C. Sirard (2003). "Smad4 and beta-catenin co-activators functionally interact with lymphoid-enhancing factor to regulate graded expression of Msx2." *J Biol Chem* **278**(49): 48805-48814.

Iglesias, D. M., P. A. Hueber, L. Chu, R. Campbell, A. M. Patenaude, A. J. Dziarmaga, J. Quinlan, O. Mohamed, D. Dufort and P. R. Goodyer (2007). "Canonical WNT signaling during kidney development." *Am J Physiol Renal Physiol* **293**(2): F494-500.

Ille, F. and L. Sommer (2005). "Wnt signaling: multiple functions in neural development." *Cell Mol Life Sci* **62**(10): 1100-1108.

Itaranta, P., L. Chi, T. Seppanen, M. Niku, J. Tuukkanen, H. Peltoketo and S. Vainio (2006). "Wnt-4 signaling is involved in the control of smooth muscle cell fate via Bmp-4 in the medullary stroma of the developing kidney." *Dev Biol* **293**(2): 473-483.

Itoh, F., S. Itoh, M. J. Goumans, G. Valdimarsdottir, T. Iso, G. P. Dotto, Y. Hamamori, L. Kedes, M. Kato and P. ten Dijke Pt (2004). "Synergy and antagonism between Notch and BMP receptor signaling pathways in endothelial cells." *EMBO J* **23**(3): 541-551.

Jain, S., A. A. Suarez, J. McGuire and H. Liapis (2007). "Expression profiles of congenital renal dysplasia reveal new insights into renal development and disease." *Pediatr Nephrol* **22**(7): 962-974.

Kanwar, Y. S., F. A. Carone, A. Kumar, J. Wada, K. Ota and E. I. Wallner (1997). "Role of extracellular matrix, growth factors and proto-oncogenes in metanephric development." *Kidney Int* **52**(3): 589-606.

Karner, C. M., R. Chirumamilla, S. Aoki, P. Igarashi, J. B. Wallingford and T. J. Carroll (2009). "Wnt9b signaling regulates planar cell polarity and kidney tubule morphogenesis." *Nat Genet* **41**(7): 793-799.

Karner, C. M., A. Das, Z. Ma, M. Self, C. Chen, L. Lum, G. Oliver and T. J. Carroll (2011). "Canonical Wnt9b signaling balances progenitor cell expansion and differentiation during kidney development." *Development* **138**(7): 1247-1257.

Katabathina, V. S., G. Kota, A. K. Dasyam, A. K. Shanbhogue and S. R. Prasad (2010). "Adult renal cystic disease: a genetic, biological, and developmental primer." *Radiographics* **30**(6): 1509-1523.

Kett, M. M. and J. F. Bertram (2004). "Nephron endowment and blood pressure: what do we really know?" *Curr Hypertens Rep* **6**(2): 133-139.

Kim, B. S. and M. S. Goligorsky (2003). "Role of VEGF in kidney development, microvascular maintenance and pathophysiology of renal disease." *Korean J Intern Med* **18**(2): 65-75.

Kispert, A., S. Vainio and A. P. McMahon (1998). "Wnt-4 is a mesenchymal signal for epithelial transformation of metanephric mesenchyme in the developing kidney." *Development* **125**(21): 4225-4234.

Kobayashi, A., K. M. Kwan, T. J. Carroll, A. P. McMahon, C. L. Mendelsohn and R. R. Behringer (2005). "Distinct and sequential tissue-specific activities of the LIM-class homeobox gene *Lim1* for tubular morphogenesis during kidney development." *Development* **132**(12): 2809-2823.

Kobayashi, A., J. W. Mugford, A. M. Krautzberger, N. Naiman, J. Liao and A. P. McMahon (2014). "Identification of a multipotent self-renewing stromal progenitor population during mammalian kidney organogenesis." *Stem Cell Reports* **3**(4): 650-662.

Kuure, S., A. Popsueva, M. Jakobson, K. Sainio and H. Sariola (2007). "Glycogen synthase kinase-3 inactivation and stabilization of beta-catenin induce nephron differentiation in isolated mouse and rat kidney mesenchymes." *J Am Soc Nephrol* **18**(4): 1130-1139.

Labbe, E., A. Letamendia and L. Attisano (2000). "Association of Smads with lymphoid enhancer binding factor 1/T cell-specific factor mediates cooperative signaling by the transforming growth factor-beta and wnt pathways." *Proc Natl Acad Sci U S A* **97**(15): 8358-8363.

Levinson, R. S., E. Batourina, C. Choi, M. Vorontchikhina, J. Kitajewski and C. L. Mendelsohn (2005). "Foxd1-dependent signals control cellularity in the renal capsule, a structure required for normal renal development." *Development* **132**(3): 529-539.

Li, W., S. Hartwig and N. D. Rosenblum (2014). "Developmental origins and functions of stromal cells in the normal and diseased mammalian kidney." *Dev Dyn* **243**(7): 853-863.

Little, M. H. and A. P. McMahon (2012). "Mammalian kidney development: principles, progress, and projections." *Cold Spring Harb Perspect Biol* **4**(5).

Livak, K. J. and T. D. Schmittgen (2001). "Analysis of relative gene expression data using real-time quantitative PCR and the 2(-Delta Delta C(T)) Method." *Methods* **25**(4): 402-408.

Logan, C. Y. and R. Nusse (2004). "The Wnt signaling pathway in development and disease." *Annu Rev Cell Dev Biol* **20**: 781-810.

MacDonald, B. T., K. Tamai and X. He (2009). "Wnt/beta-catenin signaling: components, mechanisms, and diseases." *Dev Cell* **17**(1): 9-26.

Maezawa, Y., M. Binnie, C. Li, P. Thorner, C. C. Hui, B. Alman, M. M. Taketo and S. E. Quaggin (2012). "A new Cre driver mouse line, Tcf21/Pod1-Cre, targets metanephric mesenchyme." *PLoS One* **7**(7): e40547.

Majumdar, A., S. Vainio, A. Kispert, J. McMahon and A. P. McMahon (2003). "Wnt11 and Ret/Gdnf pathways cooperate in regulating ureteric branching during metanephric kidney development." *Development* **130**(14): 3175-3185.

Marose, T. D., C. E. Merkel, A. P. McMahon and T. J. Carroll (2008). "Beta-catenin is necessary to keep cells of ureteric bud/Wolffian duct epithelium in a precursor state." *Dev Biol* **314**(1): 112-126.

Masckauchan, T. N., C. J. Shawber, Y. Funahashi, C. M. Li and J. Kitajewski (2005). "Wnt/beta-catenin signaling induces proliferation, survival and interleukin-8 in human endothelial cells." *Angiogenesis* **8**(1): 43-51.

McPherson, E., J. Carey, A. Kramer, J. G. Hall, R. M. Pauli, R. N. Schimke and M. H. Tasin (1987). "Dominantly inherited renal adysplasia." *Am J Med Genet* **26**(4): 863-872.

Mendelsohn, C., E. Batourina, S. Fung, T. Gilbert and J. Dodd (1999). "Stromal cells mediate retinoid-dependent functions essential for renal development." *Development* **126**(6): 1139-1148.

Miyazaki, Y., K. Oshima, A. Fogo and I. Ichikawa (2003). "Evidence that bone morphogenetic protein 4 has multiple biological functions during kidney and urinary tract development." *Kidney Int* **63**(3): 835-844.

Moerman, P., J. P. Fryns, S. H. Sastrowijoto, K. Vandenberghe and J. M. Lauweryns (1994). "Hereditary renal adysplasia: new observations and hypotheses." *Pediatr Pathol* **14**(3): 405-410.

Mugford, J. W., P. Sipila, J. A. McMahon and A. P. McMahon (2008). "Osr1 expression demarcates a multi-potent population of intermediate mesoderm that undergoes progressive restriction to an Osr1-dependent nephron progenitor compartment within the mammalian kidney." *Dev Biol* **324**(1): 88-98.

Murugasu, B., B. R. Cole, E. P. Hawkins, S. H. Blanton, S. B. Conley and R. J. Portman (1991). "Familial renal adysplasia." *Am J Kidney Dis* **18**(4): 490-494.

Nakagawa, N., C. Xin, A. M. Roach, N. Naiman, S. J. Shankland, G. Ligresti, S. Ren, S. Szak, I. G. Gomez and J. S. Duffield (2015). "Dicer1 activity in the stromal compartment regulates nephron differentiation and vascular patterning during mammalian kidney organogenesis." *Kidney Int* **87**(6): 1125-1140.

Neu, A. M., P. L. Ho, R. A. McDonald and B. A. Warady (2002). "Chronic dialysis in children and adolescents. The 2001 NAPRTCS Annual Report." *Pediatr Nephrol* **17**(8): 656-663.

Nicolaou, N., K. Y. Renkema, E. M. Bongers, R. H. Giles and N. V. Knoers (2015). "Genetic, environmental, and epigenetic factors involved in CAKUT." *Nat Rev Nephrol* **11**(12): 720-731.

Park, J. S., W. Ma, L. L. O'Brien, E. Chung, J. J. Guo, J. G. Cheng, M. T. Valerius, J. A. McMahon, W. H. Wong and A. P. McMahon (2012). "Six2 and Wnt regulate self-renewal and commitment of nephron progenitors through shared gene regulatory networks." *Dev Cell* **23**(3): 637-651.

Park, J. S., M. T. Valerius and A. P. McMahon (2007). "Wnt/beta-catenin signaling regulates nephron induction during mouse kidney development." *Development* **134**(13): 2533-2539.

Paroly, S. S., F. Wang, L. Spraggon, J. Merregaert, E. Batourina, B. Tycko, K. M. Schmidt-Ott, S. Grimmond, M. Little and C. Mendelsohn (2013). "Stromal protein Ecm1 regulates ureteric bud patterning and branching." *PLoS One* **8**(12): e84155.

Piscione, T. D. and N. D. Rosenblum (1999). "The malformed kidney: disruption of glomerular and tubular development." *Clin Genet* **56**(5): 341-356.

Popova, A. P., J. K. Bentley, A. C. Anyanwu, M. N. Richardson, M. J. Linn, J. Lei, E. J. Wong, A. M. Goldsmith, G. S. Pryhuber and M. B. Hershenson (2012). "Glycogen synthase kinase-3beta/beta-catenin signaling regulates neonatal lung mesenchymal stromal cell myofibroblastic differentiation." *Am J Physiol Lung Cell Mol Physiol* **303**(5): L439-448.

Quaggin, S. E. (2016). "Kindling the Kidney." *N Engl J Med* **374**(3): 281-283.

Quaggin, S. E., L. Schwartz, S. Cui, P. Igarashi, J. Deimling, M. Post and J. Rossant (1999). "The basic-helix-loop-helix protein pod1 is critically important for kidney and lung organogenesis." *Development* **126**(24): 5771-5783.

Reginensi, A., R. P. Scott, A. Gregorieff, M. Bagherie-Lachidan, C. Chung, D. S. Lim, T. Pawson, J. Wrana and H. McNeill (2013). "Yap- and Cdc42-dependent nephrogenesis and morphogenesis during mouse kidney development." *PLoS Genet* **9**(3): e1003380.

Robert, B., P. L. St John and D. R. Abrahamson (1998). "Direct visualization of renal vascular morphogenesis in Flk1 heterozygous mutant mice." *Am J Physiol* **275**(1 Pt 2): F164-172.

Rosenbluh, J., D. Nijhawan, A. G. Cox, X. Li, J. T. Neal, E. J. Schafer, T. I. Zack, X. Wang, A. Tsherniak, A. C. Schinzel, D. D. Shao, S. E. Schumacher, B. A. Weir, F. Vazquez, G. S. Cowley, D. E. Root, J. P. Mesirov, R. Beroukhim, C. J. Kuo, W. Goessling and W. C. Hahn (2012). "beta-Catenin-driven cancers require a YAP1 transcriptional complex for survival and tumorigenesis." *Cell* **151**(7): 1457-1473.

Rosenblum, N. D. (2012) "Overview of congenital anomalies of the kidney and urinary tract (CAKUT)."

Rosselot, C., L. Spraggon, I. Chia, E. Batourina, P. Riccio, B. Lu, K. Niederreither, P. Dolle, G. Duester, P. Chambon, F. Costantini, T. Gilbert, A. Molotkov and C. Mendelsohn (2010). "Non-cell-autonomous retinoid signaling is crucial for renal development." *Development* **137**(2): 283-292.

Sanna-Cherchi, S., G. Caridi, P. L. Weng, F. Scolari, F. Perfumo, A. G. Gharavi and G. M. Ghiggeri (2007). "Genetic approaches to human renal agenesis/hypoplasia and dysplasia." *Pediatr Nephrol* **22**(10): 1675-1684.

Sarin, S., F. Boivin, A. Li, J. Lim, B. Svajger, N. D. Rosenblum and D. Bridgewater (2014). "beta-catenin overexpression in the metanephric mesenchyme leads to renal dysplasia genesis via cell-autonomous and non-cell-autonomous mechanisms." *Am J Pathol* **184**(5): 1395-1410.

Saxen, L. and H. Sariola (1987). "Early organogenesis of the kidney." *Pediatr Nephrol* **1**(3): 385-392.

Schmidt-Ott, K. M., X. Chen, N. Paragas, R. S. Levinson, C. L. Mendelsohn and J. Barasch (2006). "c-kit delineates a distinct domain of progenitors in the developing kidney." *Dev Biol* **299**(1): 238-249.

Schmidt-Ott, K. M., T. N. Masckauchan, X. Chen, B. J. Hirsh, A. Sarkar, J. Yang, N. Paragas, V. A. Wallace, D. Dufort, P. Pavlidis, B. Jagla, J. Kitajewski and J. Barasch (2007). "beta-catenin/TCF/Lef controls a differentiation-associated transcriptional program in renal epithelial progenitors." *Development* **134**(17): 3177-3190.

Schnabel, C. A., R. E. Godin and M. L. Cleary (2003). "Pbx1 regulates nephrogenesis and ureteric branching in the developing kidney." *Dev Biol* **254**(2): 262-276.

Schwab, K., L. T. Patterson, B. J. Aronow, R. Luckas, H. C. Liang and S. S. Potter (2003). "A catalogue of gene expression in the developing kidney." *Kidney Int* **64**(5): 1588-1604.

Seifert, R. A., C. E. Alpers and D. F. Bowen-Pope (1998). "Expression of platelet-derived growth factor and its receptors in the developing and adult mouse kidney." *Kidney Int* **54**(3): 731-746.

Seikaly, M. G., P. L. Ho, L. Emmett, R. N. Fine and A. Tejani (2003). "Chronic renal insufficiency in children: the 2001 Annual Report of the NAPRTCS." *Pediatr Nephrol* **18**(8): 796-804.

Sequeira-Lopez, M. L., E. E. Lin, M. Li, Y. Hu, C. D. Sigmund and R. A. Gomez (2015). "The earliest metanephric arteriolar progenitors and their role in kidney vascular development." *Am J Physiol Regul Integr Comp Physiol* **308**(2): R138-149.

Sims-Lucas, S., C. Schaefer, D. Bushnell, J. Ho, A. Logar, E. Prochownik, G. Gittes and C. M. Bates (2013). "Endothelial Progenitors Exist within the Kidney and Lung Mesenchyme." *PLoS One* **8**(6): e65993.

Slegers, J. F. and W. M. Moons (1985). "Influence of renal capsule on kidney function in hypertension." *Clin Exp Hypertens A* **7**(12): 1751-1768.

Squiers, E. C., R. S. Morden and J. Bernstein (1987). "Renal multicystic dysplasia: an occasional manifestation of the hereditary renal adysplasia syndrome." *Am J Med Genet Suppl* **3**: 279-284.

Stark, K., S. Vainio, G. Vassileva and A. P. McMahon (1994). "Epithelial transformation of metanephric mesenchyme in the developing kidney regulated by Wnt-4." *Nature* **372**(6507): 679-683.

Suzuki, Y., K. Montagne, A. Nishihara, T. Watabe and K. Miyazono (2008). "BMPs promote proliferation and migration of endothelial cells via stimulation of VEGF-A/VEGFR2 and angiopoietin-1/Tie2 signalling." *J Biochem* **143**(2): 199-206.

Takahashi, M. (2001). "The GDNF/RET signaling pathway and human diseases." *Cytokine Growth Factor Rev* **12**(4): 361-373.

Thomas, R., S. Sanna-Cherchi, B. A. Warady, S. L. Furth, F. J. Kaskel and A. G. Gharavi (2011). "HNF1B and PAX2 mutations are a common cause of renal hypodysplasia in the CKiD cohort." *Pediatr Nephrol* **26**(6): 897-903.

Trnka, P., M. J. Hiatt, L. Ivanova, A. F. Tarantal and D. G. Matsell (2010). "Phenotypic transition of the collecting duct epithelium in congenital urinary tract obstruction." *J Biomed Biotechnol* **2010**: 696034.

Valdimarsdottir, G., M. J. Goumans, A. Rosendahl, M. Brugman, S. Itoh, F. Lebrin, P. Sideras and P. ten Dijke (2002). "Stimulation of Id1 expression by bone morphogenetic protein is sufficient and necessary for bone morphogenetic protein-induced activation of endothelial cells." *Circulation* **106**(17): 2263-2270.

Wang, X., Y. Xiao, Y. Mou, Y. Zhao, W. M. Blankesteyn and J. L. Hall (2002). "A role for the beta-catenin/T-cell factor signaling cascade in vascular remodeling." *Circ Res* **90**(3): 340-347.

Wang, Z., A. Havasi, J. M. Gall, H. Mao, J. H. Schwartz and S. C. Borkan (2009). "Beta-catenin promotes survival of renal epithelial cells by inhibiting Bax." *J Am Soc Nephrol* **20**(9): 1919-1928.

Weber, S., V. Moriniere, T. Knuppel, M. Charbit, J. Dusek, G. M. Ghiggeri, A. Jankauskiene, S. Mir, G. Montini, A. Peco-Antic, E. Wuhl, A. M. Zurowska, O. Mehls, C. Antignac, F. Schaefer and R. Salomon (2006). "Prevalence of mutations in renal developmental genes in children with renal hypodysplasia: results of the ESCAPE study." *J Am Soc Nephrol* **17**(10): 2864-2870.

Wiley, D. M. and S. W. Jin (2011). "Bone Morphogenetic Protein functions as a context-dependent angiogenic cue in vertebrates." *Semin Cell Dev Biol* **22**(9): 1012-1018.

Wingen, A. M., C. Fabian-Bach, F. Schaefer and O. Mehls (1997). "Randomised multicentre study of a low-protein diet on the progression of chronic renal failure in children. European Study Group of Nutritional Treatment of Chronic Renal Failure in Childhood." *Lancet* **349**(9059): 1117-1123.

Winyard, P. and L. S. Chitty (2008). "Dysplastic kidneys." *Semin Fetal Neonatal Med* **13**(3): 142-151.

Woolf, A. S., K. L. Price, P. J. Scambler and P. J. Winyard (2004). "Evolving concepts in human renal dysplasia." *J Am Soc Nephrol* **15**(4): 998-1007.

Xie, H., Z. Huang, M. S. Sadim and Z. Sun (2005). "Stabilized beta-catenin extends thymocyte survival by up-regulating Bcl-xL." *J Immunol* **175**(12): 7981-7988.

Yallowitz, A. R., S. M. Hrycaj, K. M. Short, I. M. Smyth and D. M. Wellik (2011). "Hox10 genes function in kidney development in the differentiation and integration of the cortical stroma." *PLoS One* **6**(8): e23410.

Yan, Y., J. Frisen, M. H. Lee, J. Massague and M. Barbacid (1997). "Ablation of the CDK inhibitor p57Kip2 results in increased apoptosis and delayed differentiation during mouse development." *Genes Dev* **11**(8): 973-983.

Yang, J., A. Blum, T. Novak, R. Levinson, E. Lai and J. Barasch (2002). "An epithelial precursor is regulated by the ureteric bud and by the renal stroma." *Dev Biol* **246**(2): 296-310.

Yu, J., T. J. Carroll, J. Rajagopal, A. Kobayashi, Q. Ren and A. P. McMahon (2009). "A Wnt7b-dependent pathway regulates the orientation of epithelial cell division and establishes the cortico-medullary axis of the mammalian kidney." *Development* **136**(1): 161-171.

Zeng, X., H. Huang, K. Tamai, X. Zhang, Y. Harada, C. Yokota, K. Almeida, J. Wang, B. Doble, J. Woodgett, A. Wynshaw-Boris, J. C. Hsieh and X. He (2008). "Initiation of Wnt signaling: control of Wnt coreceptor Lrp6 phosphorylation/activation via frizzled, dishevelled and axin functions." *Development* **135**(2): 367-375.

Zhang, H., R. Palmer, X. Gao, J. Kreidberg, W. Gerald, L. Hsiao, R. V. Jensen, S. R. Gullans and D. A. Haber (2003). "Transcriptional activation of placental growth factor by the forkhead/winged helix transcription factor FoxD1." *Curr Biol* **13**(18): 1625-1629.

Zhang, P., N. J. Liegeois, C. Wong, M. Finegold, H. Hou, J. C. Thompson, A. Silverman, J. W. Harper, R. A. DePinho and S. J. Elledge (1997). "Altered cell differentiation and proliferation in mice lacking p57KIP2 indicates a role in Beckwith-Wiedemann syndrome." *Nature* **387**(6629): 151-158.

Zhou, D., Y. Li, L. Lin, L. Zhou, P. Igarashi and Y. Liu (2012). "Tubule-specific ablation of endogenous beta-catenin aggravates acute kidney injury in mice." *Kidney Int* **82**(5): 537-547.

Zhurinsky, J., M. Shtutman and A. Ben-Ze'ev (2000). "Plakoglobin and beta-catenin: protein interactions, regulation and biological roles." *J Cell Sci* **113** (Pt 18): 3127-3139.